

Control of Flow And Oxygen In A 3-D Perfused Micro-Environment Fosters Balanced Survival Of Hepatocyte-Non-Parenchymal Cell Co-Cultures.

By
Ajit Dash

Bachelor of Medicine, Bachelor of Surgery (M.B.B.S.)
Utkal University, 1995.

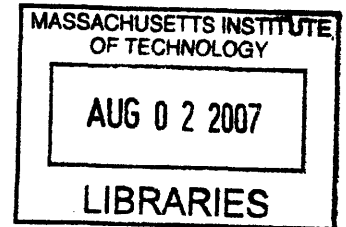
Doctor of Medicine, (Pharmacology) (M.D.)
Mumbai University, 2000.

Submitted to the Biological Engineering Division in partial fulfillment of the requirements for the degree of

Doctor of Philosophy
at the
Massachusetts Institute of Technology

June, 2007

©2007 Massachusetts Institute of Technology
All Rights Reserved



Signature of author: _____
Biological Engineering Division

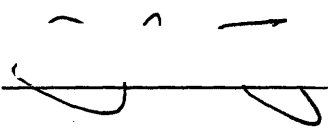
Certified by: _____
Linda Griffith
Professor of Biological Engineering and Mechanical Engineering
Thesis Advisor

Certified by: _____
Steven R Tannenbaum
Professor of Biological Engineering and Chemistry
Thesis Advisor

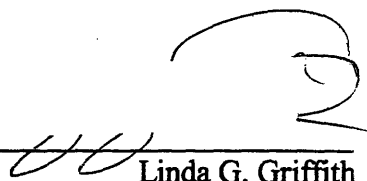
Accepted by: _____
John Essigmann
Professor of Biological Engineering Division
Chairperson, Graduate Thesis Committee

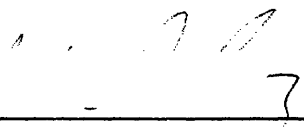
ARCHIVES

This doctoral thesis has been examined by a committee of the Biological Engineering Division as follows:

Chairperson, Graduate Thesis Committee:  _____
John S. Essigmann
Professor of Biological Engineering and Chemistry
MIT

Thesis Advisor, Committee Member: _____
Steven R. Tannenbaum
Professor of Biological Engineering and Chemistry
MIT

Thesis Advisor, Committee Member: _____
 Linda G. Griffith
Professor of Biological Engineering and Mechanical Engineering
MIT

Thesis Committee Member: _____
 Alan Wells
Professor of Pathology
University of Pittsburgh

Abstract

Creating a physiologically relevant *in vitro* liver model requires reproducing the cellular heterogeneity of *in vivo* liver in a functional state. However differentiated sinusoidal endothelial cells (SECs), marked by SE-1 expression are difficult to maintain in culture while stellate cells easily activate and over-proliferate. We hypothesized that recreating a liver tissue system that captured *in vivo* like paracrine influences would foster survival of these cells, and predicted that stimuli resulting from flow and oxygen gradients close to physiological conditions would preserve the delicate balance between the cell types. Spheroids containing hepatocytes with incorporated non-parenchymal cells (NPCs) were seeded into capillary bed sized channels in polycarbonate scaffolds, housed in a three-dimensional perfused system, and maintained for two weeks. Micro-flow rates of different media through the formed tissue units in scaffolds were controlled using pneumatic pumps and microfluidics. Staining and confocal imaging of endpoint tissue showed that lower flow rates closer to physiological regimes allowed the survival of SE-1+ SECs, regardless of exogenously added growth factors in the medium. Higher flow rates, exogenous growth factors, and scaffold contact were associated with activation of stellate cells (alpha-smooth muscle actin staining). Since oxygen measurements in the system coupled low flow rates with hypoxic tissue outlet concentrations, we parsed out these variables by repeating flow experiments in low oxygen environments. Retention of SE-1 staining cells even in higher flow rates demonstrated that hypoxic conditions in the tissue could play a role in aiding their survival by overcoming negative effects brought about by high flow. The relationship of stellate cells with flow rate was unaffected by oxygen concentrations. To explore if the negative effects of high flow on SE-1 expression were mediated by transforming growth factor-beta (TGF- β), we added a TGF- β inhibitor SB-431542 in our cultures, and found that it greatly enhanced the presence of SE-1 staining SECs at high flow rates. In conclusion we successfully created a three-dimensional flow controlled hepatic culture system that allows balanced survival of hepatocytes and non-parenchymal cells, making it useful as a potential model for studies such as cancer metastasis that require interactions between tumor cells and heterotypic host tissue.

Key Words: Liver, *In vitro*, co-culture, sinusoidal, endothelial, stellate, oxygen, flow, shear

Thesis Advisors: Linda G. Griffith and Steven R. Tannenbaum

Acknowledgements

I had the good fortune of having not one but two thesis advisors, Steven Tannenbaum and Linda Griffith, a situation that allowed me to get perspectives that not only reflected two individual viewpoints, but also two different areas of expertise. My early years at MIT were spent mostly in Steve's laboratory. In addition to the academic insights provided by him, I deeply value the constant support and encouragement I received on every possible front. My final thesis work involved a closer interaction with Linda and I truly consider it a rewarding experience. I believe that the ability of getting one to pose relevant questions and set about finding ways to answer them is the best form of imparting advice. And Linda was very effective in doing that, in the process helping me achieve my potential to the fullest. Having the combined resources of both Linda and Steve at my disposal also offered me the freedom to plan my project without any worries.

I am thankful to my Thesis Committee members John Essigmann and Alan Wells. Their advice not only widened the experience and expertise I had as a resource, but also helped me overcome stumbling blocks along the way. Additionally they have always been very accommodating about scheduling committee meetings. I would also like to sincerely acknowledge Donna Stoltz for her useful advice. Spending a week at her laboratory in Pittsburgh introduced me to the fascinating world of imaging and triggered me off in the path of being a 'cellular voyeur'.

My first interaction in Linda's lab was with Albert Hwa whose earlier work was a useful reference point for me and who was instrumental in teaching me the endothelial isolation skills that I used in my project. Working in Linda's laboratory also offered me a chance to team up with Matthew Lim and Ta-Chun Hang. Our interactions coupled the seriousness of scientific discussions with an intrinsic camaraderie that we shared. The experiments that I successfully carried out over the last year would have been impossible without their collaborative efforts. I would like to thank Karel Domansky, Walker Inman and Jim Serdy for designing the system I used – the multi-well reactor, and being around to help analyze and solve any operational hurdles. In spite of short deadlines, Jim Serdy invariably delivered my requirements for reactor components on time. Laura Vineyard was another person who was extremely accommodating about carrying out the demanding double perfusions at short notice as per the needs of the project. Academic discussions with Anand Sivaraman, Nathan Tedford and Ben Cosgrove among others were a big help in overcoming practical problems along the way. An essential part of smooth operations is administrative help, and having Megan Whittemore and Romie Littrel eased life considerably on that front. Being in the Griffith lab also allowed me to be a part of joint meetings with the Lauffenberger lab, a valuable forum for discussing my project results and getting a wide array of expert advice on how to overcome problems.

Working in the Tannenbaum lab was like being with family away from home. Kevin Leach was the first close friend I made in the US and he helped me with most of what I learned about hepatocyte cultures. Ji-Eun Kim, Anna Stevens and Patty Sun were not just lab mates, they were

always there to discuss any work related problems that I needed to talk about. Pete Wishnok and the rest of the laboratory members were a ready source of help for anything that I needed. And not to forget Amy Francis who not only made administrative hassles disappear, but also lent a patient ear whenever I needed to talk.

I would like to thank Professor Frank Gertler for allowing me the use of the confocal microscopy facility at his lab and Craig Furman and Hyung Do Kim from the Gertler lab for their helping me get started. I am also grateful to Ram Sasisekharan for being instrumental in my initial evaluation and admission into the program and a source of support throughout.

Professional progress goes hand in hand with support on the personal front. I would specifically like to thank my close friends Siddharth Jain and Mikhail Elkin for being around for me through good times and bad times. Susan Stewart and Kathleen Howley were my 'family' here in the US and made the lonely holiday seasons bearable. Carlos Pacheco, Annie Frazer and Albert Chan were part of my early 'Rainbow Coffeehouse' years - a period that helped me grow tremendously as a person. Till this day, the Coffeehouse and its members are an integral part of my life outside work. Discussions with friends like Vikas Prabhakar from BE helped balance life at work with life outside. Last but not the least, I would like to express my thanks to my mother and real family back home - for being there and standing by me all these years, in spite of the difficulties they faced by virtue of my being away from them.

Finally I would like to thank Douglas Lauffenberger, director of the Biological Engineering Division, for providing me the opportunity and resources to spend my time and efforts in such a stimulating and rewarding environment, and the administrative staff of BE (particularly Dalia Fares and Mariann Murray) for making life in the division so much easier.

Contents

CHAPTER 1.

IN VITRO LIVER CULTURE: CHALLENGES AND APPROACHES.....12

1.1 Normal Liver Microenvironment.....13

1.1.1. Functional Versatility Matched By Structural Complexity.....13

1.1.2. Cellular Component.....15

1.1.3. Extracellular Matrix.....17

1.2. Local Environmental Determinants Of Cellular Function And Survival.....17

1.2.1. Paracrine Interdependence.....18

1.2.2. Direct Cell-Matrix And Cell-Cell Interactions.....23

1.2.3. Effects Of Local Circulation On Cell Phenotype.....25

1.3 Challenges Of *In vitro* Liver Culture.....27

1.3.1. Preserving Sinusoidal Endothelial Survival And Phenotype.....27

1.3.2. Controlling Stellate Cell Overproliferation And Activation.....30

1.3.3. Hepatocyte Dedifferentiation.....32

1.4.Evolving Trends In *In vitro* Liver Culture.....33

1.4.1. From Monocultures To Co-Cultures.....34

1.4.2. From 2-D To 3-D Culture.....35

1.4.3. Towards Facilitated Microcirculation.....36

1.5. Special Considerations While Studying 3-D Perfused Systems.....36

1.5.1. Determining Scales Based On Tissue Requirements.36

1.5.2. Scaffold Material And Geometry.....38

1.5.3. Calculating Physiologically Appropriate Flow Rates.....39

1.5.4. Measuring Oxygen In Live Cultures.....39

1.5.5. Modeling Complex 3-D Systems.....40

1.5.6. Choice Of Imaging Techniques.....40

1.5.7. Choice Of Markers For Imaging Functional Liver Cells.....42

1.6. 3-D Perfused Organotypic Liver Bioreactor Systems.....44

1.6.1. Perfused Bioreactor With *In vivo* Like Function.....44

1.5.2. A High Throughput System With Controlled Flow.....47

1.7 Hypotheses And Specific Thesis Aims.....51

CHAPTER 2.
ESTABLISHING OPERATIONAL PARAMETERS IN THE SYSTEM52

2.1 Characterizing Cellular Input:.....53

- 2.1.1. Materials And Methods.....53
 - 2.1.1.1. Animals And Cell Isolation Procedures.....53
 - 2.1.1.2. Medium And Spheroid Preparation.....54
 - 2.1.1.3. Staining And Imaging Endothelial Isolates.....55
 - 2.1.1.4. Staining And Imaging Spheroids.....55
- 2.1.2. Results.....56
 - 2.1.2.1. Characterization Of Endothelial Isolates.....56
 - 2.1.2.2. Characterization Of Spheroids.....59
- 2.1.3. Discussion.....63

2.2. Selection Of Operating Conditions.....65

- 2.2.1. Optimizing Working Parameters.....65
 - 2.2.1.1. Overall Design.....65
 - 2.2.1.2. Parameters Tested.....67
 - 2.2.1.3. Results.....69
 - 2.2.1.4. Discussion.....75
- 2.2.2. Predicting Outer Bounds For Operational Flow Rates.....77
 - 2.2.2.1. COMSOL Modeling For Oxygen Predictions.....77
 - 2.2.2.2. Results.....78
 - 2.2.2.3. Discussion.....79

CHAPTER 3.
EFFECT OF MEDIUM AND FLOW RATE ON NON-PARENCHYMAL CELL SURVIVAL AND PHENOTYPE.....81

3.1. Overall Rationale.....82

3.2. Materials And Methods.....82

- 3.2.1. Setting Up Co-Cultures.....82
- 3.2.2. Staining Tissue For Non-Parenchymal Markers.....85
- 3.2.3. Confocal Microscopy And Image Processing.....85
- 3.2.4. Oxygen Measurements.....86
- 3.2.5. Total Cell Number By RNA Estimation.....87

3.3. Results.....87

- 3.3.1. Effect Of Medium And Flow On Non-Parenchymal Cells.....87
- 3.3.2. Effect Of Flow Rate On Oxygen Difference Across Tissue.....99

3.4. Discussion.....102

CHAPTER 4.	
UNCOUPLING THE EFFECTS OF OXYGEN AND FLOW ON NON-PARENCHYMAL CELL SURVIVAL AND PHENOTYPE.....	105
4.1. Overall Rationale.....	106
4.2. Materials And Methods.....	106
4.2.1. Setting Up Co-Cultures.....	106
4.2.2. Staining Tissue For Non-Parenchymal Markers.....	109
4.2.3. Oxygen Measurements And Total Cell Number	109
4.3. Results.....	110
4.3.1. Overall Tissue Formation.....	110
4.3.2. Non-Parenchymal Cell Staining And Oxygen Measurements.....	111
4.4. Discussion.....	118
CHAPTER 5.	
EFFECT OF TRANSFORMING GROWTH FACTOR – BETA INHIBITION ON NON-PARENCHYMAL CELL SURVIVAL AND PHENOTYPE.....	122
5.1. Overall Rationale.....	123
5.2. System And Operational Modifications.....	123
5.3. Materials And Methods.....	124
5.3.1. Setting Up Co-Cultures.....	124
5.3.2. Staining Tissue For Non-Parenchymal Markers.....	127
5.3.3. Oxygen Measurements And Total Cell Number	127
5.4. Results.....	128
5.4.1. Overall Tissue Formation.....	128
5.4.2. Non-Parenchymal Cell Staining And Oxygen Measurements.....	128
5.5. Discussion.....	134
CHAPTER 6.	
CONCLUSIONS AND FUTURE DIRECTIONS	137
6.1 Summary Of Conclusions	138
6.2 Future Recommendations	140
REFERENCES	141

APPENDICES.....154

Appendix 1 - Hgm Formulation155

Appendix 2 – Isolation And Viability Test Of Hepatocytes.....156

Appendix 3 - Isolation And Viability Test Of Primary Liver Endothelial Cells158

Appendix 4 - Immunostaining Of Isolated Non-Parenchymal Cells.....160

Appendix 5 – Assembly And Priming Of Multiwell Reactors.....162

Appendix 6 – Protocol For Co-Culture Spheroid Formation164

Appendix 7 – Setup And Seeding The Multiwell Reactors.....166

Appendix 8 – Maintaining And Disassembling The Multiwell Reactors.....168

Appendix 9 - Immunostaining Spheroids Or Tissue From Reactors.....170

Appendix 10 – Protocol For Oxygen Measurement In Reactor System.....172

Appendix 11 - Protocol For RNA Isolation From Samples174

Chapter 1

***In vitro* Liver Culture: Challenges And Approaches**

1.1. Normal Liver Microenvironment:

1.1.1. Functional versatility matched by structural complexity

The liver is the one of the most important and versatile metabolic organs in the body responsible for a repertoire of functions ranging from metabolism (of all classes of foods -lipids, proteins and carbohydrates- and drugs and xenobiotics) to synthesis of a host of endogeneous substances (various proteins, hormones and coagulation factors), as well as detoxification and breakdown of endogenous nitrogeneous wastes into urea (1). The liver is also the major site of storage of glucose (as glycogen), vitamin B₁₂, iron, copper and the main site of fetal red blood cell production. The reticuloendothelial system of the liver acts as an immunological filter for antigens carried to it via the portal system. The complexity of function of the liver goes hand in hand with unique structural features that make it very different from all other organs. The liver is characterized by heterogeneous cellular units that are perfused by sinusoidal networks to create a balanced haemodynamic environment (Figure 1). The 3-dimensional architecture is described as “isotropic parenchyma” (2), and no matter at whatever angle it is sectioned, it has the same histologic appearance of a central vein surrounded by about 4–6 portal areas (each consisting of a triad of structures – branches of a hepatic artery, portal vein and a bile duct). Between the central veins and the portal triads lie the primary liver cells, the hepatocytes, arranged in one cell thick plates that branch and anastomose in a continuous labrynth with surrounding hepatic plates. The resulting intervening network of spaces are lined by sinusoidal endothelial cells and are bathed in blood originating from the branches of the hepatic artery and portal vein ultimately draining into the central vein. Hepatocytes secrete bile into an anastomosing network of bile canaliculi, which then

drain peripherally into ductules at the margins of the portal triads, ultimately emptying into the interlobular bile ducts. Macrophages (Kupffer cells) and circulating lymphocytes reside in the sinusoids whereas fat and retinoid storing stellate cells are present in the narrow space of Disse between the hepatocytes and the endothelial cells.

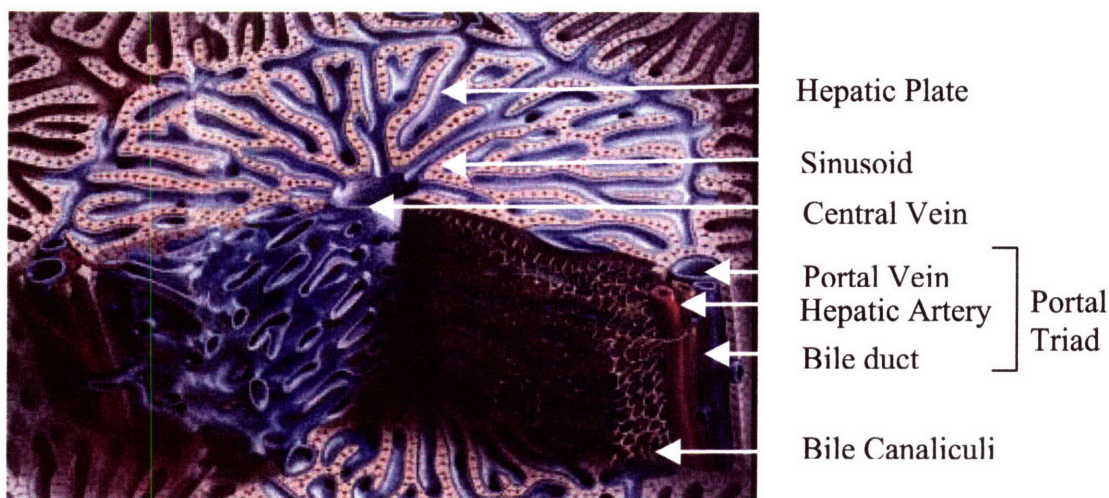


Figure 1. Anatomy of a Hepatic Lobule [Figure adapted from Volwiler et al 2006 (3)]

Hepatocyte plates, and intervening sinusoids are arranged radially around a central hepatic venule with surrounding portal triads, (each containing a portal venule, a hepatic arteriole, and a intralobular bile duct). Bile flows outward through bile canaliculi, draining into the bile ducts while blood flows from the hepatic artery and portal vein inward through sinusoids draining into the central vein.

Making the liver microenvironment different from other tissues is not just the numerous cell types present, and their defined structural and functional interrelationships, but also the unique circulatory pattern resulting from the dual blood supply it receives from the portal vein and the hepatic artery. Unlike other organs that are uniformly perfused by highly oxygenated arterial blood at a high pressure, the liver receives both venous blood at low pressure through the portal vein as well as arterial blood at high pressure via the hepatic artery. The complexity of both the flow and the cellular architecture of the liver make it a challenging system to recapitulate *in vitro*.

1.1.2. Cellular component

Hepatocytes are the predominant cell type in the liver and form the liver parenchyma. They comprise 60% of the total cells and 80% of the volume of liver(4). In their normal healthy differentiated state, they perform a diverse array of functions ranging from synthesis, catabolism, intermediary metabolism, and detoxification of drugs and xenobiotics in the body. However, the harmonized activity of these cells depends greatly on their cellular and non-cellular environment, and can be altered vastly in diseased states as well as *in vitro* culture.

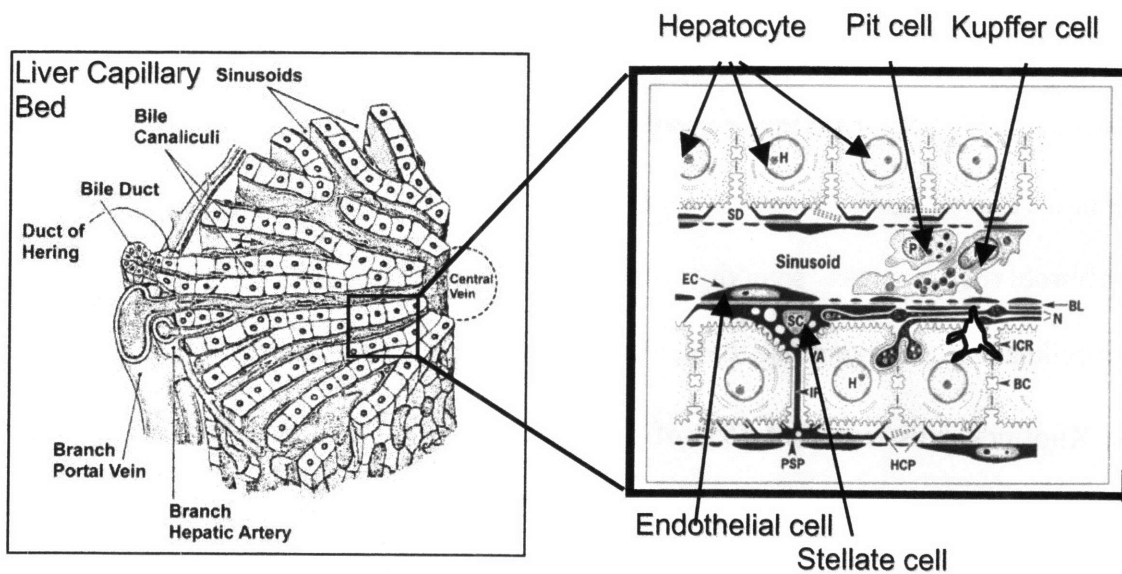


Fig 2. Histological architecture of a section of the hepatic lobule. Inset shows the sinusoids between the hepatocyte plates lined by endothelial cells, the space of Disse, and the proximal location of other non-parenchymal cell types to hepatocytes [Figures adapted from (left) Bloom & Fawcett 1968 and (right) Wake et al.1997 (5,6)] .

The largest fraction of the non-parenchymal cells (NPCs) are the sinusoidal endothelial cells that comprise about 19-21% of all liver cells (7). Lining the sinusoids, they separate the hepatocytes from blood, and filter fluids, solutes, and particles between the blood and

space of Disse. They are differentiated from regular capillary endothelial cells by the presence of numerous characteristic tiny pores called fenestrations, a sparse and rudimentary basement membrane underneath the cells and the functional feature of endocytosis. Fenestrations, with an average diameter of 160nm, are clustered in groups of 10 to 50, commonly referred to as sieve plates (8). The number and size of fenestrations vary across species and in different regions of the liver, and can change in response to a variety of hormones, drugs, toxins, diseases, and underlying extracellular matrix (8) .

Hepatic stellate cells (HSC), previously called Ito cells, comprising about 5% of liver cells by number are stromal cells, and a major player in hepatic regeneration as well as fibrogenesis and cirrhosis (9-12). Present in the space of Disse, they are responsible for producing extracellular matrix, controlling microvascular tone, storing and metabolizing vitamin A and lipid. When activated as in disease states, they transform into myofibroblasts, express smooth muscle actin filaments and produce excess of extracellular matrix giving rise to the characteristic changes seen in liver fibrosis.

The Kupffer's cells represent 15% of the liver cells (30% of sinusoidal cells) and are derived from circulating monocytes (7,13,14). They are the body's largest population of tissue macrophages and form an important part of the reticuloendothelial system. Their major functions include phagocytosis of foreign particles, removal of endotoxins and other noxious substances, and modulation of the immune response through the release of cytokines and mediators of inflammation. Additionally there are a few more cell types such as Pit cells, lymphocytes etc. present in small numbers that play a role in the homeostasis of the liver.

1.1.3. Extracellular matrix

The extracellular matrix (ECM) refers to the network of various macromolecules that comprise the scaffolding of the liver. ECM is important in the regulation and modulation of hepatic function in both normal and diseased state (15,16). Being at the interface between the blood flow and the parenchyma, any changes in ECM, whether quantitative, topographic, or qualitative, have a direct effect on liver functions. ECM which forms 5 to 10% of the liver by weight, is mostly collagen (mainly types I, III, and V around the portal tract and central vein and IV along the sinusoid wall). The ECM has numerous other components including matrix metalloproteinases; the glycoproteins laminin, fibronectin, vitronectin, undulin, nidogen (entactin); and proteoglycans such heparan sulfate (15,17,18). Though the major function of ECM is mechanical support and resistance of the liver, by virtue of its ability to trap and store secreted soluble factors, it also has a role in major biological functions such as cell proliferation, migration, differentiation, and gene expression.

1.2. Local environment determines cellular function and survival:

Understanding the complex effect that local environmental parameters, (surrounding cells, matrix and local microcirculation) have on the survival and functionality of hepatic cells is extremely relevant to any attempt at establishing a fully functional culture of liver cells, whether for experimental studies or with the aim of creating a bio-artificial liver. In an *in vivo* milieu, owing to the close spatial configuration of cells and matrix, the phenotype and survival of each of the cell types in the liver is influenced by the environment, either by paracrine effects of secreted soluble factors, or by direct cell

matrix and cell-cell interactions, and mechanico-chemical stimuli brought about by local perfusion flow (Fig 3).

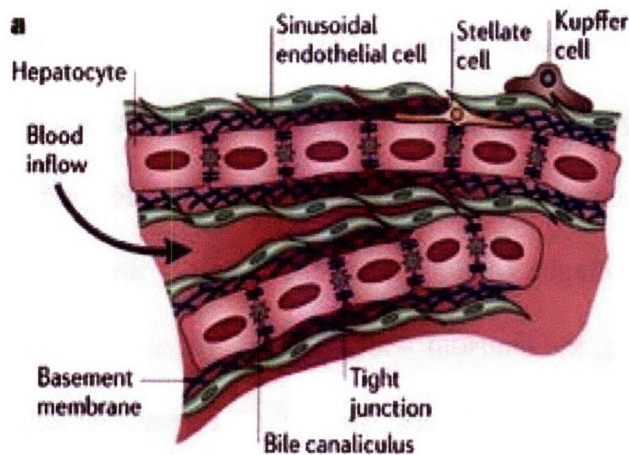


Fig 3. Schematic of microenvironment of liver showing spatial arrangement of cell types allowing both chemical as well as mechanical cues from each other and extra-cellular matrix facilitated by the flow through of blood. [Figure from Griffith and Schwartz, 2006 (19)].

1.2.1. Paracrine Interdependence:

The paracrine effects of the different NPCs and hepatocytes in supporting each others growth, survival and function has been the focus of research for a while. However, one has to bear in mind that it is very difficult and almost impossible to view the effect of one cell type, cytokine or parameter in isolation, since the interaction is always more complex and multi-factorial. Furthermore, most studies examining these effects, are done in an *in vitro* setting which in itself can impart very different properties to all the kinds of cells being studied making their interaction harder to correlate with an *in vivo* setting. Reductive isolated cell experiments can perturb the intimate relationships on which paracrine influences depend and purity of the isolated cell population is always suspect, resulting in activation of the cells before they can be studied. Lastly, in most cases the key mediators of growth are often produced by more than one cell population.

Both *in vitro* experiments as well as liver regeneration studies show that NPCs influence hepatocyte growth and survival either positively and/or negatively through the effect one or multiple secreted cytokines (Fig 4.).

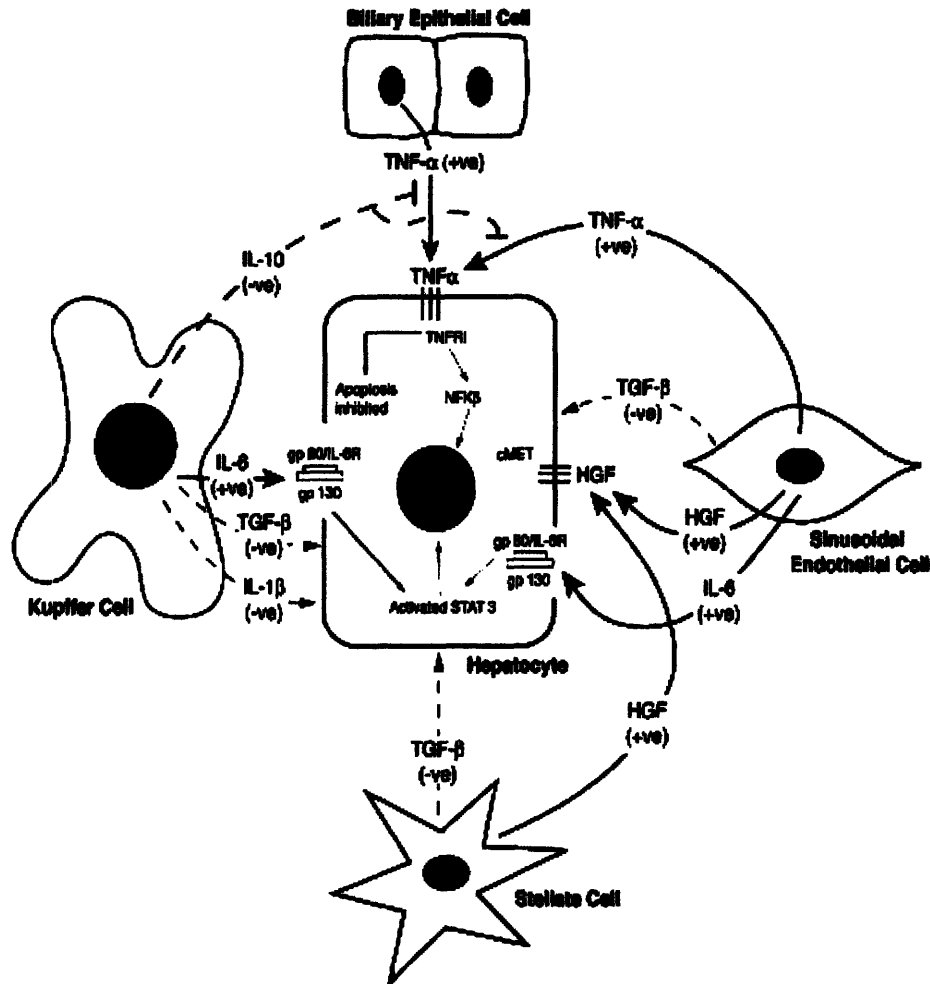


Fig 4. Hepatocyte Growth Factor (HGF) secreted by stellate and sinusoidal endothelial cells is the major mitogen for hepatocyte growth and proliferation (others being interleukin-6 and tumor necrosis factor – α) while transforming growth factor beta ($TGF-\beta$) secreted by all the cell types except the biliary cells is inhibitory. [From Malik et al 2002 (13)]

Kupffer cells release both pro-proliferative (e.g. $TNF-\alpha$, $IL-6$) and anti-proliferative ($IL-1$, $TGF-\beta$) cytokines (20-23) but there is rapid and phasic change in the production of

these after a stimulus such as partial hepatectomy. Hepatocyte Growth Factor (HGF), a very strong mitogen for hepatocytes and is synthesized by quiescent HSCs (24). HGF is stored within the extracellular matrix and early after a partial hepatectomy, there is release of pre-formed HGF from the matrix, and cleavage of the active form from pre-pro-HGF, mediated by plasminogen activator. Studies using co-cultures of hepatocytes with sinusoidal endothelial cells (25,26) demonstrated that these cell types support long term hepatocyte functional activity. Studies using hepatocyte co-cultures with endothelial cell lines (27) show that hepatocytes can migrate towards endothelial vascular structures in response to HGF secreted by endothelial cells and form sinusoid like structures. The stability of these structures is further augmented and preserved by addition of supportive fibroblasts. The inhibitory cytokine, transforming growth factor beta (TGF- β) can also be secreted from sinusoidal endothelial, stellate and Kupffer cells and is responsible for the arrest of hepatic proliferation after hepatectomy.

The survival of sinusoidal endothelial cells which are notoriously hard to cultivate *in vitro* has been prolonged by the use of hepatocyte co-cultures (28,29). The beneficial effects of hepatocytes on their growth are attributed to the secretion of factors such as vascular endothelial growth factor (VEGF) and platelet derived growth factor (PDGF), which are instrumental for their functioning. VEGF and angiopoietin produced by hepatocytes are also believed to play a role in endothelial cell proliferation post-hepatectomy (30-32) Along with survival, in the case of a differentiated functional cell like the sinusoidal endothelium, it is important to preserve the phenotype. Studies implanting fetal liver fragments into quail chorioallantoid membrane resulted in the acquisition of a sinusoidal phenotype by the chorioallantoid microvessels (33)

demonstrating the effect of hepatocytes in maintenance of the specific sinusoidal endothelial phenotype. Another recent study demonstrated that the paracrine effect of hepatocytes and stellate cells in preserving sinusoidal endothelial cell phenotype was mediated by VEGF (34). Transforming growth factor beta TGF- β (secreted by all the cell types) is known to change the phenotype and have a 'capillarizing' effect by stimulating the synthesis of basement membrane proteins laminin, collagen type IV and entactin in rat liver sinusoidal endothelial cells (35) .

In stellate cells, while the role of paracrine influence of surrounding cells like hepatocytes, sinusoidal endothelial cells and especially Kupffer cells in supporting survival is important, of greater consequence is their role in stellate cell activation. Conversion of quiescent stellate cells to activated proliferative, fibrogenic, and contractile myofibroblasts is seen in diseased and inflammatory states, and results in a self-perpetuating flare up of cytokines and subsequent fibrosis. Stellate cell activation is a programmed response consisting of two stages. An early initiation or preinflammatory stage mainly results from paracrine stimulation caused by effects of liver injury on the homeostasis of neighboring cells and from changes in ECM composition. The subsequent perpetuation stage consists of cellular events amplifying the activated phenotype and results from autocrine and paracrine stimulation, as well as from accelerated ECM remodeling. While insulin-like growth factor I (IGF-I) and VEGF are mainly secreted from hepatocytes, fibroblast growth factor (FGF), TGF- β 1, platelet-derived growth factor (PDGF) and endothelin-1, secreted from endothelial cells can stimulate transcription factors such as Sp1, c-myb, nuclear factor kB (NF-kB), c-jun/AP1, STAT-1, and SMAD proteins that regulate gene expression (36). Kupffer cells and sinusoidal endothelial cells

secrete IL-6 which can induce proliferation, but IL-6 stimulation can also occur via an autocrine mechanism (13). The paracrine effects of microenvironment on activation of stellate cells are summarized in Table 1.

Cytokine	Cellular Source	Main Effect
TGF-B	Kupffer cells, Endothelial cells, Lymphocytes, Platelets	Extracellular matrix production, contractility
PDGF	Kupffer cells, Endothelial cells	Proliferation
VEGF	Endothelial cells, Hepatocytes	Proliferation
IL-6	Kupffer cells, Endothelial cells	Matrix production
IGF -1	Endothelial cells, Hepatocytes	Proliferation
bFGF	Kupffer cells, Endothelial cells	Proliferation
Endothelins	Kupffer cells, Endothelial cells	Contractility

Table 1. Some of the main cytokines involved in stellate cell activation.

Some of these soluble growth factors and cytoines like transforming growth factor-beta (TGF- β), vascular-endothelial-cell growth factor (VEGF) and hepatocyte growth factor (HGF) are bound by the ECM, greatly slowing their diffusion and modulating their local concentrations and gradients (37). Alternatively binding with ECM can create locally higher concentrations of autocrine growth factors, allowing smaller amounts of the factor to signal more effectively (38).

1.2.2. Direct Cell- Matrix And Cell- Cell Signaling Effects.

Apart from the effects mediated by soluble factors, the architecture of the liver creates close physical proximity between the different cells and matrix, and gives rise to direct interactions between them. Some of these interactions are believed to affect their survival and phenotype through integrin and cadherin mediated signaling.

In isolated hepatocytes integrin activation by extracellular matrix is known to contribute to inhibition of apoptosis (39,40). These studies showed that embedding of hepatocytes within their normal liver ECM surroundings maintains their survival. When detached from their natural surrounding, hepatocytes enter into apoptosis, unless treated with anti- β 1-integrin antibodies or synthetic RGD (arginine–glycine–aspartate)- peptides. Similar studies looking at sinusoidal endothelial cell survival have also shown that adhesion molecules linking endothelial cells to each other or to perisinusoidal matrix plate play an important role in cell viability (41,42). Others have shown that a detached endothelial cell, with its integrin receptors free, irreversibly enters an apoptotic process, while an endothelial cell in suspension, but with its integrin receptors blocked by RGD peptides may survive (43). Normal sinusoidal endothelial cells are known to express a distinctive set of cell-adhesion molecules (different from other endothelial cells), adapted to their structural and microenvironmental characteristics. When the extracellular matrix changes during liver cirrhosis leading to sinusoidal capillarization (deposition of ECM and formation of a continuous basement membrane), this repertory is dramatically modified, possibly as a consequence of the concomitant matrix changes (44). Additionally it has been seen that in hepatic fibrosis, the number of fenestrations on sinusoidal endothelial cells (reflective of their effective functionality) decreases corresponding to an increase in

interstitial collagen in the liver (8). This change correlates with deposition of extracellular matrix in the space of Disse. *In vitro* experiments (45) have validated this finding by demonstrating that maintenance of endothelial fenestrations requires a complex matrix made of physiologically derived basement membrane (collagen types IV and V and laminin) as opposed to interstitial collagen matrix (types I and III).

Adhesion to extracellular matrix is known to induce tyrosine phosphorylation of focal adhesion kinase, and promote actin stress fiber formation and focal adhesion assembly in stellate cells leading to an activated state(46). These events have been shown to be inhibited by soluble RGD peptides. Stellate cells are also notorious for the alteration of ECM subsequent to their activation (47) giving rise to the fibrotic changes seen in cirrhosis. However it is also suggested that an initiating event in their activation can arise as a result of modification of the surrounding ECM such as de novo synthesis of a spliced variant of cellular fibronectin (48).

The idea of direct cell-cell interactions promoting survival was suggested and subsequently demonstrated by reports that hepatocytes maintain their differentiated phenotypes by forming spheroids or multi-layer cell aggregates, which require cell-cell interactions mediated by E-cadherin, an intercellular adhesion molecule known to regulate hepatocyte cell functions (41,49). While similar spheroid studies have not been carried out with sinusoidal endothelial cells, there are reports that endothelial cells that apoptose in suspension even in the presence of survival factors such as VEGF and FGF-2, survive when allowed to establish cell-cell contacts in three-dimensional spheroid models (50) .

1.2.3. Effects of local circulation on cell phenotype

A vital component of the hepatic microenvironment is the circulation. Blood flow not only provides nutrients and oxygen to the cells, but is also responsible for transfer of other soluble substances like hormones and cytokines and removal of toxic metabolites produced by the hepatocytes. Flow through the tissue additionally provides stimuli in the form of shear stresses that can potentially affect cellular signaling and phenotype.

Unidirectional sinusoidal blood flow along the metabolic hepatocytes from the portal triad to the central vein causes a gradient in all the soluble factors as they get utilized by the cells, dividing the lobule different zones, a phenomenon called zonation (Fig 5).

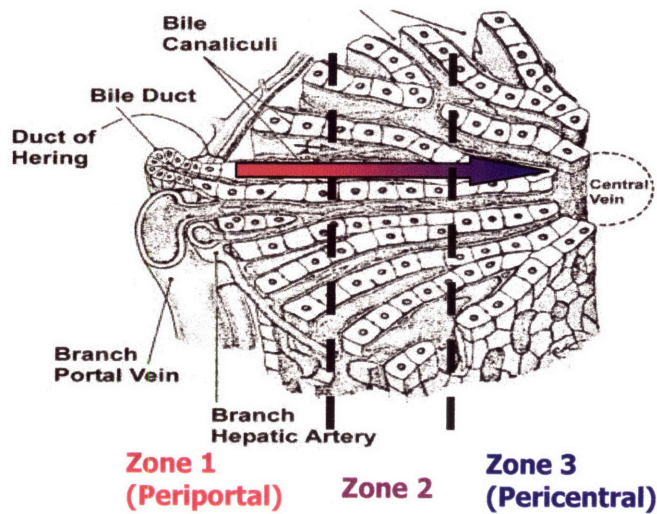


Fig 5. Zonation of the hepatic lobule arising due to oxygen gradient as blood flows from portal triad to central vein. [Adapted from Bloom and Fawcett 1968 (5)]

The periportal region receiving blood directly from the hepatic artery is oxygen rich whereas the pericentral zone is relatively hypoxic. The gradients in oxygen, nutrients, hormones and soluble factors has effects on the phenotype and metabolic functions of hepatocytes (51-53). Certain metabolic processes such as fatty acid oxidation, gluconeogenesis, cholesterol synthesis and ureagenesis and bile acid production are much higher in the periportal zone whereas glycolysis and lipogenesis are more common in the

perivenous zone. Of the drug metabolism processes, glutathione peroxidation is more common in the periportal region while glutathione conjugation and glucuronidation are common in the perivenous zone.

The effects of zonation and the resulting oxygen gradient are not only limited to hepatocyte function. Sinusoidal endothelial cells also show differences in phenotype across the zones with larger number of fenestrations and greater porosity noted in the hypoxic pericentral zone (54). Studies in the porcine liver (55) demonstrate a heterogeneity in the morphology of stellate cells between the pericentral zones (more dendritic with longer processes) and periportal regions (more desmin staining and Vitamin A storage). In the case of Kupffer cells, a higher phagocytic and lysosomal enzyme activity with increased oxygen radical production is noted in the periportal zone, probably related to its status as the port of entry for antigens presenting in the liver (56).

Apart from zonation, the hepatic circulation is also different from other tissues due to the unique circulation pattern resulting from the dual inflow from the portal vein and hepatic artery into the sinusoids. The physiological flow of blood through the tissue exposes it to shear stresses that are known to modulate the activity of some of the cell types. Experimental studies where sinusoidal endothelial cells were subjected to physiological shear stresses demonstrated an upregulation of various receptors such as VEGFR-1 and VEGFR-2 (57). Stellate cells have long since been known to regulate sinusoidal microcirculation pressure but a recent study shows that shear stress by the sinusoidal stretching effect of increased blood flow can induce increased TGF- β formation in these cells (58).

1.3. Challenges of *in vitro* liver culture

Growing any heterotypic cellular system *in vitro* is challenging on account of the inability to accurately recreate the multiple complex interactive components of *in vitro* tissue dynamics outside the physiological system. This is especially true in the case of attempts to create and maintain functional hepatic tissue *in vitro*, due to altered responses of each of the various cell types in an environment lacking all the components and stimuli provided by *in vivo* tissue. While a lot of literature and research efforts are directed at retaining the differentiated status of hepatocytes in cultures, what is equally important in any 'complete' *in vitro* hepatic model is balancing the survival, functioning and phenotypes of the non-parenchymal cell types.

1.3.1. Preserving sinusoidal endothelial survival and phenotype

Sinusoidal endothelial cells are particularly difficult to cultivate in cultures. Not only are they relatively cumbersome to isolate with high purity, they also have a low plating efficiency (28). After plating, these cells rapidly develop vacuoles (Fig 6A) starting as early as 8 hours of culture, leading to the formation of foamy cells after 3 days of culture(59). Sinusoidal endothelial cells have a phenotype that is different from other endothelial cells due to the presence of fenestrations, loose gap junctions and a sparse basement membrane. The functionality of these cells (endocytosis and filtration) goes hand in hand with the retention of their differentiated phenotype. Apart from the difficulty in having these cells survive in culture, it is even harder to retain their phenotype. Over a period of time they rapidly lose their phenotypic characteristics like fenestrations (Fig 6B) and are known to undergo apoptosis in the absence of vascular endothelial growth factor (VEGF) in the growth medium (60).

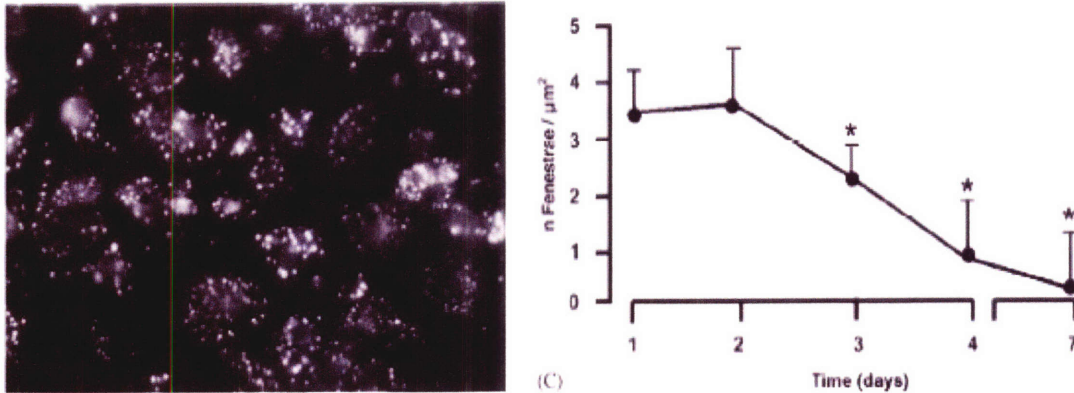


Fig 6. Rapid de-differentiation of rat sinusoidal endothelial cells *in vitro*

(A). Rat liver sinusoidal endothelial cells *in vitro*. after 8 h culture incubated for 1 hr with FITC-labeled collagen demonstrating perinuclear vacuolization [Smedsrød et al. 1985 (59)]

(B) Influence of the culture time on the number of fenestrae per micrometer squared. [DeZanger et al., 1997 (61)]

The markers used to stain functional sinusoidal endothelium are also different from regular vascular endothelium since these cells do not express the standard markers like platelet endothelial cell adhesion molecule (PECAM 1 or CD 31), CD34 and E-selectin *in vivo* (44). In fact, surface expression of CD31 on sinusoidal endothelial cells is considered to be a marker reflecting a de-differentiated state (34). Appearance of CD31 staining on cell surface is associated with the disappearance of another important functional characteristic - fenestrations. Methods that employ anti-CD31 antibodies as a means of purifying endothelial cell fractions during isolation end up with a cell population characterized by absence of fenestrations (62). Very few functional markers are known to be specific to sinusoidal endothelium, and in the rat, SE-1 is one such marker (63). *In vitro* studies looking at survival and functionality of rat sinusoidal endothelial cells in *in vitro* look for either presence of fenestrations or SE-1 expression.

The changes that occur in SECS in *in vitro* culture over time to produce a vascular phenotype with loss of fenestration and formation of an organized basement membrane are referred to as capillarization. Approaches to improve the survival of SEC while retaining their differentiated state have included addition of glycine, dexamethasone, heparin, and insulin to the growth medium (64-66). Some have used serum-containing medium supplemented with either tumor cell-conditioned media (67), phorbol ester (60) or vascular endothelial growth factor (VEGF) (68). While VEGF seems to be a frequently used factor required for extending the survival and proliferation *in vitro* (66,69), most studies also use serum while cultivating sinusoidal endothelial cells. Commercially available standard endothelial growth medium also contains added growth factors such as fibroblast growth factor, insulin like growth factor etc.

Interestingly, in a study where liver extracts were transplanted in chorioallantoic membrane (which contains capillary type microvasculature), proximity to liver tissue was found to induce the SEC phenotype in the proliferating vessels indicating the role of hepatocytes in maintenance of the characteristic phenotypic features (33). In another *in vitro* study where co-cultures of SECs with other liver cells were set up, a more stable endothelial phenotype and function was noted (29). In instances where endothelial survival has been attempted in serum-free medium (28), hepatocyte-conditioned medium was used to provide the necessary growth factors, and noted to improve the survival in culture till 5-6 days. This was attributed to a paracrine relationship between hepatocytes and sinusoidal endothelial cells, with hepatocyte-made VEGF and hepatocyte growth factor (HGF) from sinusoidal endothelial cells being reciprocally beneficial for both the

cell types. However survival of endothelial cells occurred with concomitant overgrowth of stellate cells (probably induced by some of the same factors).

A recent paper (70) using pig liver sinusoidal endothelial cells with various different media and growth factors added, reports a much longer survival time (about 30 days). However, even in their cultures, there is a loss of fenestrations by the 4th day and their chosen indicator of functionality, endocytic activity of the cells sharply declined after the 8th day. So, regardless of the medium composition and culture system, existing *in vitro* methods for survival of sinusoidal endothelial cells fail to retain functionally active cells over a long period, and there is a need to develop systems that would support their survival.

1.3.2. Controlling overproliferation and activation of stellate cells

Unlike sinusoidal endothelial cells, stellate cells are fairly resistant and tend to dominate older *in vitro* cultures. Apart from proliferating *in vitro*, they also undergo the process of activation, similar to the phenomenon seen *in vivo* in diseased and cirrhotic conditions. In co-cultures containing hepatocytes, endothelial cells or Kupffer cells, not only do the cytokines listed earlier in table 1 easily activate stellate cells, substrate and medium are also known to play a major role in the process. Properties of the substrate such as rigidity and presence of extracellular matrix can affect the phenotype of stellate cells. Various studies show that stellate cells maintained on uncoated plastic, and plastic coated with collagen proliferate rapidly and produce abundant amounts of type I collagen (reflective of an activated state) as compared to when they are grown on a thick layer of matrigel (71-73).

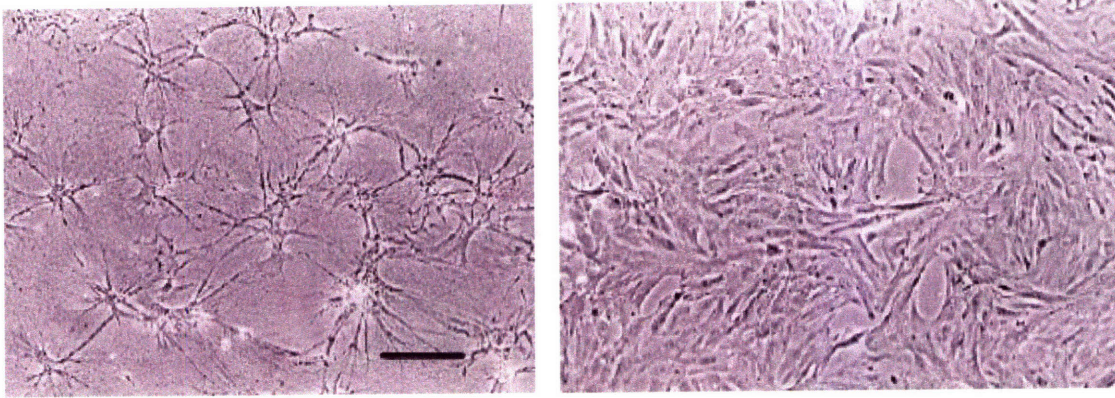


Fig 7. (A) Branched morphology of stellate cells that appear quiescent on a soft thick layer of matrigel. (B) Proliferation and activation of stellate cells on rigid substrates along with fibroblastic transformation [Senoo 1996 (74)]

Rigidity of the substrate is believed to exert its activating effect in part by shear caused by the mechanical stretching of the cells and stimulation of TGF- β (58). Another important component in *in vitro* cultures that can activate stellate cells is the composition of the medium. Most growth media used to cultivate hepatic cells contain various individually added growth factors such as EGF, FGF, IGF, VEGF etc, each of which can initiate the process of activation. Alternatively the presence of serum in the medium can serve to activate the cells through any of the numerous uncharacterized growth factors it may contain.

All the components of an *in vitro* heterotypic co-culture system that can potentially cause the proliferation and activation of stellate cells have been summarized in Fig 8.

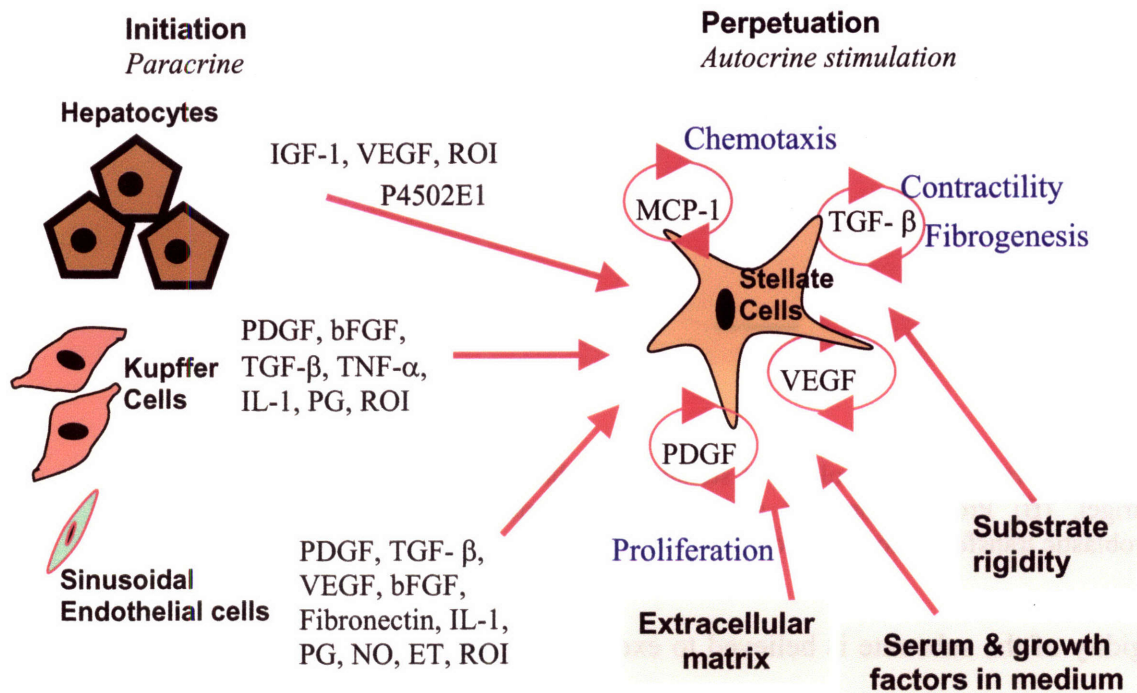


Fig 8. Cellular and culture conditions cause stellate cells to activate and proliferate *in vitro* [Adapted from Friedman 2000 (75)]

1.3.3. Hepatocyte dedifferentiation

A long standing problem in *in vitro* liver studies has been maintaining the functionally differentiated state of the hepatocyte. When isolated and placed in culture, there is a rapid loss of drug-metabolizing enzymes during the first few days along with loss of other phenotypic features – a process known as de-differentiation. Research in the past has focused on rectifying, or at least attempting to minimize this phenomenon. Approaches have ranged from adjusting cell plating density, to altering medium composition to incorporate a range of growth factors and anti-oxidants to changing the substrate rigidity from plastic to surfaces coated with collagen monolayers or softer thicker gels like collagen or matrigel (reviewed in (76)). It had been long noted that configurations that

encourage a three-dimensional arrangement of hepatocytes allowing cell-cell contact (like sandwiching between two layers of collagen gel and culturing on matrigel) better preserve phenotype. Subsequent studies focused on setting up hepatocytes in three dimensional cultures with or without other cell types (which progressed from initial spheroids to seeding tissue into three dimensional scaffolds) and have been found to be effective in retaining a differentiated status. (77-80).

1.4. Evolving Trends in *in vitro* liver culture

Over the last couple of decades a lot of effort in tissue engineering has been devoted to recreating functional hepatic tissue *in vitro*. Running in parallel are two aims of this field of research

1. Either achieving successful clinical therapies for replacing human liver
2. Or engineering liver-like tissue that can be used to study hepatic pathophysiology *in vitro* and even test new drugs.

While both tracks have different goals, the underlying principles and ground rules guiding them are the same. Both face the challenges of retaining functionality coupled with viability of each of the cell types, as well as balancing their numbers in order to generate a tissue that behaves as close to it should in a physiological setting. Cell-based *in vitro* models not only need to be organotypic (i.e. recapitulate both the 3-D organization and multicellular complexity of an organ) in order to be accurate, predictive and physiologically relevant, but at the same time be designed to allow systematic experimental intervention. As knowledge in the broader field of tissue engineering grows,

the trends in each of these areas changes while incorporating findings from across the board that go towards creating a more balanced functional system.

1.4.1. From monocultures to co-cultures

Organs are rarely monotypic and usually comprise numerous cell types, matrices and other environmental factors with interwoven autocrine and paracrine interactions. In order to preserve the complex function arising out of these relationships and to study them at a molecular and cellular level, reproduction of a total organ environment has to be attempted in culture models. Tissue engineers across various organ systems are displaying an interest in the broader role of the stroma in regulating normal epithelial cell function (81,82) .

In the case of liver, some of the earlier studies used purified hepatocyte populations for their *in vitro* models. The biggest problem that these faced was poor long term survival and extremely rapid dedifferentiation of the cells in culture with loss of metabolic functionality. An abundance of literature (table 2) over the last few decades has shown the beneficial effects of each of the non-parenchymal cell types in not only extending the survival of hepatocytes, but also maintaining its differentiated state. This interaction has been shown to be reciprocal in enhancing the survival and retention of phenotype of the non-parenchymal cells as well.

Co-culture with hepatocyte	Effect	References
Stellate cells	Growth, Differentiation, Prolonged survival	(83,84)
Endothelial Cells	Differentiated function	(25,26)
Kupffer Cells	Inhibition, Cytotoxicity	(85,86)
Biliary Cell	Differentiated function	(87,88)
Entire NPC fraction	Growth, differentiated function	(89,90)

Table 2. Effects of co-culture on hepatocyte function

1.4.2. From 2-D to 3-D

Across all kinds of tissue research, it is believed that a physiologically relevant model should recognize that organs and tissues function in a 3-D environment (91-95). The spatial constraints imposed by a 3-D environment on cells determines how they perceive and interpret biochemical cues from the surrounding microenvironment (96-100). Additionally it provides another dimension for external mechanical inputs and for cell adhesion, dramatically affecting integrin ligation, cell contraction and associated intracellular signaling (101,102). In a 3-D environment, the surrounding extracellular matrix both not only controls solute diffusion, but also binds many effector proteins, such as growth factors and enzymes, thereby establishing tissue-scale solute concentration gradients, as well as local pericellular gradients. In the liver, the earliest 3-D systems consisted of spheroids either of hepatocytes alone or co-cultured with non-parenchymal cells (103-106). Over time, more complex 3-D setups have been developed across both fields of liver tissue culture (107,108).

1.4.3. Towards facilitated microcirculation

Efforts at ensuring adequate delivery of oxygen to the tissue in the 3-D systems have driven design considerations in bioartificial liver devices to attempt creating fluid flow past the tissue surface. These include membrane-based reactors (in which cells are cultured outside semi-permeable, hollow-fibre membranes), perfusion reactors (in which cells are grown in porous scaffolds and fluid is pumped around them) and stirred-suspension-culture reactors (in which aggregates of cells are kept in suspension) (109-112). The large scale of these devices makes them impractical to use in basic research applications. Perfusing flow through the tissue can overcome the oxygen transport limitation by increasing the amount of oxygen available to cells deep in the tissue and this can be achieved in small setups with the help of microfluidic pumps and valves. These are designed to circulate culture medium through small culture units in the order of a few thousand cells over a period of time (113) and are starting to be applied to 3-D formats (77).

1.5. Special considerations while studying perfused 3-D systems

1.5.1. Determining scales based on predicted tissue requirements:

As with the liver *in vivo*, in a 3-D hepatic tissue unit, concentration gradients can exist for any soluble and diffusible culture-medium component that is consumed or produced by cells — from oxygen to basic nutrients or secreted factors, giving rise to localized heterogeneity in cellular behavior, or certain gradient-dependent cell responses within the tissue unit. In order to achieve a physiologically relevant 3-D microenvironment it is important to know or predict the various cellular requirements and accordingly come up with length scales for design. In the liver, oxygen is an important parameter and is

usually easily depleted due to its relatively low solubility in culture medium. Existing experimental values of cellular utilization are available in literature (114,115) and can be used as the basis for determining the upper bounds of length scales versus diffusion limitations. However one has to take into account certain other factors that can affect distance scales. Oxygen consumption *in vivo* is very heterogeneous across the whole organ due to zonation. At periportal regions where gluconeogenesis occurs, the oxygen consumption is higher than at pericentral regions where glycolysis occurs. Across the organ, oxygen consumption also increases as it metabolizes xenobiotics. In cases of floating spheroids where all the surfaces are exposed to oxygen saturated media, oxygen transport by diffusion can support a cellular mass of greater diameter than when oxygen transport can only occur across one plane – such as tissue packed into a well. Knowing this, we are thus able to define length scales for design.

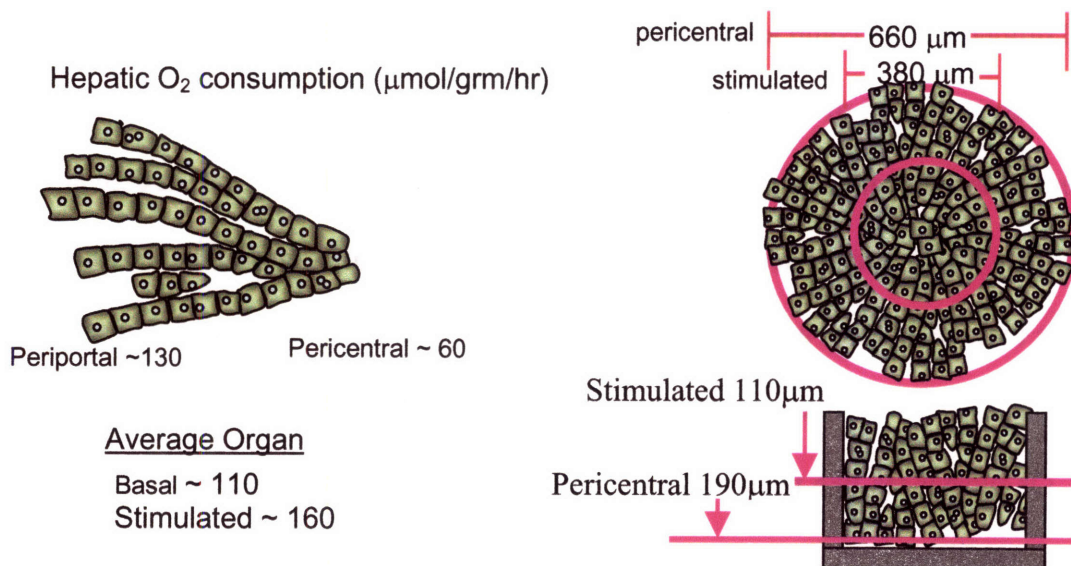


Fig 9. Oxygen Diffusion Limits On Size Of 3-D Cultures [Matsumura & Thurman, Am. J. Physiol, 1983 (116) , Matsumara et al 1992. (117)]

For example (Fig 9), based on known oxygen consumption rates and cell size scales, a spherical mass of tissue at an elevated oxygen consumption rate would need to be smaller than $380\mu\text{m}$ to allow oxygen to diffuse into the center. Likewise a static culture would need to be less than $110\mu\text{m}$ deep to allow for enough oxygen to reach the bottom layer of cells.

One also has to account for the significant oxygen diffusion barrier posed by the height of static unperturbed medium column on the tissue surface. It has been seen that at regular cell densities used in tissue culture, a depth of 2 mm can reduce oxygen availability to as low as 10-20 % of the oxygen concentration at the air-liquid interface (118).

1.5.2. Scaffold material and geometry:

In order to provide support for 3-D organization of cells, many models utilize a scaffold. While choosing a scaffold material, one has to take into account the physical and chemical properties that could affect cellular behavior. For example certain materials may not allow easy adhesion of cells and may need to be coated with substances to facilitate attachment. Mechanical properties such as rigidity of the scaffold can result in activation of certain cell types. Sometimes, the choice of scaffold material is guided by the kind of procedures that the cultures are subjected to after the cultures are harvested. For instance, if the tissue needs to be fixed and sectioned one may prefer polycarbonate to a silicon scaffold. Or substances like peek may be avoided if fluorescent microscopy is intended. Once the scaffold material is chosen, the geometry of the individual channels housing the tissue is calculated, based on earlier described considerations. Based on the material used, channels may be created by etching holes or drilling, and can be used to organize cells in capillary bed sized dimensions (119).

1.5.3. Calculating physiologically appropriate flow rates:

In a system that is perfused, one has to keep in mind the potential effects of shear stresses induced by the flow of culture medium through the tissue. Higher than physiological shear rates such as seen after partial hepatectomy are known to perturb the different cell types, giving rise to a range of cell signaling events and cell growth seen in hepatic regeneration.

Reference flows

Interstitial velocity: $0.1 \sim 5 \mu\text{m/s}$
Microvascular velocity: $100 \sim 300 \mu\text{m/s}$



Fig.10. A ‘high’ flow rate of $1 \mu\text{l/min}$ falls in the realm of microvascular flow rates while a flow rate as ‘low’ as $0.2 \mu\text{l/min}$ is closer to interstitial flow rates though still on the higher side.

We can get a sense of whether the flow rates used in a 3-D *in vitro* system, fall in the realm of physiologically appropriate flow rates, based on known reference values for microvascular and interstitial flow and the surface area of the channels or tissue being perfused. (Fig.10)

1.5.4. Measuring oxygen in live cultures

Various measurements are made in systems to look for temporal effects. However in order to measure oxygen concentrations in the perfused *in vitro* systems, one has to adopt

methods that can do so without placing strain on the oxygen requirements of the live cultures. In other words, not only would an ideal assay be non-toxic to cells in the culture, it should also not utilize oxygen from within the system while measuring it. There are chemiluminescence based assays that operate on the principle of particles getting activated and luminescent in the presence of light and getting quenched by interaction with molecular oxygen. These assays are known not to utilize oxygen in the process and offer a suitable option for making oxygen measurements in live culture systems.

1.5.5. Modeling complex 3-D systems

Mathematical modeling of variables within a system allows us to make prior predictions about the effect changes in certain variables may have on others. In the case of perfused heterotypic culture systems, in addition to simple diffusion gradients of solutes and oxygen, we have the added element of flow that provides a new level of complexity. Finite element modeling methods are effective in such systems and work by dividing them into a complex system of points called nodes that make up a mesh. This mesh is programmed to contain the material and structural properties that define how the system will react to certain conditions as described by selected Partial Differential Equations (PDEs). Several PDEs can be linked or coupled together to arrive at a solution that satisfies all the equations. As the equations are solved iteratively, one has to choose an initial condition and make use of specific software for these finite element studies.

1.5.6. Choice of imaging techniques

Imaging 3-D tissue is a challenging process. Conventional wide field microscopy not only suffers from the physical resolution limits imposed by using visible light as the

illumination source, but also from out-of-focus light degrading the image quality due to specimen thickness. Although electron microscopy offers good resolution, it requires skill in preparing and sectioning specimens and artifacts can often be introduced during specimen preparation. Confocal microscopy and two-photon microscopy are two methods that are very useful for studying the architecture of 3-D tissues but the latter is more cumbersome and time consuming.

In confocal microscopy (Fig 11), a laser is reflected by a dichroic mirror and is focused by the objective lens at the desired "Plane of Focus".

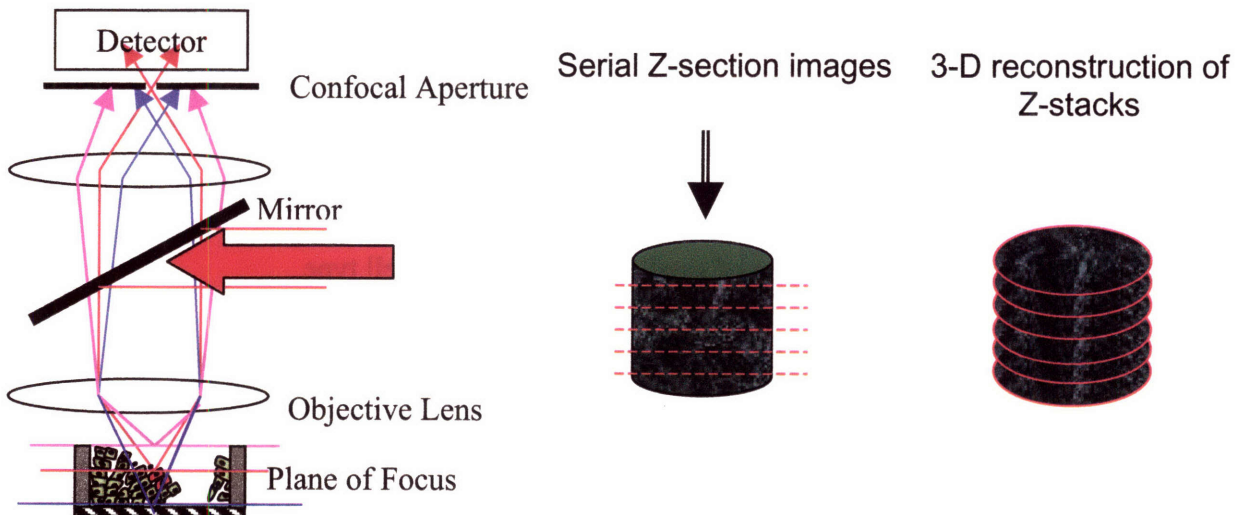


Fig.11. Schematic of principle of confocal microscopy (see text for description) and recreation of 3-D tissue structures from Z-stacks [Adapted from Rigby 1999 (120)].

Fluorescence emitted by the specimen from the point of focus (red rays) and passes back through the lens, mirror and confocal aperture to the detector. Fluorescence emitted from planes above and below the plane of focus (blue and pink lines), are prevented from reaching the detector by the confocal aperture. To collect a two-dimensional (2-D) image,

the laser beam is usually scanned across the specimen in the plane of focus. After each 2-D image is collected, the plane of focus is moved in the Z direction to generate serial 2-D images (Z-sections). These images are then stacked together using appropriate software to reconstruct a 3-D image of the tissue. Since these images are digitalized they can be also analyzed using cell-counting software if needed.

1.5.7. Choice of markers for imaging functional liver cells

As mentioned earlier, demonstrating the behavior of liver cells to be as close to 'in-vivo' is as important as their survival, since the culture environment is known to change the differentiation status. Hence while visualizing such systems, we need an adequate battery of markers that reflect their existence in a specific functional state (differentiated or de-differentiated in case of hepatocytes and sinusoidal endothelial cells, and quiescent or activated in the case of stellate cells). These markers have to be adequately specific, and yet sensitive enough for detection of small numbers of each cell type.

For sinusoidal endothelium, using conventional endothelial markers may not work, since they do not consistently express a lot of the classical markers such as platelet endothelial cell adhesion molecule (PECAM 1 or CD 31), CD34 and E-selectin on their surface. The monoclonal antibody, SE-1, is known to specifically recognize and exclusively react with a 45 kD (M.W.) antigen expressed only in rat liver SEC and in no other type of endothelial cell (63,121). In the in-vivo rat liver, SEC associated directly with hepatocytes (without basal lamina) express SE-1 antigen, whereas no SE-1 antigen expression is seen in endothelial cells of the hepatic vein. While its nature and function is not entirely characterized yet, the antigen is considered to be related to the specific function of SEC in adult rat livers. Based on its cellular localization (surface of plasma

membrane and inner surface of pinocytotic vesicles), it is suggested to be a kind of receptor molecule specifically expressed in SEC for that function. Newer markers like stabilin have been developed that stain sinusoidal type of endothelial cells but they additionally stain Kupffer cells and macrophages and hence would not be specific in a hepatic co-culture. Apart from visualization of fenestrations, SE-1 antigen marker is the best choice of marker to demonstrate phenotypic maturation of SEC. Though PECAM or CD31 is present at intercellular junctions on most endothelium, it has been reported that surface expression of PECAM on sinusoidal endothelial cells is a de-differentiation marker(34). Normally expressed intracellularly, its appearance on cell surface of SECs seems to coincide with the disappearance of fenestrations. However it is strongly expressed on any large-vessel endothelium such as those lining the hepatic and central veins in the liver.

Stellate cells present a different kind of problem since they are extremely hard to retain in an inactivated state *in vitro*. Quiescent stellate cells express a couple of different markers such as desmin, glial fibrillary acidic protein (GFAP), and vimentin that are fairly reliable and predictive markers. In the activated state, they proliferate rapidly and acquire a lot of features of myofibroblasts (which in the liver also originate from other non-stellate cell types), develop stress fibers, over-synthesize basal lamina-like material and collagen fibers, and classically express alpha smooth muscle actin (α -SMA), which is regarded as a standard marker for activated stellate cells. However one has to keep in mind that this is not absolutely specific and can be expressed by myofibroblasts from any other source.

Kupffer cells that serve a macrophagic function in the liver cultures can be identified by macrophage markers ED1 and ED2 (122).

Hepatocytes being extremely metabolic cells, express a host of markers. Among them, albumin and cytokeratin 18 (CK 18) are known to be specific for differentiated hepatocytes.

1.6. 3-D Perfused Organotypic Liver Bioreactor Systems

1.6.1. Perfused bioreactor for *in vivo* like function

An early prototype reactor that integrated 3-D microscale tissue with flow, was developed in our laboratory, taking the earlier described considerations into account [Figure 12A, (78)]. The system consisted of a microfabricated 3-D scaffold with multiple channels that was perfused with a chemically defined serum free medium by an independent peristaltic pumping mechanism. It fostered the formation of 3-D tissue structures from primary rat liver cells or spheroids that were seeded into the channels (Fig. 12B,). Each of the channels within the scaffold held 500–1,000 cells forming a functional tissue unit similar to capillary bed dimensions [Fig 12 C,(19)], and the overall system could be scaled to hold in the range of 10,000–1,250,000 cells, by creating larger scaffolds with different numbers of channels (77,123) . These tissue-like morphological structures (Fig 12 D) formed in the microreactor, maintained liver specific functions like albumin secretion and ureagenesis for at least two weeks (79,80). More importantly, they retained several important liver-enriched genes, including drug-metabolizing enzymes that are usually rapidly lost in culture, at levels much closer to *in vivo* expression and activity than 2-D collagen gel sandwich culture controls (77). Studies that seeded cancer cells into the hepatic tissue mimics of this system showed tumor like outgrowths even in

a serum free medium, demonstrating the potential of the system to be used as a cancer model (Fig 12 E).

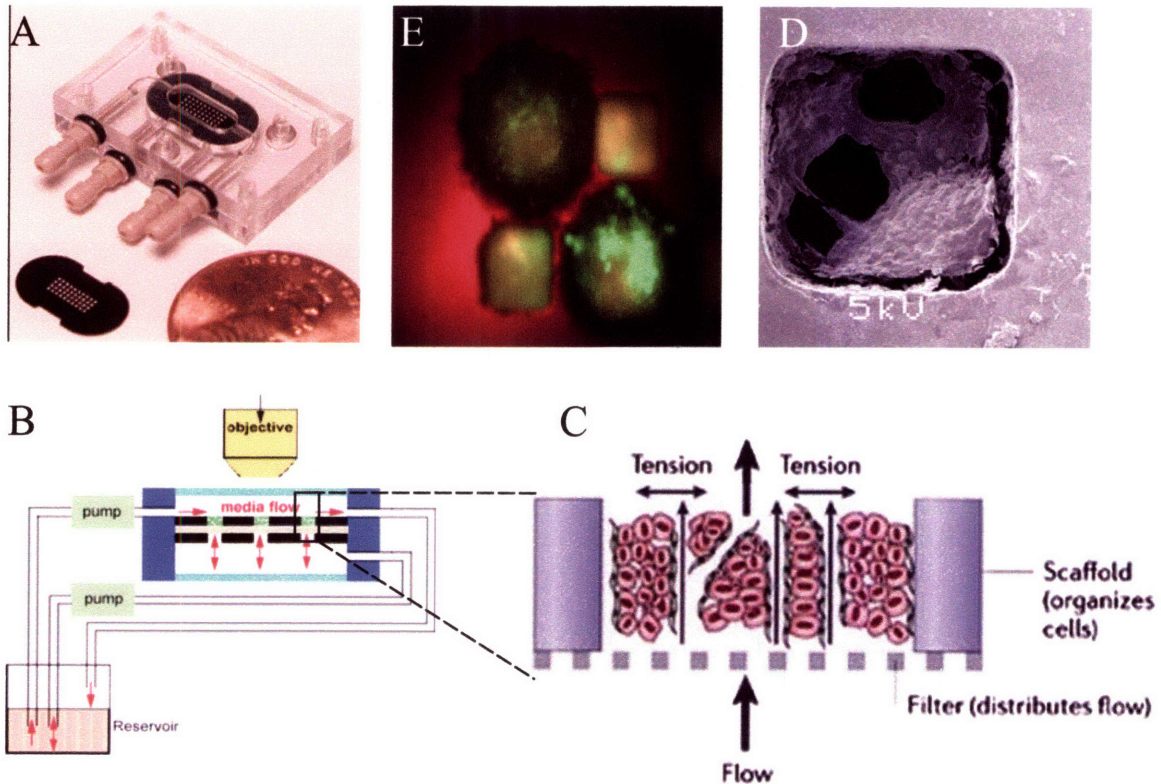


Fig .12.(A) 3-D perfused bioreactor model containing a scaffold with channels encased in a polycarbonate casing. (B) schematic of flow through system (c) Blow up of individual channel with perfused tissue (D) SEM image of tissue mimic from channel (E) DU-145 cells seeded into the liver tissue mimics produce outgrowths.

Though the results with the early prototype 3-D reactor were encouraging, there was room for improvement on a couple of fronts. These reactors were limited by mechanical peristaltic pumps that allowed flow of medium across the tissue, at rates considerably higher than physiological levels that cells are exposed to *in vivo*. As a result, the tissue was exposed to shear stresses that could have possibly have had an impact on non-parenchymal function. Staining data from early prototype reactors set up showed few endothelial cells and a number of activated stellate cells. Furthermore, the seeding

protocol in this model required hepatocyte spheroids to be injected into a closed system. The exact number of spheroids used to pack the channels varied from experiment to experiment making the input into the system variable and hard to quantify. Last but not the least, this system was not high throughput enough to study the effect of more than one variable at a time.

1.6.2. A high throughput system with controlled flow

A newer generation 3-D perfused reactor developed in the Griffith laboratory [Fig. 13 (124,125)] addresses most of the above-described issues. It keeps the same basic design features, but is scaled up to a multi-well format, allowing for up to $\sim 10^6$ cells per each reactor (well) in the system. Channels have a diameter of $300\mu\text{m}$ and depth of $230\mu\text{m}$ and contain tissue in the size scale of a capillary bed. There are several hundred such channels in each scaffold. Perfused flow enters the bottom of the scaffold through a $5\mu\text{m}$ filter, which distributes the flow evenly and is given mechanical rigidity by a support plate. Each reactor is coupled with a reservoir and flow of medium between the two is through micro-fluidic channels and controlled by pneumatic pumps. The overall format is of a 24 well plate (with 12 pairs of reactor-reservoir combinations) allowing for easy integration with existing technologies. The easier multi-well set-up not only allows direct seeding into the channels with a pipette tip, thereby giving better control over the input into the system, but also allows *in situ* observation of cells by optical imaging. Additionally it allows us to easily perturb functions and measure the associated response. The pneumatic pumping system in this case is different from the earlier mechanical pumps, and allows flow rates to be reduced by more than an order of magnitude expanding the regime of flow rates to interstitial regime. Most importantly, the multi-well

format allows easy comparison of different parameters such as flow rate or medium composition in the same experimental setup, thereby minimizing animal to animal or instrument variation between compared groups.

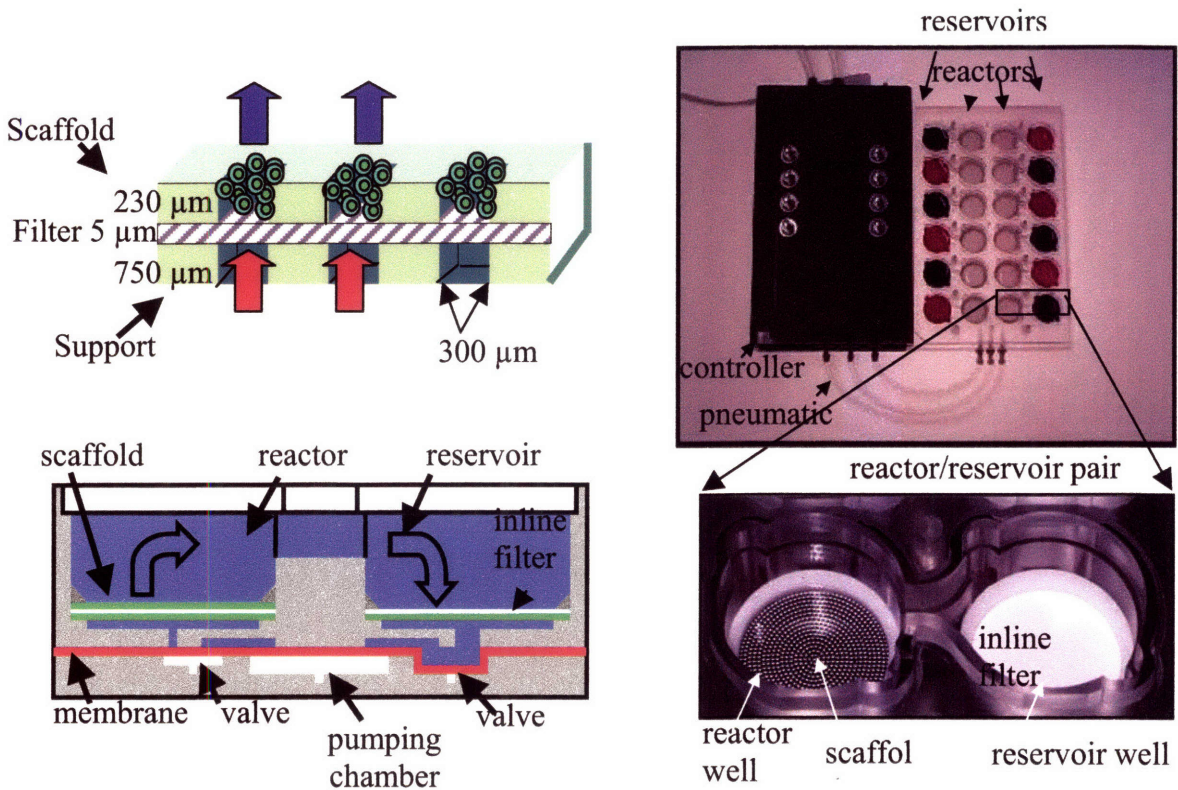


Fig 13. Multiwell 3-D perfused bioreactor. (A) 3-D perfused microenvironment is formed in each channel (B). A flow loop from reactor to reservoir maintained by a novel pneumatic pumping system enables the re-oxygenation of media (C) The system contains 12 pairs of reactor-reservoir units, housed in a (D) conventional 24 well plate format

1.7. Hypothesis and Specific Objectives

The working hypotheses guiding this thesis were that:

- Survival of differentiated sinusoidal endothelial cells may be achieved by recreating a three dimensional co-culture environment that recapitulates the necessary paracrine interactions.
- Control of microscale flows and oxygen concentrations in the perfused 3-D coculture system of hepatocytes and non parenchymal cells, would influence the survival and proliferation of sinusoidal endothelial cells, Kupffer cells, and stellate cells.

Based on this hypothesis the specific aims of this thesis were to:

- Create a 3-D co-culture environment that captures appropriate paracrine cell interactions and demonstrate that it improves SE-1+ liver endothelial cell survival
- Study the effect of changing flow rates through the 3-D *in vitro* tissue, on SE-1+ cell survival and phenotype.
- Determine whether SE-1+ cell survival and phenotype at different flow rates is regulated by oxygen tension within the paracrine environment.

Explore a potential mechanistic aspect of the effect brought about by flow or oxygen.

Chapter 2:

Characterizing The System And Optimizing Operating Parameters

2.1 Characterizing The Cellular Input Into The System

While studying a heterotypic culture system, it is important to have an accurate idea about the different cellular inputs into the system in order to draw inferences about the effects of variables on individual cell types while assessing the tissue structures formed. For our experiments we used purified hepatocytes and endothelial cells derived from two different animals (one being wild type and the other genetically modified to express a fluorescent protein) so that we could follow their individual fates easily by visual imaging. Since most purification protocols are not absolute, we also employed the use of specific markers that stained each cell type as a tool in our characterization efforts.

2.1.1. Materials and Methods:

2.1.1.1. Animals And Isolation Procedures For Hepatocytes And Endothelial Cells:

All animals used for the experiments were treated according to protocols approved by the MIT Committee of Animal Care. Hepatocytes were isolated from male Fischer rats (150g-250g) by a modification of Seglen's two-step collagenase perfusion procedure (77) using a 25 mL/min flow rate (Details in Appendix 1). An enriched hepatocyte population (~95% purity) was obtained by two sequential 50g centrifugation and washing cycles. The viability of hepatocytes was determined by Trypan blue (Gibco, Carlsbad, CA) exclusion test and was consistently over 85%.

Endothelial cells were isolated from 150-250g female GFP-positive Sprague-Dawley rats by a second perfusion (Details in Appendix 2) using a 15 mL/min flow rate, and a modification of the two-step Percoll density gradient procedure(126). These rats were bred from EGFP-positive males that were a generous gift of M. Okabe (127). After the

collagenase perfusion procedure, supernatants from the 50g spins were subjected to two sequential spins (5 minutes at 100g followed by centrifugation of the supernatant for 7 minutes at 350g). The pellets formed were re-suspended in PBS (Gibco), loaded very gently on top of a two layer Percoll (Sigma-Adrich) density gradient (25% on top of 50%) and centrifuged for 20 minutes at 900g. Endothelial cells which formed a ring at the interface were collected, diluted 1:1 with PBS, and subjected to an additional 10 minutes of 900g spin. The resultant pellet contained non-parenchymal cells highly enriched in liver endothelial cells. The viability and concentration of primary endothelial cells isolations were determined by Hoechst (Molecular Probes) and Sytox Orange (Molecular Probes) staining and were consistently above 90%.

2.1.1.2. Medium Used And Co-Culture Spheroid Preparation:

A serum-free hepatocyte growth medium (HGM) medium described previously (128) was used with the following modifications (125): niacinamide, 0.305 g/l; glucose 2.25g/l; 1 mM L-glutamine; ZnCl₂, 0.0544 mg/l; ZnSO₄·7H₂O, 0.0750mg/l; CuSO₄·5H₂O, 0.020mg/l; MnSO₄, 0.025mg/l; EGF (Collaborative, Bedford, MA), 20 ng/ml; and 0 ng/ml HGF (Detailed constituents listed in Appendix 3). Endothelial Growth Medium (EGM-2 bullet-kit, Cambrex, Walkersville, MD) was mixed with HGM 1:1 (v/v) to create “mixed medium”. Immediately after isolation, 20 million hepatocytes and 40 million endothelial cells were added to 500 ml spinner flasks (Bellco Glass, Vineland, NJ) containing 100 mL of mixed medium, and spun at 85 rpm for 48 hours to produce spheroids of wild type hepatocytes with incorporated GFP positive sinusoidal endothelial cells. Spheroids ranging from 50-300 μm in diameter were selected by

sequential size exclusion filtration (nylon meshes from SEFAR, Depew, NY), and resuspended in mixed medium.

2.1.1.3. Staining And Imaging Endothelial Isolates (Details in Appendix 4):

Characterization of the freshly isolated endothelial cell fractions was done by plating them on collagen-coated (30 mg/mL collagen) sterilized glass cover slips in 24-well plates (300,000 cells per well). Cells were allowed to attach to the cover slips for 4 hours before they were washed in PBS and fixed in 2% paraformaldehyde (EMS) for 20 min. Each cover slip was stained with primary antibodies against SE-1 (IBL America), CD31 (Chemicon), ED2 (Serotec), GFAP (Serotec), or SMA (Sigma) followed by secondary antibody goat-anti-mouse Cy3 (Jackson ImmunoResearch) and Hoechst nuclei stain (Molecular Probes). Fluorescent Microscopy was used to acquire images from two biological replicates and at least 6 images per replicate per group were used to quantify the percentage of SE-1+, CD31+, ED2+, GFAP+ and SMA+ cells. Images were imported into Metamorph (Universal Imaging) for quantitation.

2.1.1.4. Staining And Imaging Spheroids (Details in Appendix 9):

To estimate endothelial presence within the co-culture spheroids, we stained them for the different NPC markers mentioned earlier. After 48 hours, the spheroids were removed from the spinner flasks and selected by size-based exclusion to be in the 50-300 micron range. These were resuspended in PBS and then fixed in 2% paraformaldehyde for 45 min. In order to stain them, we experimented with various embryo-staining protocols before customizing the conditions to suit our protocol. To achieve penetration of the stains into the cells in these three dimensional spheroids, we permeabilized them with 0.1% Triton-X for 30 mins, following which they were washed with PBS and then

blocked with 5% goat serum for an hour. The spheroids were then incubated overnight at 4°C with primary antibodies for the various non-parenchymal cell markers mentioned earlier. Following repeated washes with 2% BSA in PBS, they were incubated with secondary antibody goat-anti-mouse Cy3 and Draq 5 (Alexis) nuclear stain for an hour before washing and placing in chamber slides for Confocal microscopy.

Spinning disc confocal microscopy was done using the McBain spinning-disk confocal with a Nikon TE2000U inverted microscope equipped with a laser from Coherent (Innova 70C). The objectives chosen to were 20x with a working distance of 3 mm. From z-stacks of images, we reconstructed top down view 3-D composite images superimposing all the sections. For each stain, we analyzed at least six different images (with an average of 3-6 spheroids per field). Image acquisition, 3-D reconstruction and quantitative analysis were performed by using Metamorph software (Universal Imaging).

2.1.2. Results:

2.1.2.1. Characterization Of Endothelial Isolates:

Staining for the different non-parenchymal markers followed by fluorescent microscopy showed that most of the cells from the isolated endothelial purified cell fraction, plated and fixed after 4 hours, stained positive for the functional sinusoidal endothelial marker SE-1 (Fig 2.1). Few of the cells stained for the large vessel endothelial marker CD31 (PECAM). The various other non-parenchymal cells were also present in the isolate in low numbers and stained for their respective markers such as ED-2 (for Kupffer cells), GFAP (for quiescent stellate cells) and SMA (for activated stellate cells). These are shown in Fig 2.2 (A-D).

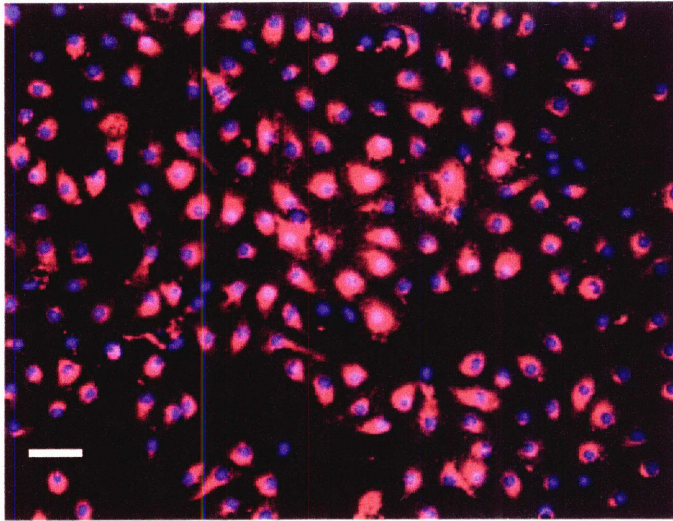


Fig 2.1 (Left) Staining pattern of the freshly isolated endothelial fraction purified by our protocol for endothelial cells shows about 80 % of the cells staining positive for SE-1, a functional marker of sinusoidal endothelial cells. Scale bar 20 μ m

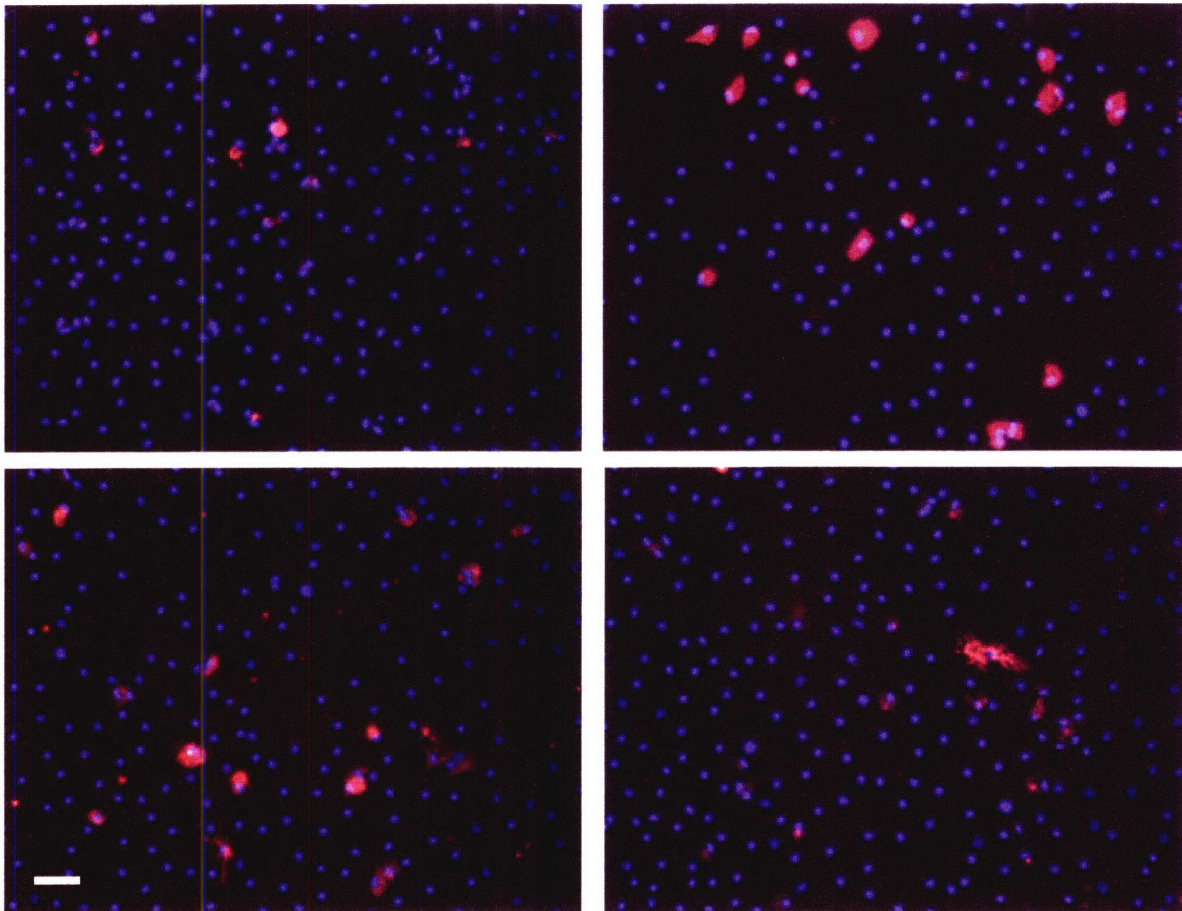


Fig 2.2 Staining pattern of the freshly isolated endothelial fraction purified by our protocol for (A) large vessel endothelial marker CD31 (PECAM) shows few cells. Kupffer cells staining for ED-2 (B), and quiescent stellate cells staining for GFAP (C) are scattered. Very few cells stain for SMA, the marker of activated stellate cells at this point (D). Scale bar 20 μ m

Quantitative analysis of images stained for the non-parenchymal markers, from over 2 biological replicates (at least 6 images per replicate per group), using METAMORPH software, demonstrated a purity of about 80% endothelial (mostly SE-1 + but few CD31+ cells), 10% Kupffer (ED2+), and 10% Stellate cells (including GFAP+ and SMA+). This is represented in the form of a pie chart in Fig 2.3. These results were confirmed separately in our laboratory by other investigators using a combination of staining and flow cytometry (data not shown).

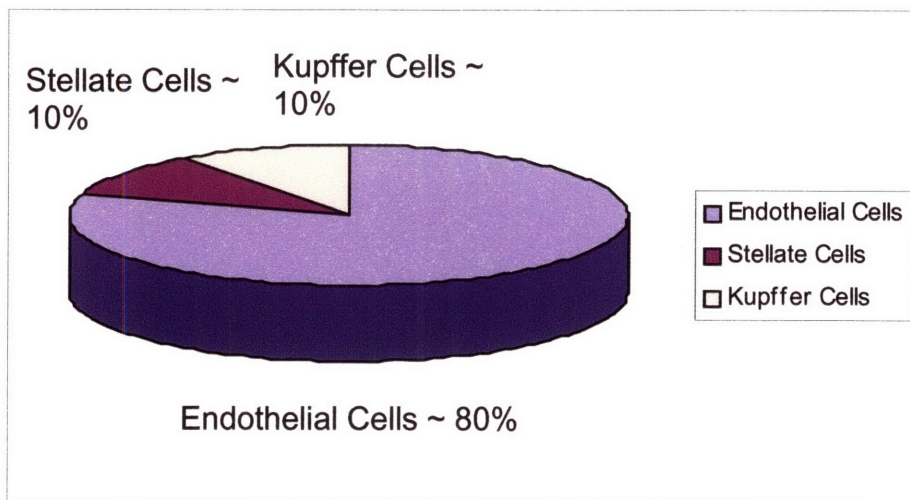


Fig 2.3. Quantification of composition of 'purified endothelial isolate' by two-step Percoll density gradient procedure. We consistently got a yield characterized by about 80% sinusoidal endothelial cells and about 10% each of stellate and Kupffer cells.

2.1.2.2. Characterization Of Spheroids:

Unlike the high numbers of SE-1 positive cells seen in our isolates, staining and confocal imaging of the 48 hour spheroids for the NPC markers showed a much lower incorporation rate (Fig 2.4. A & B). Counting the positively stained cells and expressing them as a fraction of the total number of Hoechst stained nuclei in a spheroid showed SE-1+ cells to be in the range of 15 %. The spheroids also demonstrated a large number of

GFAP and SMA positive activated stellate cells coating the surface (Fig 2.4. C&D). CD 31 expression seemed to follow a similar pattern as the SMA with some cells on the surface of the spheroids expressing it while Kupffer (ED-2+) cells were few and scattered inside the spheroids (data not shown).

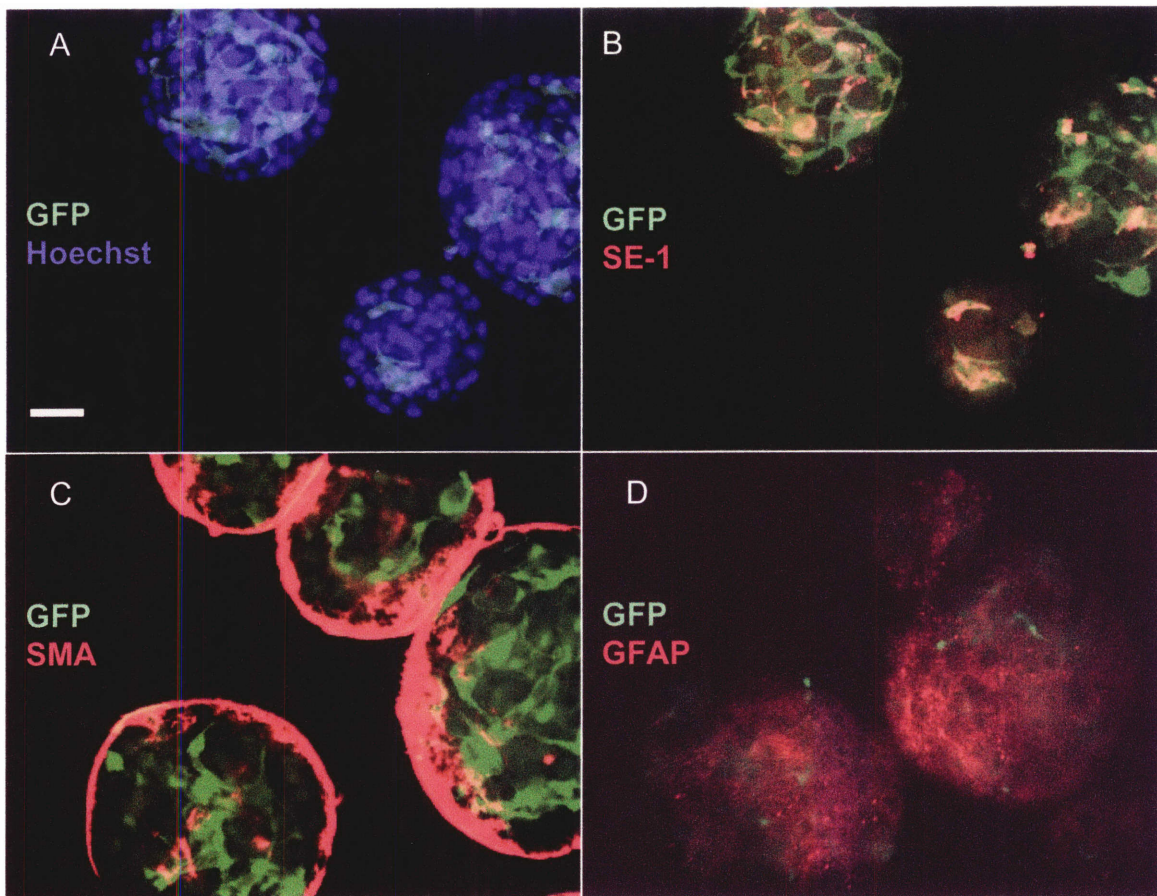


Fig 2.4. Characterizing the NPC incorporation into 48 hour spheroids: (A & B) Sinusoidal endothelial cells - Hoechst and SE-1 staining of same spheroids allowed estimation of incorporation rates of endothelial cells estimated to be about 15 % (C) Activated stellate cells /fibroblasts as evidenced by SMA staining coat the outer surface of the spheroids. (D) GFAP staining confirms these surface fibroblasts to be of stellate origin. Scale bar 20 μ m

2.1.3. Discussion:

Characterizing the cellular composition of our isolate was an important first step not only to judge the efficiency of isolation protocol and have an idea about the input, but also to validate the staining markers that we were subsequently going to use in the study. Our perfusion protocol for the isolation of endothelial cells was not entirely effective in getting a 100% pure population of endothelial cells. There is considerable literature devoted to improving endothelial purity ranging from simple techniques such as selective adherence of Kupffer cells on glass slides to remove them(129), to more complex methods such as elutriation (130) and immunomagnetic bead columns (131). However we chose to stick with our protocol and work with an endothelial isolate with 80% purity because we did not want to eliminate the other cell types entirely, as they contribute to the recreation of an *in vivo* like paracrine environment. A finding of interest was that the endothelial cells in our isolate hardly stained for CD31. The few cells that did could have derived from the larger vessels like the central and hepatic veins during the perfusion, or they may be dedifferentiated sinusoidal endothelium. The scarcity of CD31 staining from the freshly isolated sinusoidal endothelial fraction supports literature that suggests they do not express it in a differentiated state. Another observation to note is that at this stage, stellate cells are mostly non-activated (with few SMA staining cells) in spite of the stress of the perfusion procedure.

Spheroid seeding protocols are used since they select for the most viable cells and are already compacted three-dimensional aggregates of the cells. Though we had already quantified the composition of non-parenchymal cells in our fresh isolates, it was necessary that to characterize their presence in the 48-hour co-culture spheroids, since

they were the actual input being seeded into our reactors. Interestingly the data from our spheroid analysis showed that the actual incorporation of SE-1 cells into the spheroids was much lower (in the range of 15%) than the composition of the isolates. This is possibly due to the fact that hepatocytes aggregate much more effectively into spheroids as compared to the endothelial cells. Liver endothelial cells do not have direct cell-cell contact with hepatocytes *in vivo* and are normally associated with each other through ECM interactions in the Space of Disse. Earlier studies done in our laboratory (Albert's thesis), that used different methods of co-culturing these two cell types in the early prototype reactor, noted an endothelial incorporation rate at least seven times in these co-culture spheroids than spheroids prepared only from hepatocyte fractions. Going forward, one has to bear in mind that in spite of the benefits of spheroid seeding, the technique does handicap us with low starting numbers of endothelial cells.

The other finding of relevance was that fibroblastic cells covered these spheroids. This is consistent with reports in literature (Hong-Fang Lu 2005) about spheroid formation. It has been shown that the fibroblasts contract and envelope the aggregates of hepatocytes in response to substances secreted by them when co-cultures are seeded on certain surfaces. Our experiments showed a similar structure of the spheroids formed by rotation in a spinner flask. Additional factors contributing to the activation in our case could be the presence of serum and growth factors in the medium as well as the shear stress that the spheroids are subjected to during the spinning process. Regardless of the causative factors, the importance of this finding is that it highlights that we are introducing stellate cells into our system in an already activated state.

2.2. Selection Of Operating Conditions

For any new system to be developed, a lot of effort goes into determining the very basic operational parameters for its functioning. While a lot of these are based on the various considerations described in chapter 1, and some are based on computational models, one cannot overlook an iterative process of experimentally testing a lot of variables that have to be established before using the system in any way. Described in this section are results of some of the experimental and computational experiments that determined the working conditions in our reactor system.

2.2.1. Optimizing Working Parameters

2.2.1.1. Overall Design:

To optimize the working parameters, we set up co-cultures as per an experimental layout shown in Fig 2.5. Briefly, spheroids were prepared from hepatocytes obtained from a wild type rat and endothelial cells from a GFP expressing rats. Day 2 spheroids ranging from 50-300 μm in diameter were selected by sequential size exclusion filtration (nylon meshes from SEFAR, Depew, NY), resuspended in mixed medium, and seeded into the channels of the reactor scaffolds. Since the multi-well reactor allowed direct seeding into the reactor channels, the approximate number of spheroids seeded into the scaffolds was controlled to be the same for all the wells. The reactors were followed up for 7 days under different operating conditions described subsequently. Tissue structures formed were examined by phase contrast and fluorescent microscopy (to track the GFP positive endothelial cells) at different time points relevant to the operational conditions and the end of the culture period.

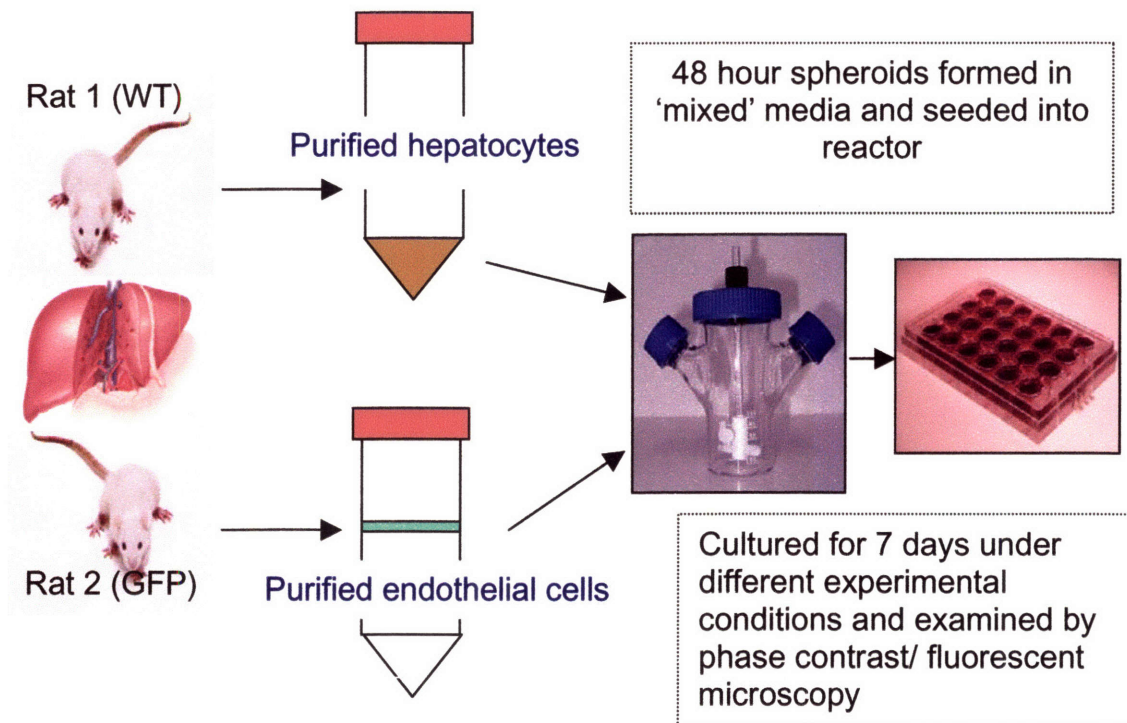


Fig 2.5. Two day co-culture spheroids prepared from wildtype hepatocytes and GFP + endothelial cells isolated from two perfusions were seeded into the scaffolds in the reactor and maintained under different operating conditions.

2.2.1.2. Parameters Tested:

Flow reversal:

In our three-dimensional perfused system, the microfluidic channels were designed to flow medium through the tissue from below upwards. However at the time of seeding and the initial hours following it, we needed to maintain a downward direction of flow in order to pull the spheroids into the channels, and not regurgitate them out. Different flow reversal times were tested, ranging from 2 to 24 hours to test for optimal tissue formation. Phase contrast images were taken post seeding and compared with images taken after reversal of flow for overall tissue distribution patterns.

Scaffold material types:

Though the choice of scaffold material for our experiments was guided by the suitability for specific experimental procedures that we had in mind in each situation, we wanted to test the different scaffold materials being considered such as peek, polycarbonate, and permanox, for their tissue attachment properties. Wells were set up with scaffolds made up of each of the different materials, but with identical geometry (number and layout of channels) under otherwise identical conditions. Fluorescent images from each of these scaffolds seeded with co-culture spheroids were examined every day to look for overall patterns of tissue formation.

Collagen coating of filters:

In an attempt to maximize tissue attachment and retention within the channels, we tried coating the filters underlying the scaffolds with extracellular matrix constituents and looked for tissue formation patterns. Wells having similar scaffolds and other identical operating conditions were set up with filters which were either coated with rat-tail collagen (BD Biosciences concn 30 $\mu\text{g/ml}$) for an hour or uncoated. Overall tissue retention patterns were looked for after reversal of flow by using fluorescent microscopy.

2.2.1.3. Results:

Flow reversal: Of the various flow reversal times tested, it was seen that early reversal times resulted in significant loss of tissue (Fig 2.6. A & B). This was evidenced by the presence of many empty channels in these groups. At 8 hours, the tissue formation and adhesion to scaffolds seemed strong enough and did not seem to be affected much by flow reversal (Fig 2.6. C & D). Increasing the reversal to 24 hours (Fig 2.6. E & F) did not seem to improve tissue retention as compared to the 8 hour time point.

Post Seeding Images

48 hour Images

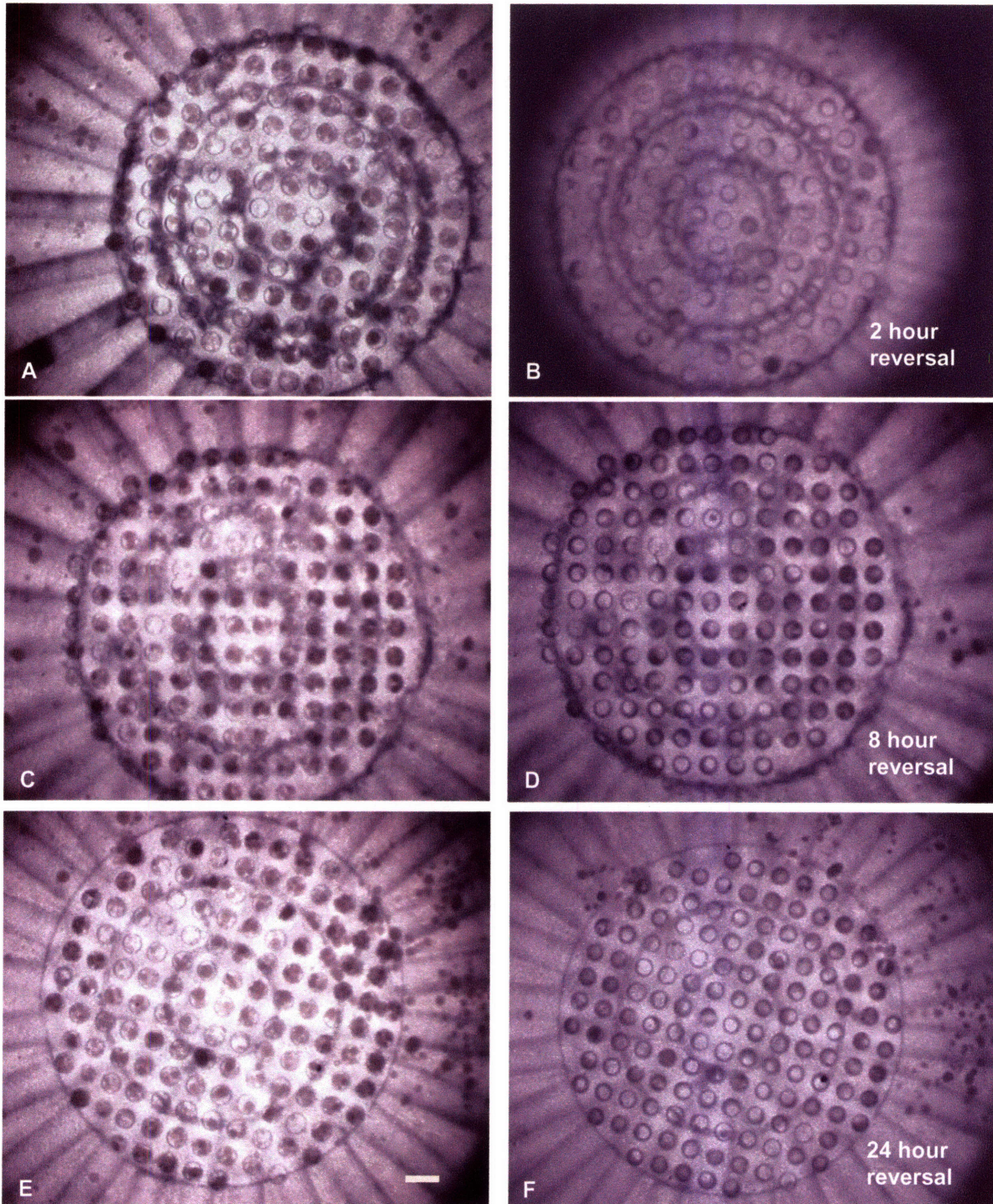


Fig 2.6. Effect of flow reversal time on tissue retention. Early flow reversal at 2 hours (B) causes significant loss of tissue from post seeded state (A). Tissue retention seems optimal with flow reversal at 8 hours with not much difference between post seeded (C) and post reversal state (D). Retention is not improved further by increasing reversal time to 24 hours (E & F). Scale bar 500 μm

Scaffold material:

Using the 8-hour flow reversal, we did not see significant differences in overall tissue formation patterns between the different materials tested. Most of the channels in the scaffolds were uniformly packed with cells from the co-culture spheroids, with the GFP expressing endothelial cells aiding easy visualization. Figs 2.7. A & B show the fluorescent images from permanox and polycarbonate scaffolds.

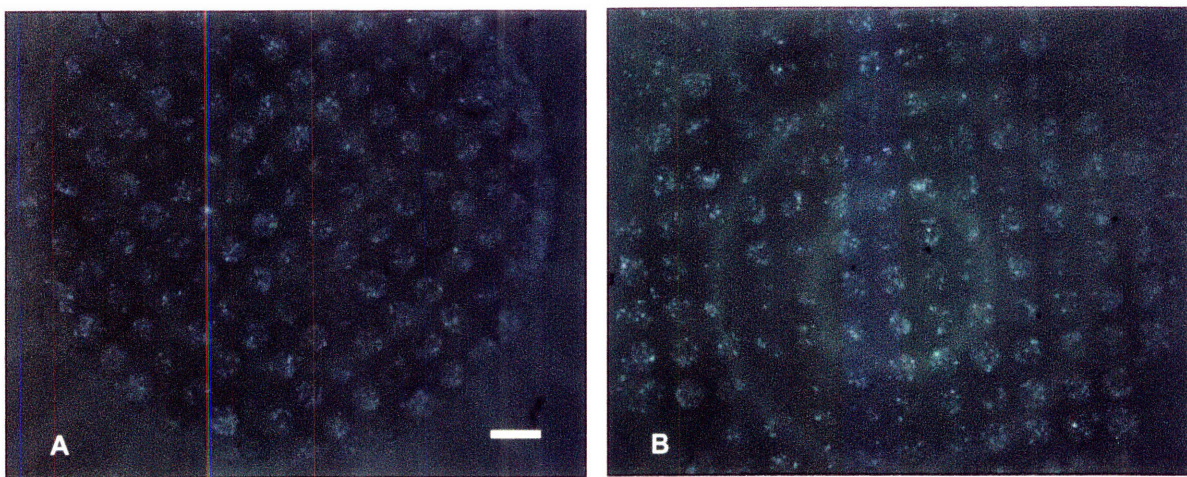


Fig 2.7. Effect of scaffold material on tissue adherence and retention: None of the materials tested showed visible differences. Pictured here are fluorescent images taken at 48 hours of (A) permanox and (B) polycarbonate scaffolds seeded with co-culture spheroids containing GFP positive endothelial cells. Scale bar 500 μm

Collagen coating of filters:

The channels in scaffolds where the underlying filters were coated with collagen seemed to display a better retention of tissue within the channels as compared to uncoated filters (Figs 2.8. A & B). Due to better attachment to the filter, these channels were more prone to loss of tissue during flow reversal in the case of filters that were not coated with collagen and ended up empty.

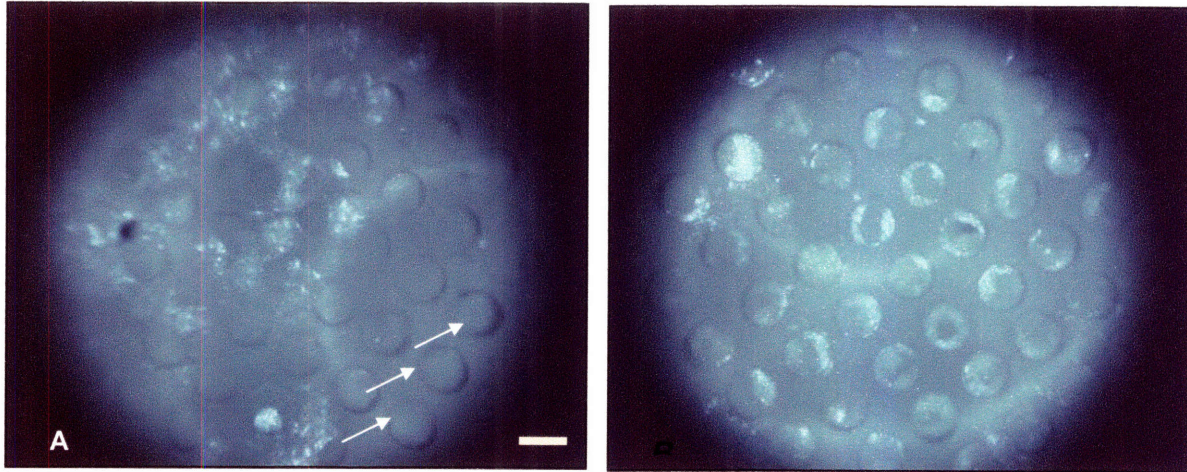


Fig 2.8. Effect of collagen coating of filters on tissue adherence and retention: Collagen coating of the filters seemed to result in better retention of the tissue structures within the channels of the scaffold. Images at 48 hours show that uncoated filters (A) were associated with loss of tissue and empty channels (white arrows) while this loss was minimized by collagen coating (B). Scale bar 300 μm

2.2.1.4. Discussion:

Though downward flow through the channels is necessary for the initial formation of tissue, we need to change flow in the upward direction over the main course of the experiment, since it is more evenly distributed on account of the filter beneath the scaffold. Additionally it serves to remove dead cells and debris from the channels. As very early flow reversal results in some degree of loss of tissue, we needed to figure out the a time point that that was relatively early in the course of our experiment and yet allowed adherence between the cell-cell and cell-scaffold contacts. Based on these results, we picked the 8-hour reversal for our subsequent experiments. Since all the scaffold materials showed similar tissue attachment patterns, the only differences between the scaffolds that were of consequence were physical properties. For instance

peek was associated with increased autofluorescence that made it unsuitable for our experiments since they involved extensive fluorescent imaging. In the case of permanox, it's low density made it float in solutions posing a hindrance during steps such as sterilization with ethanol or coating with collagen. Our approach of maximizing tissue retention in the channels by coating the filters with extracellular matrix components such as collagen seemed to help in decreasing loss of tissue from the channels. This could be on account of cell-matrix interactions between the seeded spheroids and the collagen coating on the filter.

2.2.2 Predicting The Outer Bounds For Operational Flow Rates

Note: Matthew Lim, a visiting post-doctoral researcher in the laboratory of Linda G Griffith, carried out the mathematical modeling presented in this section. Since the data is relevant for the purpose of the further experiments planned in my thesis, I have added it with his kind permission.

2.2.2.1. COMSOL[®] Modeling For Oxygen Utilization Predictions:

COMSOL[®] Multiphysics modeling software was used to determine the outer bounds of operational flow rates we could use in the system, without subjecting the entire tissue to hypoxia. As an initial step, a geometric design representative of our system was created. This design was then meshed, with the fineness of the mesh maximized around corners and the tissue-medium interface. After making certain assumptions about our system, the Navier-Stoke's partial differential equation was used for bulk fluid flow in the system and the Brinkmann's equation for flow through the filter and tissue. The solutions from

these were coupled to convection-diffusion equation (to account for mass transport of oxygen and metabolites in the system and reaction rates of consumption of O₂ by the cells) across the whole model (Fig. 2.9.). Simulations were run to get steady state oxygen concentrations in the system for different flow rates not only for conditions where media was assumed to be fully saturated, but also taking into account experimentally measured values of oxygen saturation measured in our system.

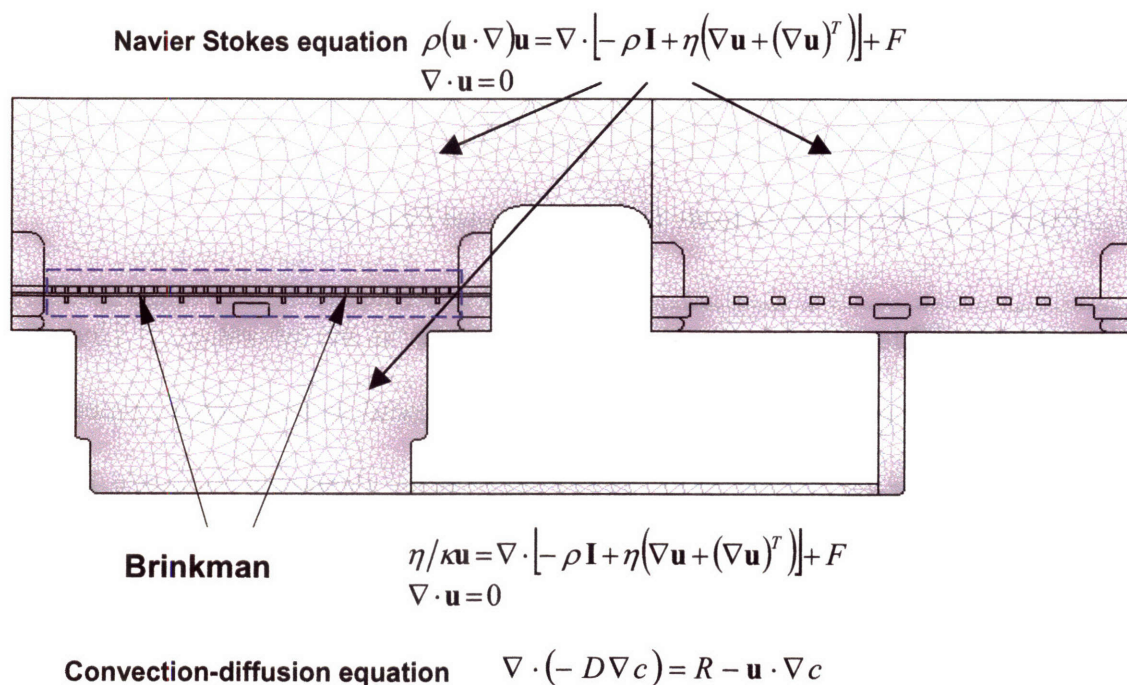


Fig 2.9. COMSOL modeling of the system utilizes Navier-Stoke's equation for bulk fluid flow and Brinkman equation for flow through the filter, scaffold and tissue region and couples them with to convection-diffusion equation to account for mass transport of oxygen and metabolites in the system.

2.2.2.2. Results:

In addition to flow patterns over the entire system, we were specifically interested in oxygen data for single channels under different flow conditions. Steady state values of oxygen concentration based on known oxygen consumption rates under ideal media

saturation values and experimentally measured of oxygen saturation values and two different flow rates are shown in Fig 2.10.

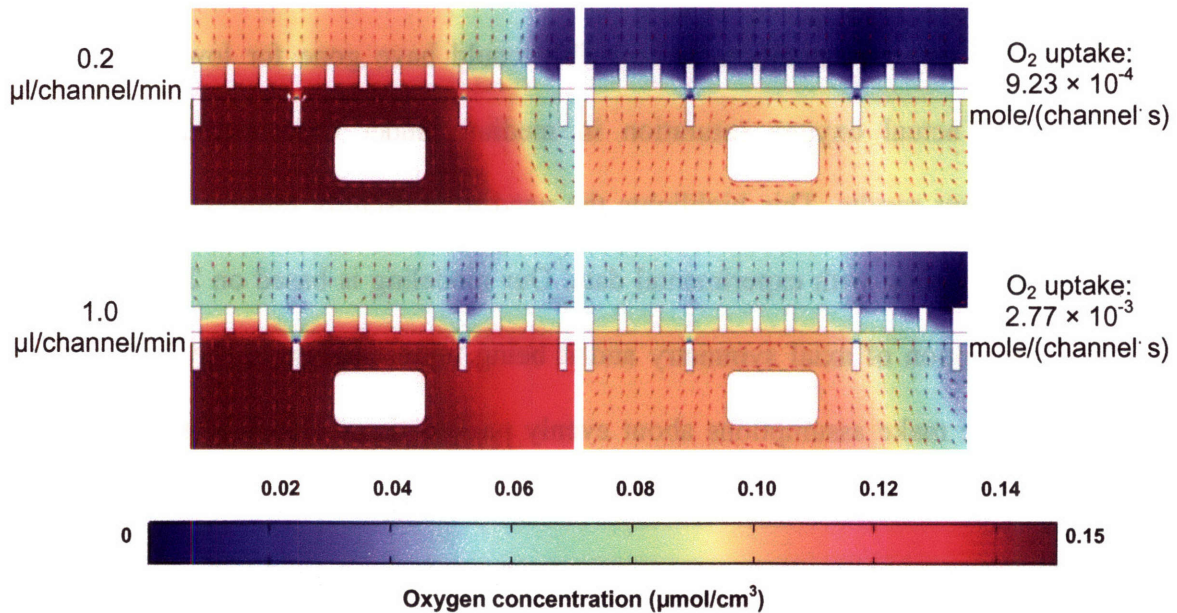


Fig 2.10. COMSOL modeling to predict outer bounds of flow rate. Steady state concentrations were calculated for both ideal (fully saturated) media conditions (left) as well as experimentally measured oxygen saturation values in media (right).

Though under ideal medium oxygen saturation conditions, at a flow rate of 0.2 µl/channel/min, the outlet concentration (of the medium exiting the tissue) would not be in the hypoxic range, under experimental conditions it was predicted to be hypoxic. Oxygen uptake rates were predicted to be higher in the higher flow rate (1 µl/channel/min) as compared to the lower rate.

2.2.2.3. Discussion:

Our goal was to zero in on two different operational flow rates that would provide the outer bounds for the flow conditions we wished to test in our system. We wanted a lower flow rate that would allow an inlet concentration (of medium entering the tissue) in the

physiological range while producing outlet concentrations that were just about hypoxic so that we might be able to create a gradient over our tissue height. The results of our modeling helped us choose these flow rates to be 0.2 and 1.0 $\mu\text{l}/\text{channel}/\text{min}$. Based on ideal values of oxygen saturation, we possibly could have gone for lower rates, but measuring the actual oxygen saturation in medium under experimental conditions provided different results. This highlights the need to constantly reinforce information gained from modeling with experimental data. Our modeling is based on 2-D geometry with the assumption of axial symmetry and it being representative of the 3-D system. Additionally we make assumptions about evenly packed tissue channels giving rise to uniform flow patterns across the scaffold. Though this may not be always possible in actual experimental settings, the model does provide us with reference values to plan our experiments on.

Chapter 3

Effect Of Medium And Flow Rate On The Non-Parenchymal Cell Survival And Phenotype

3.1. Overall Rationale

Our primary objective for this set of experiments was to study the effect of changing perfusion flow rates through the tissue in the reactors, on non-parenchymal (particularly sinusoidal endothelial) cell survival and phenotype. We also wanted to explore the relationship between flow and oxygen in our system, and if the effects seen with flow were independent of the type of medium used.

3.2. Materials And Methods

3.2.1. Setting Up Co-Cultures:

Wild type hepatocytes and GFP + endothelial cells were isolated from different animals using the isolation procedures described earlier. Day 2 spheroids ranging from 50-300 μm in diameter were selected by sequential size exclusion filtration, re-suspended in 'mixed' medium (a combination of hepatocyte growth medium described earlier and endothelial growth medium in 1:1 ratio), and seeded into the channels of the reactor scaffolds. The flow in the reactors was maintained in the downward direction through the channels for the first 8 hours, following which the direction was reversed. After reversal of flow, one row of wells in the plate (6 reactors) was maintained at an upward flow rate of 1 $\mu\text{l}/\text{channel}/\text{minute}$ while the other was set at 0.2 $\mu\text{l}/\text{channel}/\text{minute}$. For each flow rate, 3 of the reactors were filled with medium that was only HGM, while the other 3 had 'mixed' medium. The reactors were maintained at 37⁰C and 5% CO₂ and medium was changed every 24 hours for the entire duration of the culture. Partial pressure for oxygen was maintained at 20% throughout. Cultures were monitored over 2 weeks by phase contrast and fluorescent microscopy. At the end of 2 weeks, oxygen measurements were made from one reactor in each group, followed by harvesting of the same scaffold for cell

number estimation by total RNA. The other two wells were fixed and stained for the various non-parenchymal cell markers. The experimental layout is depicted in Fig 3.1 A & B.

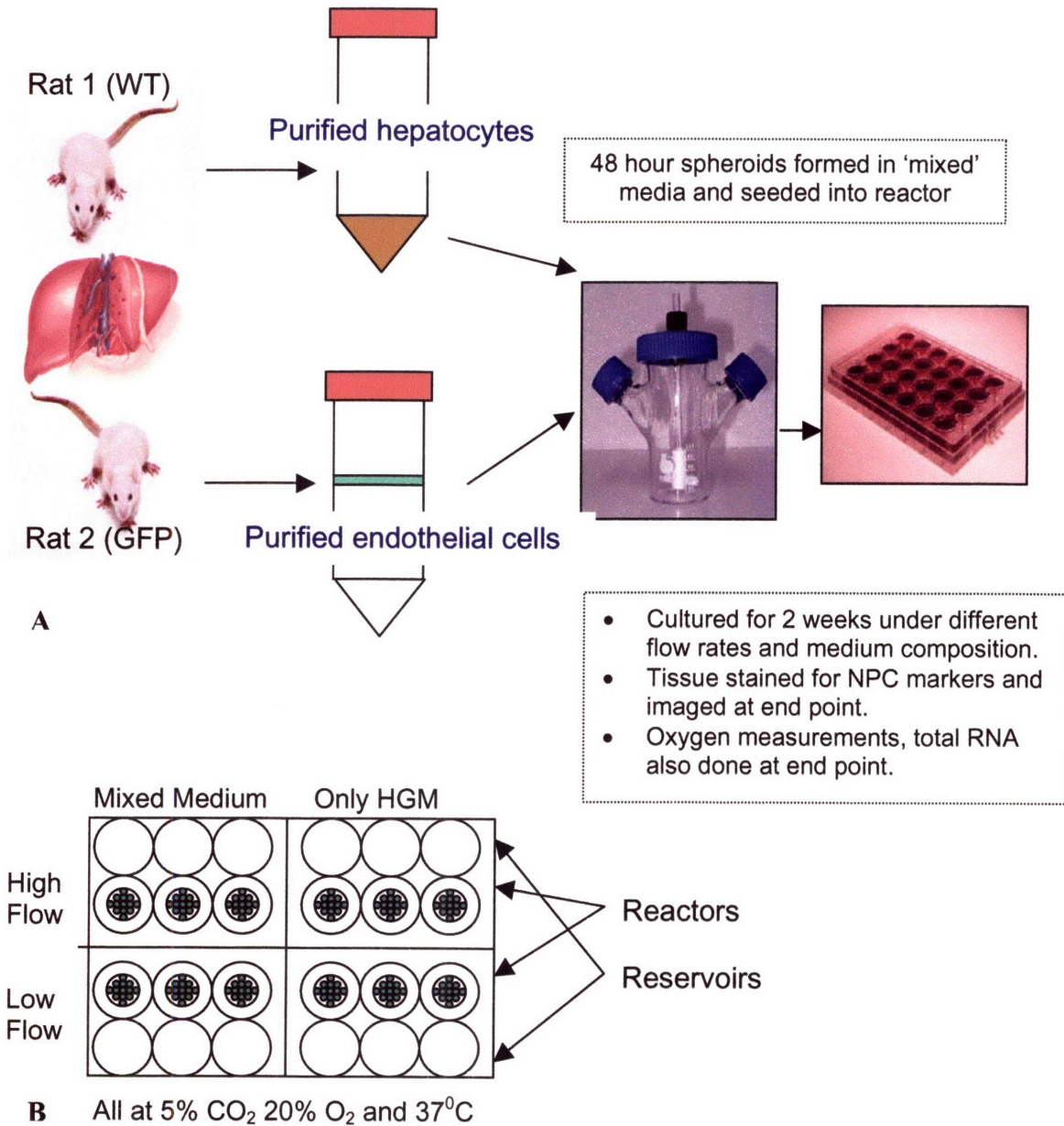


Fig 3.1. Experimental Design to evaluate effect of medium and flow:
 (A) Two day co-culture spheroids prepared from wild type hepatocytes and GFP + endothelial cells isolated from two perfusions were seeded into the scaffolds in the reactor and maintained for 2 weeks. (B) Multiwell layout for simultaneous evaluation of two flow rates and medium types.

3.2.2. Staining For NPC Markers

To characterize non-parenchymal cells in the tissue at the end of the experimental period, we adopted a staining protocol similar to the one we used to stain spheroids. The scaffolds were fixed in 2% paraformaldehyde for 60 minutes and then cut into multiple segments (each containing numerous tissue channels) using a pair of sharp scissors. After permeabilizing the scaffold segments containing channels of tissue with 0.1% Triton-X for 45 minutes, they were washed with PBS, blocked with 5% goat serum for 60 minutes. The scaffold segments were then separately incubated overnight with primary antibodies for the various non-parenchymal cell markers (SE-1 for sinusoidal endothelial cells, CD31 for large vessel endothelium and dedifferentiated SECs, ED2 for Kupffer cells, GFAP for quiescent stellate and SMA for activated stellate cells). The next day, following 3 washes with 2% BSA in PBS, the scaffolds were incubated with secondary antibody goat-anti-mouse Cy3, for an hour before washing and placing in chamber slides for confocal microscopy.

3.2.3. Confocal Microscopy And Image Processing

Spinning disc confocal microscopy was done using the McBain spinning-disk confocal with a Nikon TE2000U inverted microscope equipped with a laser from Coherent (Innova 70C). The objectives chosen to visualize one channel per field were 20x with a working distance of 3 mm. For each condition, six channels (chosen to include at least two completely filled and two partially empty tissue units) were imaged from top to bottom with 4-5 micron z sections. From z-stacks of images, we reconstructed top down view 3-D composite images superimposing all the sections as well as 3-D images with a 360 degrees view to get a lateral perspective. Image acquisition, 3-D reconstruction and

quantitative analysis were performed by using both Metamorph software (Universal Imaging) and Imaris.

3.2.4. Oxygen Measurements

Oxygen measurements were made in the system using the PreSens Oxy-4 system and the custom O₂ dipping Probes (v 1.01) (shown in Fig 3.2).

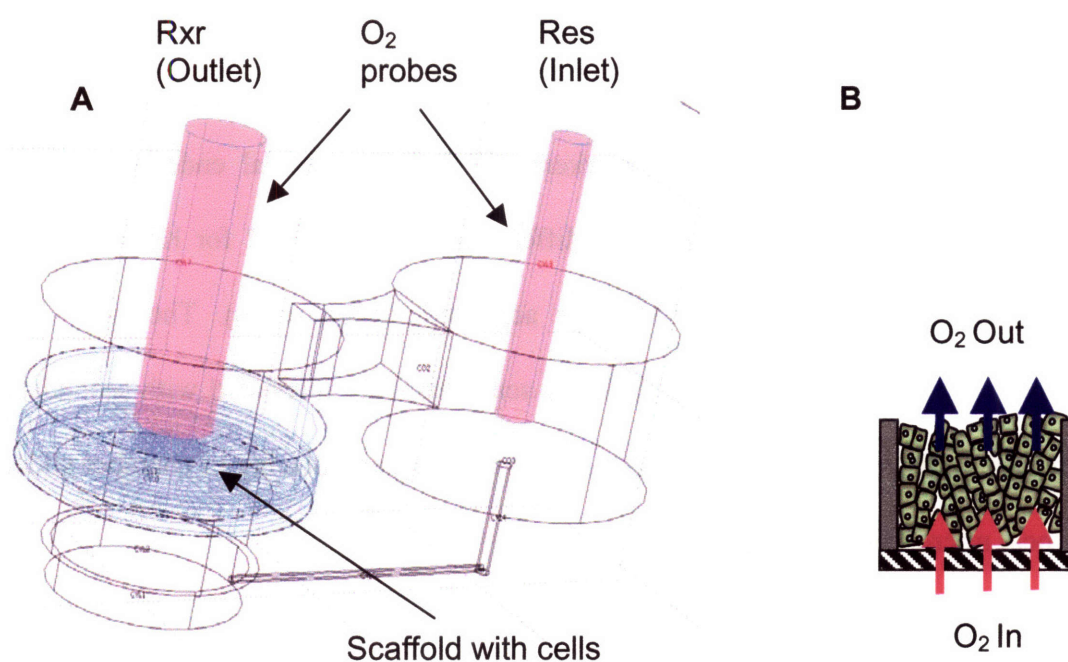


Fig 3.2. Measurement of oxygen difference across tissue units:
(A) PreSens Oxy-4 system was used to simultaneously measure the O₂ concentrations in the reservoir and the reactor to reflect (B) inlet and outlet O₂ concentrations across the tissue in the channels of the scaffolds.

Prior calibration of the probes was done using air saturated water at a known temperature (for 100% O₂), and Oakton Zero Oxygen Solution (Sodium Sulfide for 0 % O₂). Measurements were then made in the reservoir and reactor sides of the system, to reflect inlet and outlet concentrations respectively, thereby giving us an idea of oxygen

utilization across the tissue in the scaffold. Briefly, the probes were sterilized and fitted on the lid of the multiwell system, and adjusted to be immersed at a uniform depth in the medium of all the reactor or reservoir wells being measured (1 mm above the scaffold surface in reactors and 1mm above the filter in the reservoirs). Multiple measurements from each well were recorded using the Oxy 4 software with sampling rates every 5-15 mins until a steady state measurement was reached (usually within 2 hours). Data was exported into excel format for analysis.

3.2.5. Total Cell Number By RNA Estimation

Total RNA was isolated from the scaffolds of the wells where oxygen measurements were made, to estimate the total cell number for the purpose of normalizing the measurements. After the oxygen measurements, one mL of Trizol (Invitrogen) was added directly to scaffolds in 6 well plates and kept at -80°C until ready for RNA estimation. RNA isolation was performed using the RNeasy mini kit (Qiagen) according to manufacturer's protocols (for details refer to appendix). The concentration and quality of purified RNA was determined by assessing the ratio of absorbance at 260nm to 280nm.

3.3.Results:

The data presented below represent the results consistently seen consistently in three different biological replicates.

3.3.1.Effect Of Medium And Flow On Non-Parenchymal Cell Population:

Monitoring the cultures by phase contrast and fluorescent microscopy (for the GFP expressing NPCs in the tissue) over 2 weeks showed tissue filled channels distributed uniformly across the scaffolds an all the four groups. However, there were a higher

number of channels in the high flow rate group that doughnut shaped tissue structures with a thick ring of tissue attached to the walls surrounding a central conduit. Also the overall intensity of the green fluorescence appeared to be higher in the groups with mixed medium as compared to the tissue in cultures grown in HGM only.

Staining for the NPC markers and confocal imaging demonstrated that the SE1+ cells survive in serum-free medium (HGM only) within our system up to 2 weeks in perfused co-cultures. Their survival was enhanced at low flow and with serum (Fig. 3.3). The effect of flow rates on CD 31 staining pattern was the reverse of the effect seen on SE-1 staining, i.e. a higher staining was seen in the high flow rates as compared to the low flow rates (Fig 3.4). Most of the CD31 staining was localized along the tissue fluid interface. Stellate cells were found to be more prolific with serum & high flow (GFAP staining, Fig.3.5). The vastly increased number of stellate cells seen in the serum groups correlates with the earlier mentioned overall increase in green fluorescence. Additionally stellate cells were seen to be activated by mechanical stresses such as contact with rigid scaffold and high flow (SMA staining, Fig 3.6). Kupffer cells (ED2 staining, Fig. 3.7) were few and scattered in the tissue consistently across both flow conditions and medium types. An interesting observation noted on examining 3-D reconstructions of the images was that these SE-1 + cells seemed to be consistently polarized at the upper end of the tissue (Fig. 3.8).

Low Flow
(0.2 $\mu\text{l}/\text{channel}/\text{min}$)

High Flow
(1 $\mu\text{l}/\text{channel}/\text{min}$)

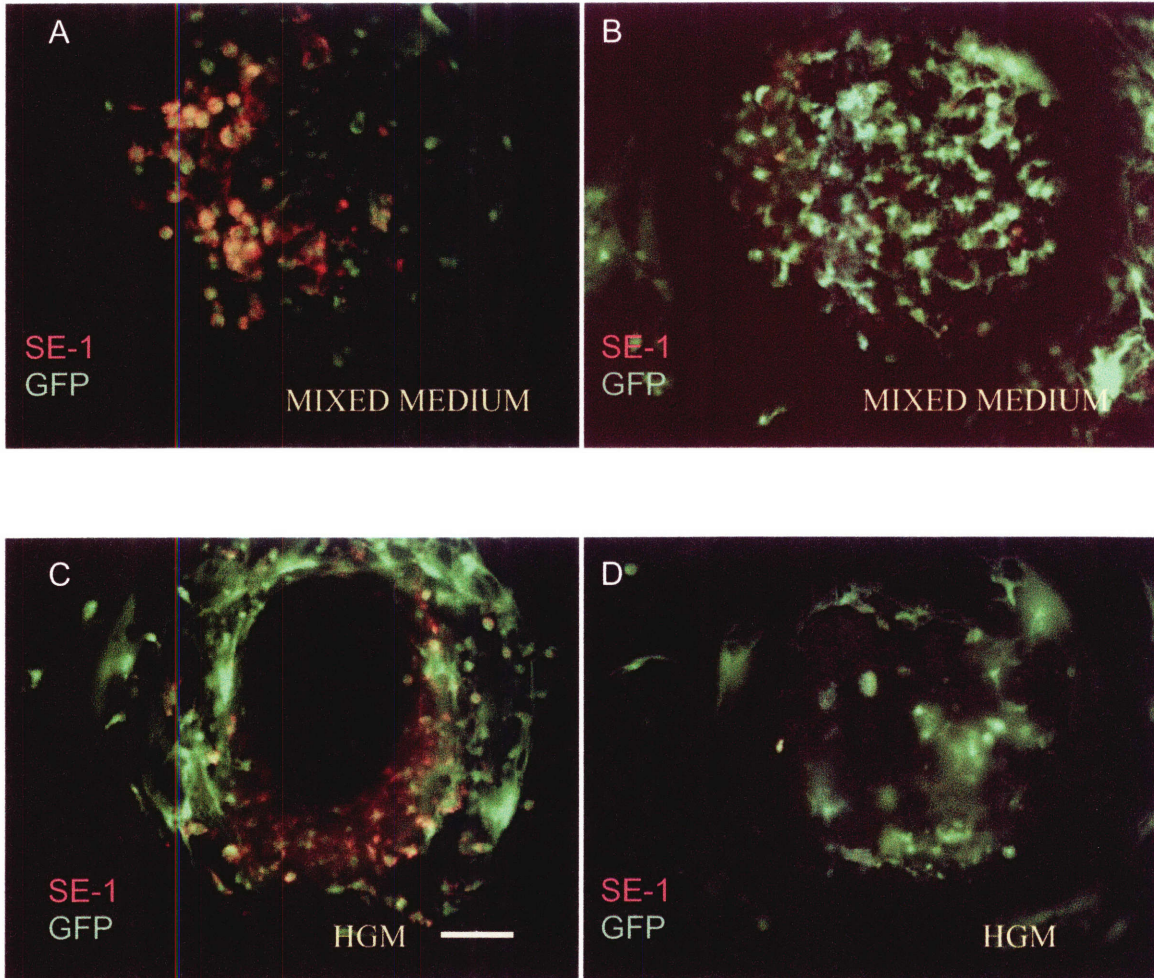


Fig 3.3. Effect of flow rate and medium composition on sinusoidal endothelial survival and phenotype. Confocal images of SE-1 (red) stained co-cultures from single representative channels of reactors with either mixed medium (A & B) or HGM only (C & D) with flow rates of either 0.2 $\mu\text{l}/\text{channel}/\text{min}$ (A & C) or 1 $\mu\text{l}/\text{channel}/\text{min}$ (B & D). Survival of SE-1 expressing endothelial was seen to be enhanced by low flow rates and serum in the medium. Scale bar 50 μm

Low Flow
(0.2 $\mu\text{l}/\text{channel}/\text{min}$)

High Flow
(1 $\mu\text{l}/\text{channel}/\text{min}$)

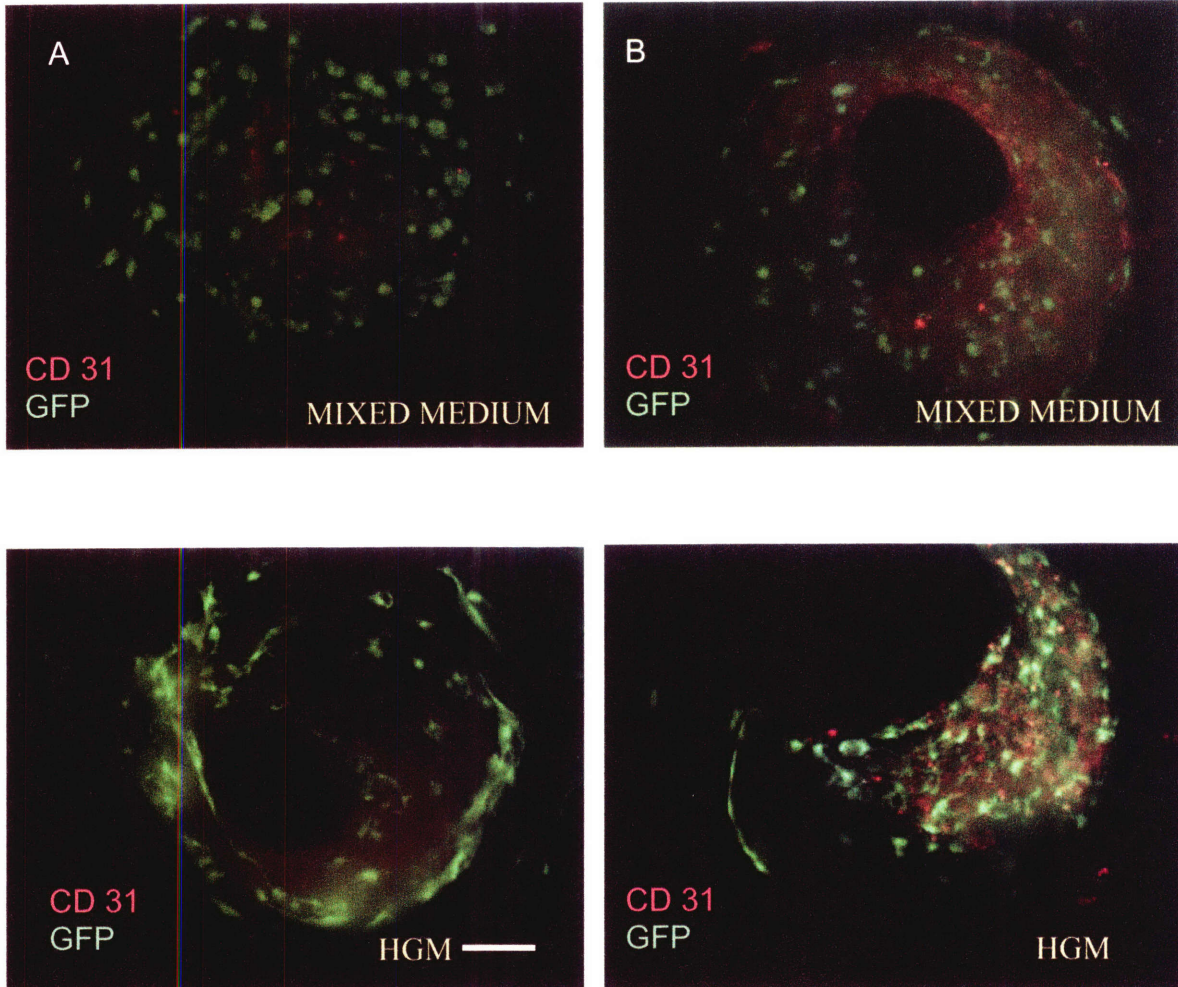


Fig 3.4. Effect of flow rate and medium composition on sinusoidal endothelial phenotype. Confocal images of CD31 (red) stained co-cultures from single representative channels of reactors with either mixed medium (A & B) or HGM only (C & D) with flow rates of either 0.2 $\mu\text{l}/\text{channel}/\text{min}$ (A & C) or 1 $\mu\text{l}/\text{channel}/\text{min}$ (B & D). Expression of CD 31, a dedifferentiation marker for sinusoidal endothelial cells was seen to be increased by high flow. Pronounced staining of this large vessel endothelial marker was seen at the fluid tissue interface. Scale bar 50 μm .

Low Flow
(0.2 $\mu\text{l}/\text{channel}/\text{min}$)

High Flow
(1 $\mu\text{l}/\text{channel}/\text{min}$)

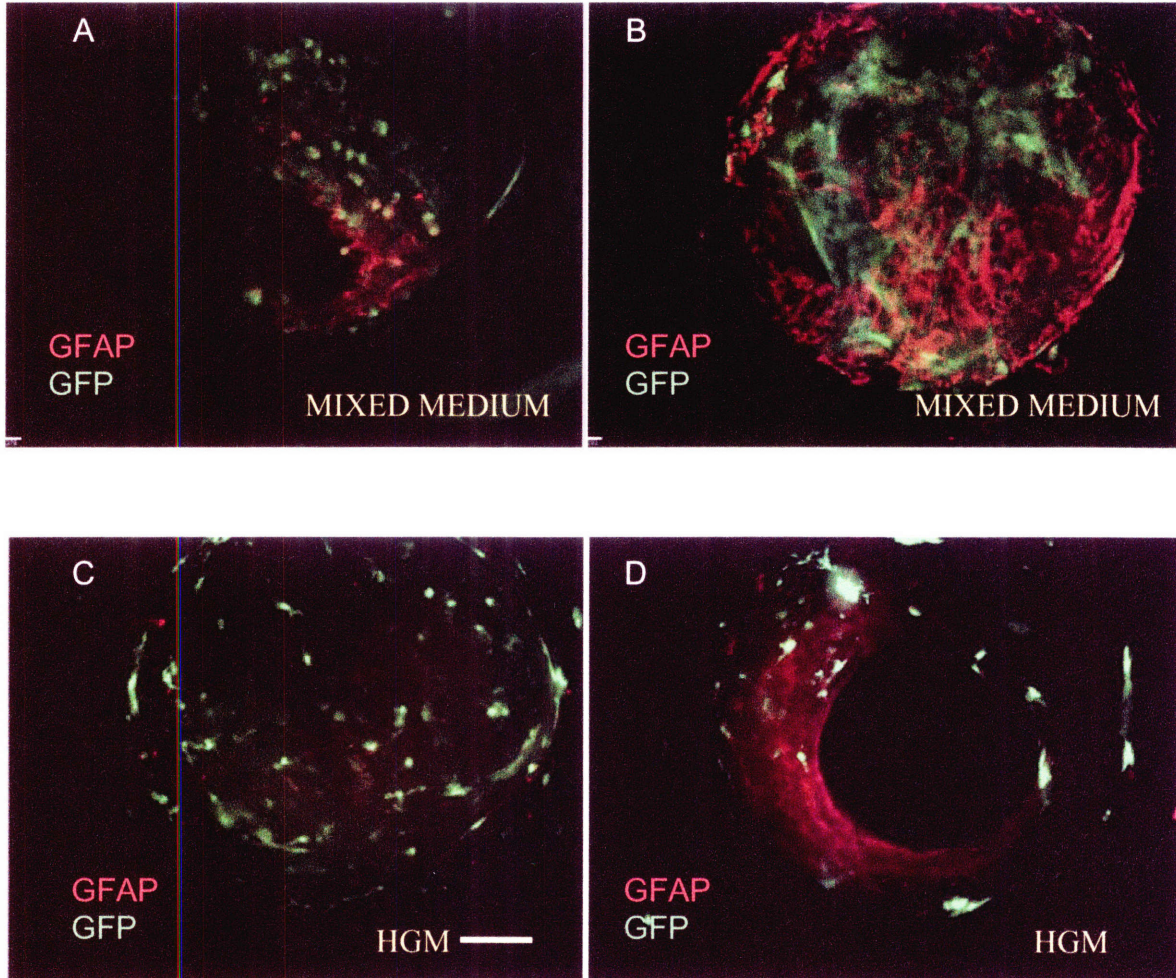


Fig 3.5. Effect of flow rate and medium composition on hepatic stellate cell survival and proliferation. Confocal images of GFAP (red) stained co-cultures from single representative channels of reactors with either mixed medium (A & B) or HGM only (C & D) with flow rates of either 0.2 $\mu\text{l}/\text{channel}/\text{min}$ (A & C) or 1 $\mu\text{l}/\text{channel}/\text{min}$ (B & D). Survival of GFAP expressing quiescent stellate cells was seen to be enhanced by high flow rates and serum in the medium. Consistent localization of these cells is seen at the fluid tissue interface of tissue structures, especially in the channels commonly seen in fast flow rate channels. Scale bar 50 μm

Low Flow
(0.2 μ l/channel/min)

High Flow
(1 μ l/channel/min)

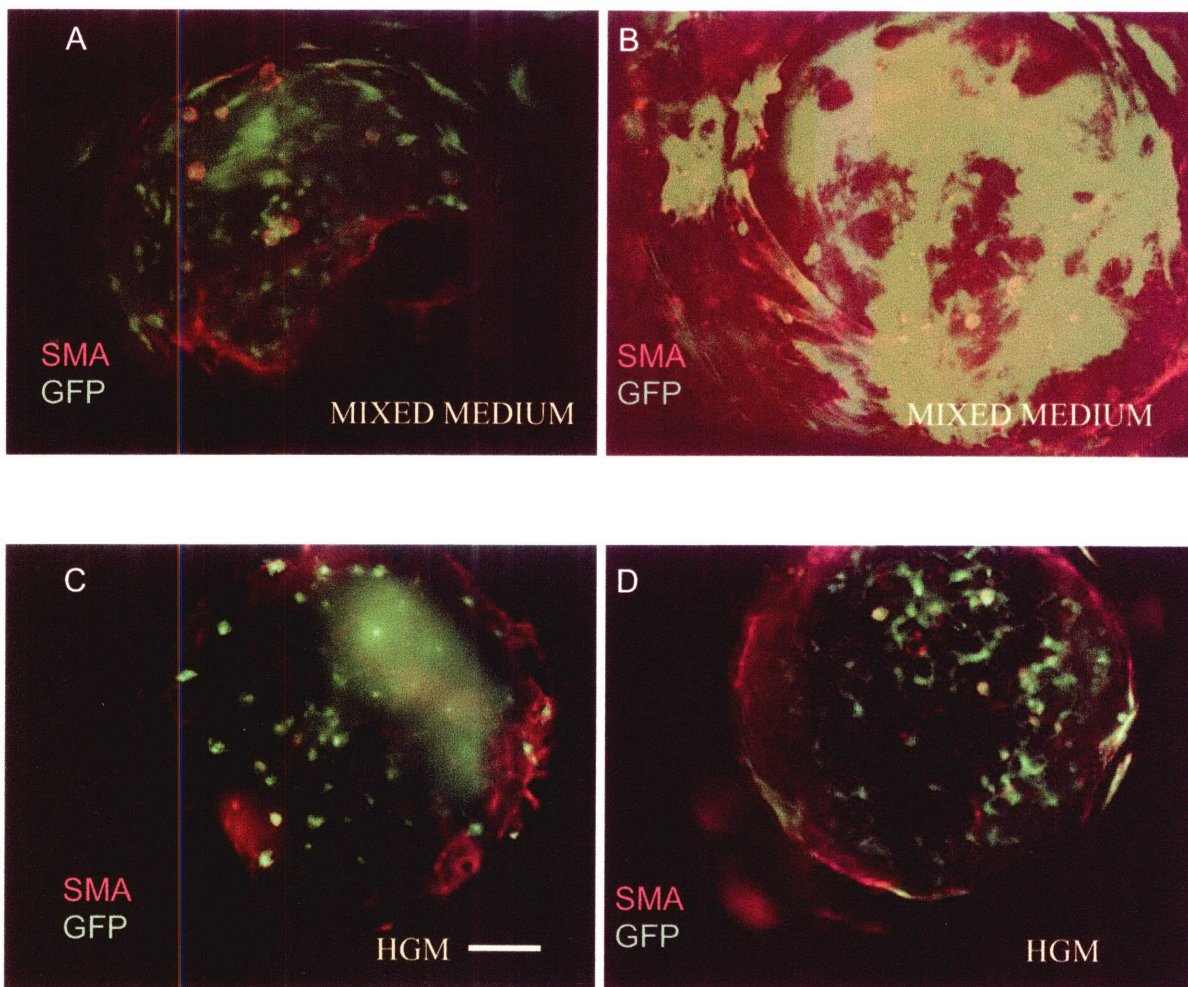


Fig 3.6. Effect of flow rate and medium composition on activation and fibroblastic transformation of stellate cells. Confocal images of SMA (red) stained co-cultures from single representative channels of reactors with either mixed medium (A & B) or HGM only (C & D) with flow rates of either 0.2 μ l/channel/min (A & C) or 1 μ l/channel/min (B & D). Stellate cells were markedly activated by high flow rates, serum in the medium and contact with the scaffold surfaces. Scale bar 50 μ m

Low Flow
(0.2 μ l/channel/min)

High Flow
(1 μ l/channel/min)

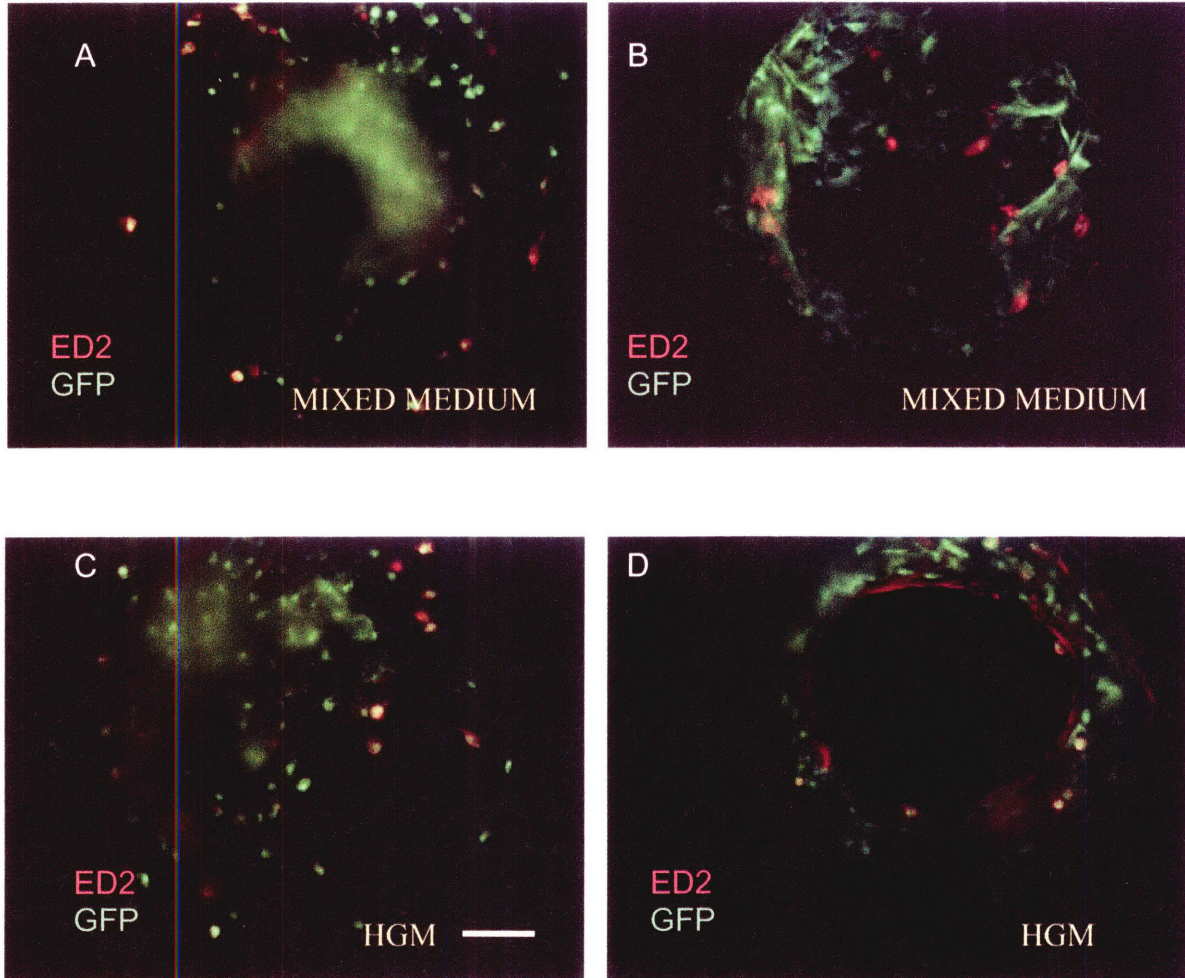


Fig 3.7. Effect of flow rate and medium composition on Kupffer cell survival. Confocal images of ED2 (red) stained co-cultures from single representative channels of reactors with either mixed medium (A & B) or HGM only (C & D) with flow rates of either 0.2 μ l/channel/min (A & C) or 1 μ l/channel/min (B & D). Kupffer cells were few and scattered throughout the tissue and appeared not to be influenced medium composition or flow rate. Scale bar 50 μ m

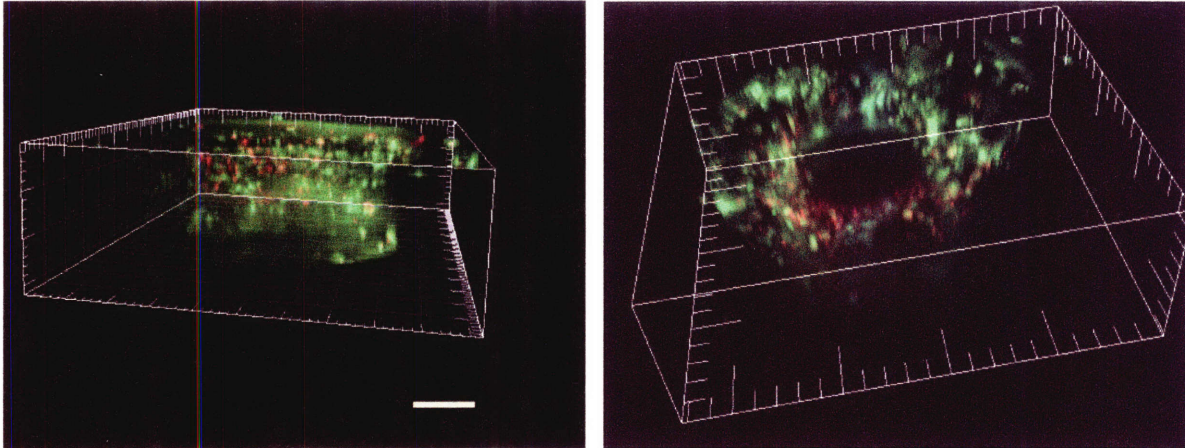


Fig.3.8. Localization patterns in the 3-D reconstructions: The SE-1 staining patterns seen in low flow conditions were consistently polarized at the upper end of the tissue. Scale bar 50 μm

3.3.2. Effect of flow rate on oxygen concentration differences across tissue

To assess if the differences seen between the two flow rates were also associated with differences in oxygen concentration and uptake, we measured the change in oxygen concentration across the tissue at both the flow rates. Measurements of the O_2 concentrations in the reservoir and the reactor using the PreSens Oxy-4 system gave us an idea of inlet and outlet O_2 concentrations. The product of difference between the inlet and outlet concentrations and the flow rate was adjusted to the cell number to give us values for oxygen uptake. We noticed that in line with our earlier modeling predictions, we found a reproducibly ($n = 3$) larger difference in oxygen gradient across the tissue in the slow flow rate reactors as compared with the high flow rate (Fig 3.9.) and lower outlet concentrations in the low flow rate groups.

The recovered cell numbers assessed from total RNA in both the flow rates were not very different with around 5×10^4 cells in the low flow rate and 6×10^4 cells in the high flow. On normalizing the data to cell number, and looking at oxygen uptake rates, it was seen

that the uptake rates in the low flow rate group was 0.52 nmol/s/10⁶ cells while that in the high flow rate group was 1.32 nmol/s/10⁶ cells (Fig 4.10).

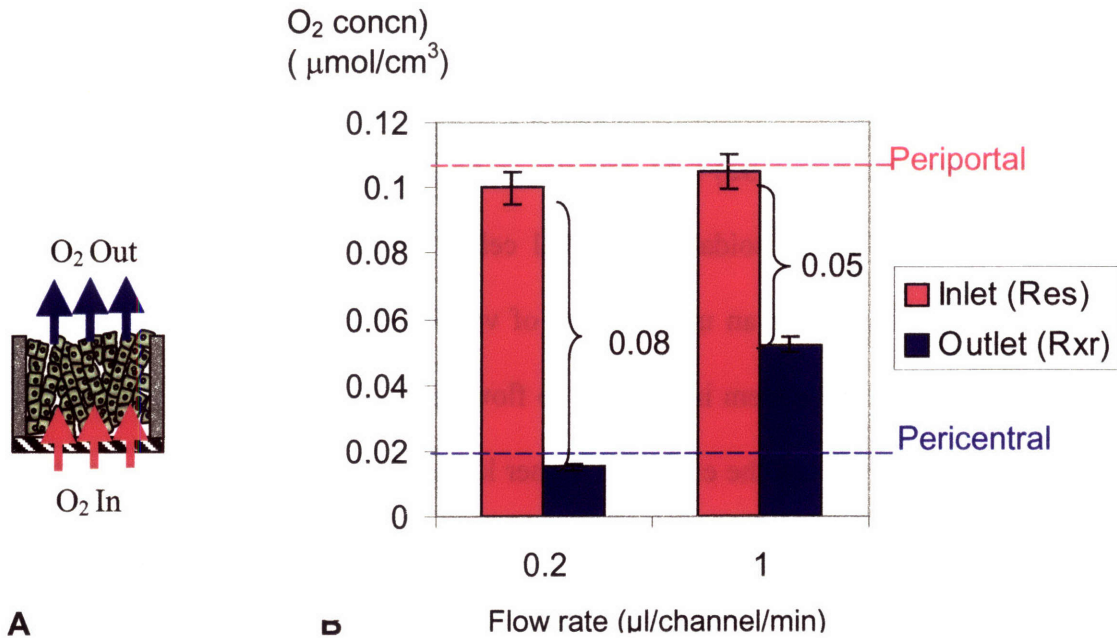


Fig 4.9. Effect of flow rate on measured value of oxygen difference across tissue units: (A) Oxygen concentration was measured in the reservoir and reactor to represent the inlet and outlet concentrations respectively. (B) The difference in oxygen concentration across the tissue was larger and the outlet concentration was lower in the slow flow rate as compared to the high flow rate reactors.

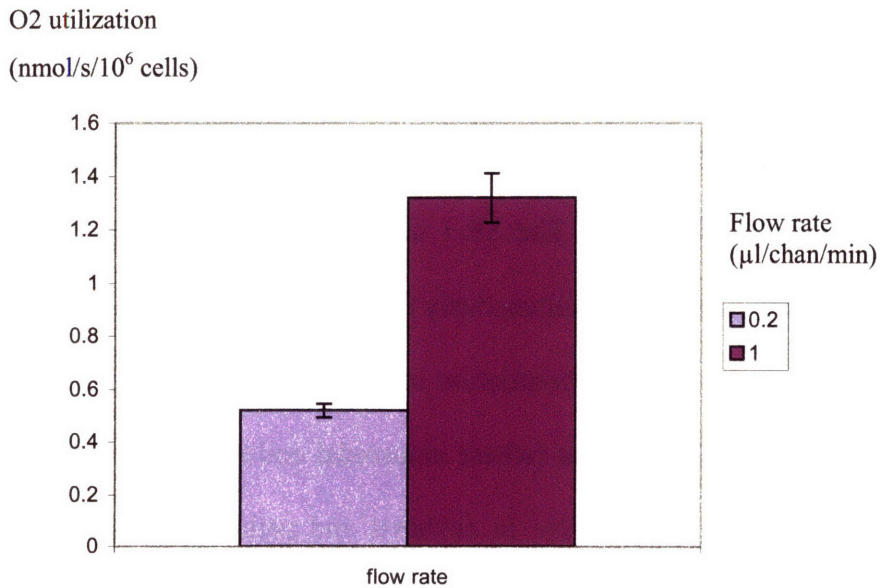


Fig 4.10. Effect of flow rate on oxygen uptake: Calculated oxygen uptake (normalized to recovered cell number estimated by total RNA) was significantly higher in the high flow rates.

3.4. Discussion:

Flow of blood *in vivo*, or of perfused medium in an *in vitro* system can directly provide mechanical stimuli to cells in the form of shear stress. Within the liver, endothelial cells and hepatic stellate cells are known not only to be major regulators of microvascular pressure in the sinusoids (132) (75), but also to be affected by shear stresses as well. In experimental studies, sinusoidal endothelial cells subjected to physiological levels of shear stresses demonstrate an upregulation of various receptors such as VEGFR-1 and VEGFR-2 (57). In our system in addition to flow rates close to physiological levels, we additionally wanted to test the effects of higher levels of flow and its associated stress on endothelial cells. High shear rates have also been demonstrated to have effects on other non-parenchymal cells. In stellate cells, shear stress by the sinusoidal stretching effect of increased blood flow is known to induce increased TGF- β formation and consequent activation (58). In cultured endothelial cells, fluid shear has been demonstrated to induce transforming growth factor beta-1 transcription and production (133).

Our experiments conducted in over three different biological replicates consistently demonstrated opposing effects of a high flow rate on endothelial and stellate cell numbers (as evidenced by immunostaining). The SE-1 staining pattern of endothelial cells that decreased in high flow rates was simultaneously accompanied by an increased expression of CD 31, a known marker of dedifferentiation in these cells (34). This finding is similar to the phenomenon of capillarization (where sinusoidal endothelial cells dedifferentiate and lose their phenotype) seen *in vivo* in cirrhosis and pathologic conditions (134) or induced *in vitro* by certain toxins (135). Presence of serum and additional growth factors in the medium was found to enhance SE-1 + survival in our experiment. This is expected

given the beneficial effects of the exogenous VEGF in the mixed medium. However it was interesting to note that even in the reactors containing only HGM (without exogenous VEGF or serum), the 3-D co-cultures with hepatocytes at low flow rates supported the survival of these cells. This points to the potential beneficial effects of the other cell types in the system (either by direct spatial contact or by paracrine regulation) supporting the sinusoidal endothelial cell survival under perfusion rates that lie closer to the physiological regime.

Though there are a lot of reports of increased pressure and shear in portal microcirculation as a result of stellate cell activation in fibrosis, no one has studied the effects of shear stress on activation of hepatic stellate cells. In our experiments we uniformly found a direct relation between increasing flow rates and stellate cell proliferation and activation (as evidenced by the GFAP and SMA staining patterns in our cultures). Though the mixed media increased the level of overall activation (once again on account of the presence of serum exogenous growth factors), the difference between the flow rates was maintained. A possible hypothesis about the increased proliferation and activation of stellate cells could be effects mediated through TGF β induction since the mechanical stresses of increased flow rates, are known to increase TGF β , a known and established player in the activation process of stellate cells (75,136).

The oxygen measurements across both the flow rates confirmed our earlier modeling predictions and the linked the variable of oxygen concentration with flow rates in our system. Lower flow rates are associated with a larger difference between inlet and outlet oxygen concentrations in the medium (across the height of tissue), probably due to the increased transit time. Consequently we also note relatively hypoxic concentrations at the

outlets in the low flow reactors. The consistent observation of localization of SE-1 staining cells at the upper end of the tissue in the low flow reactors could possibly correlate with the constant relatively hypoxic outlet concentrations seen in the same groups. When normalized to cell number, oxygen uptake rates by the cells are found to be higher in the high flow rates probably related to the increased volume of medium flowing through the tissue per unit time. These values are also slightly higher than those reported in literature using two dimensional *in vitro* models (137).

Given the differences in oxygen patterns across the two flow rates, it was important to parse out the effect of flow from oxygen on the non-parenchymal cells in our system. The next chapter describes the experiments that we conducted to solve this problem.

Chapter 4.

Uncoupling The Effects Of Oxygen And Flow On Non-Parenchymal Cell Survival And Phenotype.

4.1.Overall rationale

Though our earlier experiments generated interesting observations about the effect of flow on non-parenchymal cell phenotype and survival, they also demonstrated that the different flow rates were coupled with differences in oxygen concentrations, making the observed effects hard to comprehend. In an attempt to uncouple the effects of flow from oxygen, we wanted to carry out experiments in a setup where we could decrease the differences in oxygen concentration arising due to different flow rates. One way to achieve this was to make the overall environment more hypoxic which would decrease the inlet concentrations, and thereby possibly reduce the differences between inlet and outlet.

4.2. Materials and Methods

4.2.1. Setting up co-cultures:

The experimental layout has been schematically depicted in Fig 4.1. Wild type hepatocytes and GFP + endothelial cells were isolated as described before and co-culture spheroids were produced in spinner flasks containing mixed medium (a combination of HGM and EGM-2 in 1:1 v/v). Day 2 spheroids were then seeded into two separate multi-well reactors and set up in two different incubators containing 10% and 20% O₂ environments. The flow in the reactors was maintained in the downward direction through the channels for the first 8 hours, following which the direction was reversed. After reversal of flow, one row of wells in each multi-well plate (6 reactors) was maintained at an upward flow rate of 1 μ l/channel/minute while the other row was set at 0.2 μ l/channel/minute.

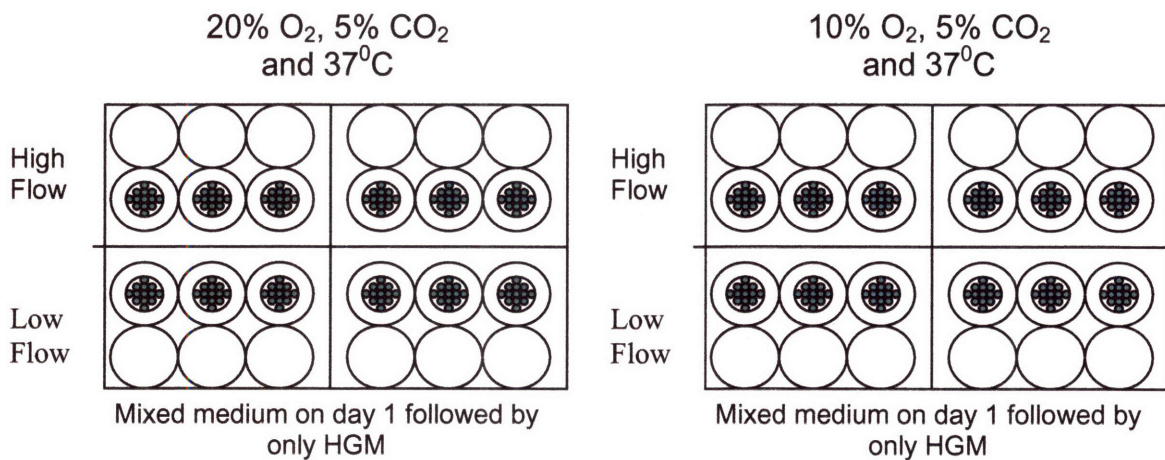
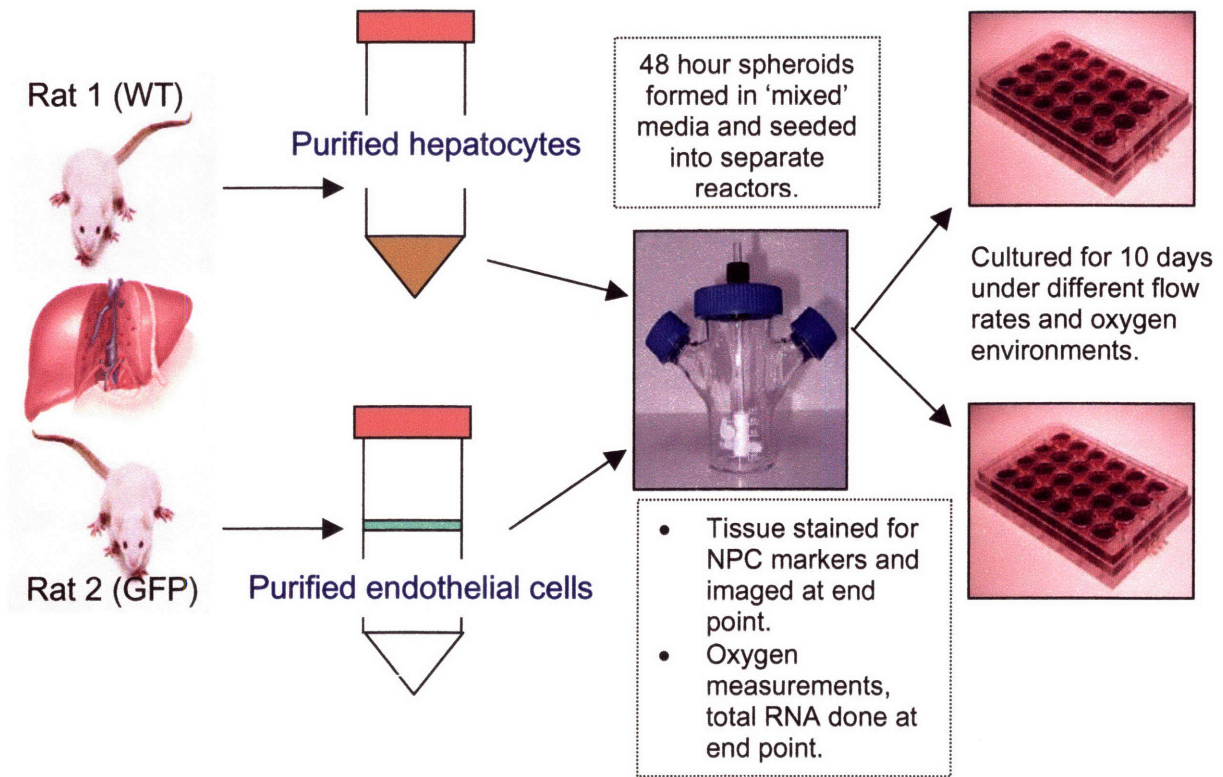


Fig 4.1. Experimental Design to evaluate effect of medium and flow:
 (A) Two day co-culture spheroids prepared from wild type hepatocytes and GFP + endothelial cells isolated from two perfusions were seeded into the scaffolds in 2 reactors and maintained under different oxygen environments for 10 days. (B) Multiwell layout for simultaneous evaluation of two flow rates and oxygen concentrations.

The reactors were maintained at 37⁰C and 5% CO₂ and medium was changed every 24 hours for the entire duration of the culture. After the first day, only HGM was used as medium in all the wells. Cultures were monitored for 10 days by phase contrast and fluorescent microscopy. At the end of the experimental period, oxygen measurements were made from two reactors in each incubator at each flow rate, followed by harvesting of the same scaffold for cell number estimation by total RNA. Three other wells were fixed and stained for the various non-parenchymal cell markers while one was used for live dead staining to assess overall viability of the cultures.

4.2.2. Staining for NPC markers and confocal microscopy:

Non-parenchymal cells in the tissue in each of the conditions at the end of the experimental period were characterized as described in the previous chapter. Briefly the scaffolds were fixed in 2% paraformaldehyde for 45 min and cut into multiple segments. These segments were permeabilized with 0.1% Triton-X for 30, mins, washed with PBS and blocked with 5% goat serum for an hour. After overnight incubation with primary antibodies for the various non-parenchymal cell markers, they were washed with 2% BSA in PBS, and incubated with secondary antibody, goat-anti-mouse Cy3, for an hour before washing and placing in chamber slides for confocal microscopy. Spinning disc confocal microscopy was done as described earlier and from z-stacks of images, 3-D composite images were reconstructed Image acquisition and 3-D reconstruction were performed by using both Metamorph software (Universal Imaging) and Imaris.

4.2.3. Oxygen Measurements And Total Cell Number By RNA Estimation:

Oxygen measurements were made from two of the reactors at each flow rate and oxygen environment as described earlier using the PreSens Oxy-4 system and custom O₂ dipping

Probes (v 1.01). Probes were calibrated prior to use with air-saturated water and Oakton Zero Oxygen Solution and measurements were made in the reservoir and reactor sides of the system to reflect inlet and outlet concentrations respectively. The sterilized probes were fitted on the lid of the multiwell system, and immersed at a uniform depth in the medium of all the wells being measured. Multiple measurements from each well were recorded using the Oxy 4 software until a steady state measurement was reached. Data was exported into excel format for analysis. Total RNA to estimate the total cell number was isolated from the scaffolds of the wells where oxygen measurements were made, to normalize the measurements. One mL of Trizol (Invitrogen) was added directly to the removed scaffolds in 6 well plates. RNA isolation was performed using the RNeasy mini kit (Qiagen) according to manufacturer's protocols (for details refer to appendix). The concentration and quality of purified RNA was determined by assessing the ratio of absorbance at 260nm to 280nm.

4.3.Results:

The data shown below represent results seen over two biological replicates.

4.3.1. Overall tissue formation:

Over the period of the study, observing the channels in the reactors by phase contrast and fluorescence microscopy showed the overall tissue formation in the hypoxic (10% oxygen) reactors to be appearing relatively sparser as compared to the normal oxygen (20%) reactors. This was later confirmed by the quantification of cell numbers as estimated by total RNA. The live dead images also showed that the overall viability in the hypoxic group was lower than regular oxygen concentrations (data not shown).

4.3.2. Non parenchymal cell staining and oxygen measurements:

The staining results at the higher O₂ (20%) environmental concentration reproduced what we had consistently seen in our earlier experiments at that oxygen level. Enhanced survival of SE-1 + cells was seen at low flow rates and increased stellate cell activation and proliferation was noted at the high flow rates (Figs.4.2 A &B and 4.3., A & B respectively). However, at the lower O₂ environment, the differential effect of flow rate on endothelial cell survival seemed to disappear, and we found SE-1+ cells at both the flow rates (Fig 4.2. C & D). On the other hand, the staining pattern of stellate cells seemed unaffected by the hypoxic conditions and showed the same trend (increased proliferation and activation in higher flow rates) in both the oxygen environments (Fig 4.3.).

On measuring the oxygen concentration in the different flow rate reactors (Fig 4.4. A), those maintained in a high oxygen environment showed the same trend as consistently noted earlier (relatively lower oxygen outlet concentrations and greater difference across the tissue in the low flow group as compared to high flow group). However measurements done in the in the low oxygen environment, found the outlet concentrations for both the flow rates to be in the hypoxic range even though the inlet concentrations were higher. The oxygen uptake rates calculated as the product of the difference in concentration across the tissue (normalized to cell number) and the flow rate, was higher in the higher flow rates for both environments (Fig.4.4 B.), though not to a factor of 5 times - the flow rate difference. The uptake values for each flow rate were lower in the high oxygen groups as compared to the corresponding values of the same flow rate in the hypoxic group.

Low Flow
(0.2 $\mu\text{l}/\text{channel}/\text{min}$)

High Flow
(1 $\mu\text{l}/\text{channel}/\text{min}$)

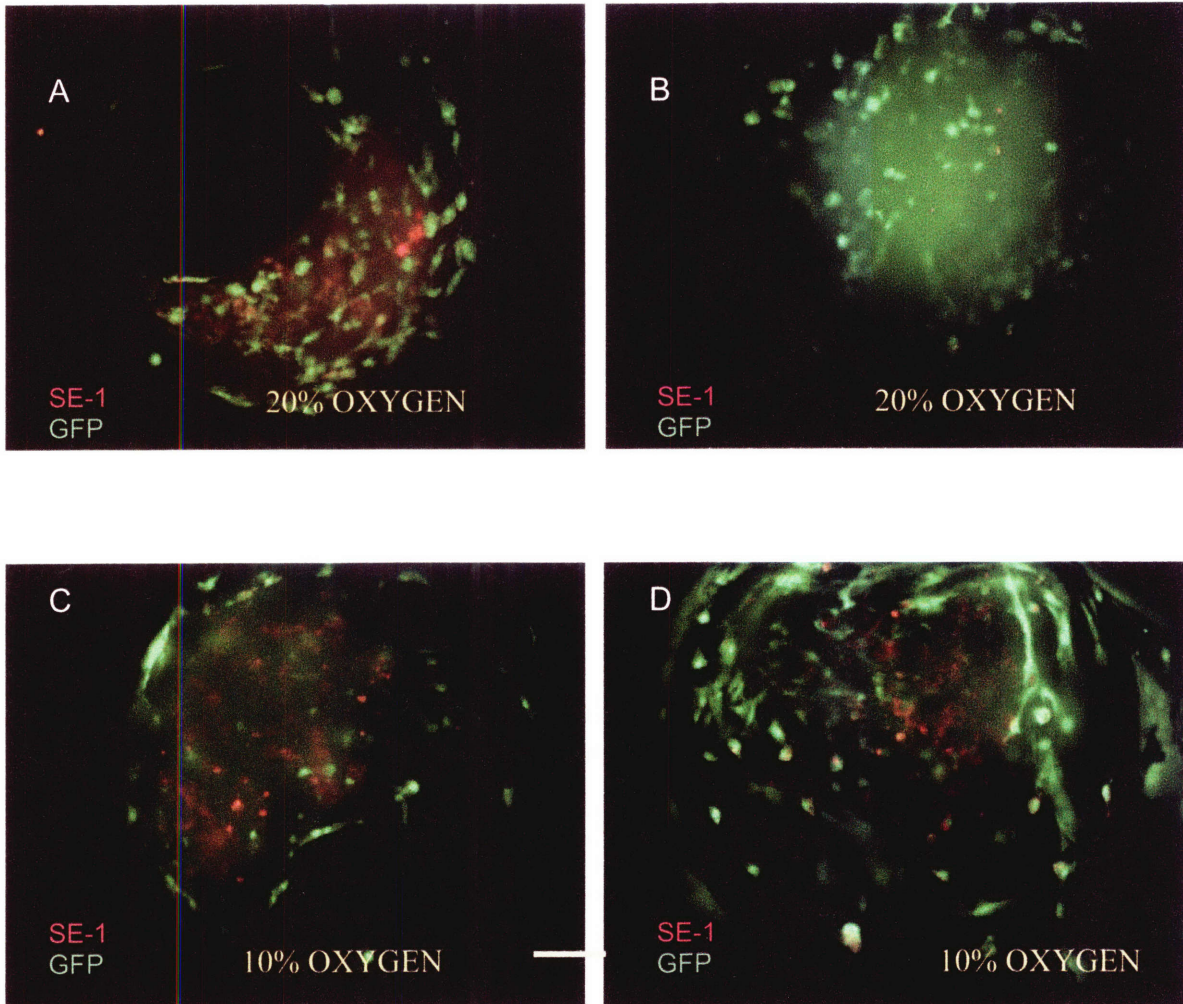


Fig 4.2. Uncoupling the effect of oxygen and flow rate on sinusoidal endothelial cell survival and phenotype. Confocal images of SE-1 (red) stained co-cultures from single representative channels of reactors in either 10% oxygen (A & B) or 20 % oxygen (C & D) with flow rates of either 0.2 $\mu\text{l}/\text{channel}/\text{min}$ (A & C) or 1 $\mu\text{l}/\text{channel}/\text{min}$ (B & D). While low flow rates aided the survival of SE-1 + cells at high (20%) oxygen environments, at lower oxygen environments, this effect low flow rate on SE-1 + cell survival was lost. Scale bar 50 μm

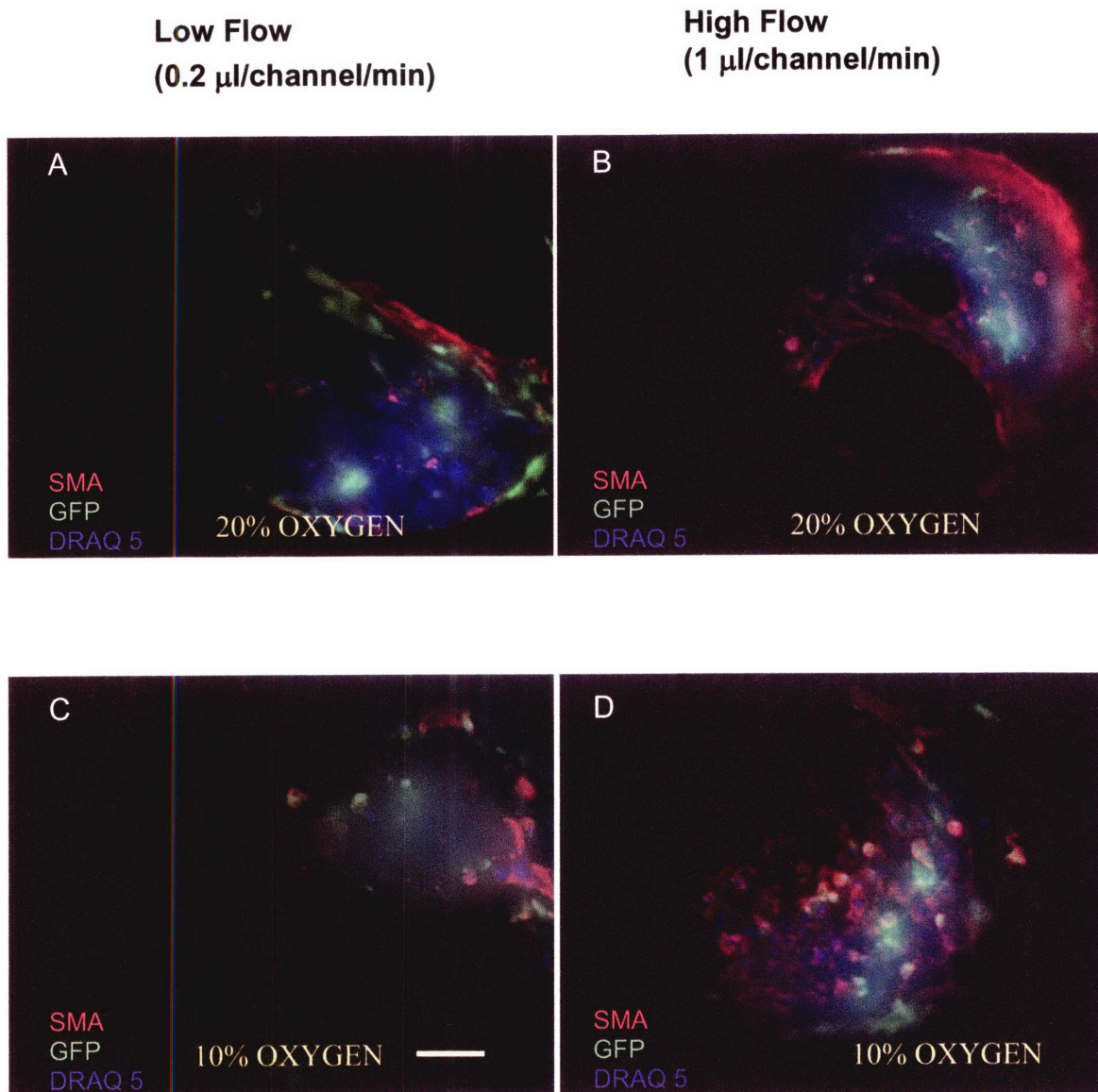
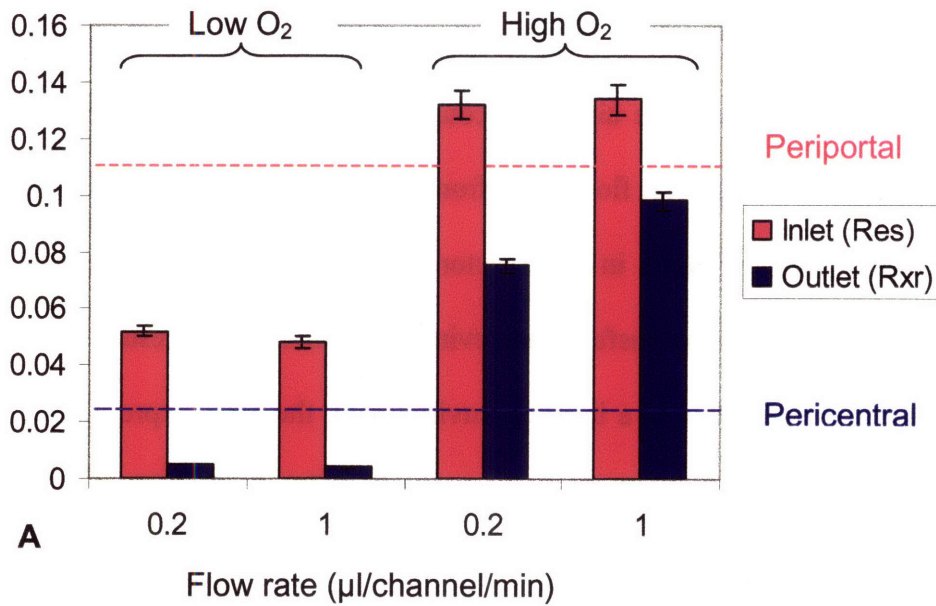
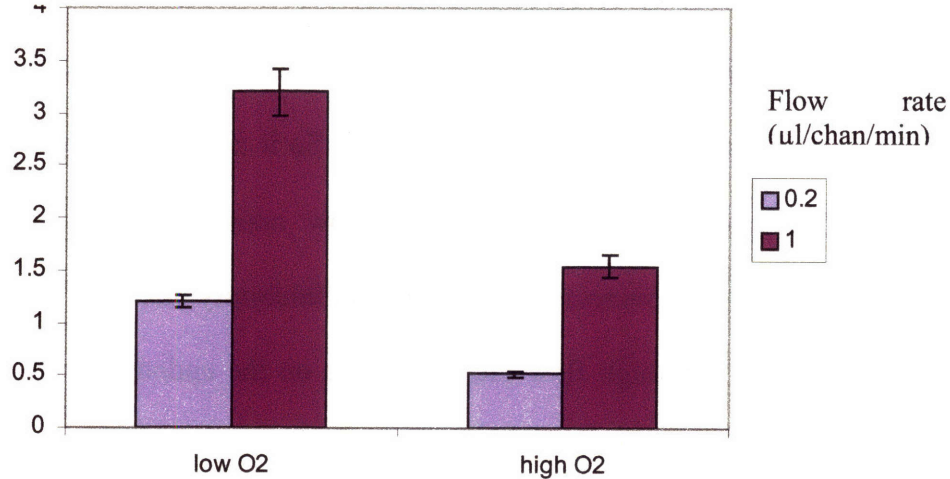


Fig 4.3. Uncoupling the effect of oxygen and flow rate on stellate cell proliferation. Confocal images of SMA (red) stained co-cultures from single representative channels of reactors in either 10% oxygen (A & B) or 20 % oxygen (C & D) with flow rates of either 0.2 $\mu\text{l}/\text{channel}/\text{min}$ (A & C) or 1 $\mu\text{l}/\text{channel}/\text{min}$ (B & D). Activation and proliferation of stellate cells was increased by high flow rates regardless of the oxygen concentrations. Nuclear staining with Draq 5 (blue) is additionally shown in this image. Scale bar 50 μm

O₂ concn
($\mu\text{mol}/\text{cm}^3$)



O₂ uptake
(nmol/s/10⁶ cells)



B

Fig 4.4. (A) Effect of oxygen environment on oxygen differences across tissue at different flow rates. Values for outlet concentrations at both flow rates in the low oxygen environment were in the hypoxic range and the concentration differences across the tissue were approximated for both rates. Values for high oxygen environment showed the same trend as seen earlier (relatively lower oxygen outlet concentrations and difference across the tissue in the low flow group as compared to high flow group). (B) Oxygen utilization rates calculated as the product of the difference in concentration across the tissue (normalized to total cell number) and the flow rate, was higher in the high flow rates. Overall utilization rates in the high oxygen groups were lower as compared to the hypoxic groups.

4.4. Discussion:

Our experiments were planned in two different environments; the normal environment we routinely use in our cultures (with 20 % O₂), and an artificially hypoxic environment (with 10% O₂). This was done with the aim of decoupling the effects of the oxygen differences seen in reactors with different flow rates, from the direct effects of flow itself. Measurement of oxygen concentrations in the reactors and reservoirs from the two environments showed that we were successful in achieving this aim. Staining results from two biological replicates showing that in a hypoxic environment, the SE-1 expression is maintained at both high and low flow rates, went hand in hand with low outlet concentrations seen at both the flow rates. This implies that the low oxygen concentrations may be a factor responsible for endothelial survival and SE-1 expression. The correlation of hypoxia with endothelial cell survival is strengthened by the fact that hypoxia is well known to upregulate VEGF in most cell types including hepatocytes, mediated via hypoxia inducible factor- alpha (HIF1- α) (138). So it is possible that the indirect effects of relative hypoxia seen at the higher flow rates in the low O₂ environment might be responsible for overcoming any potential inhibitory effects such as loss of phenotype that the effects of high flow rates can have on the endothelial cells (possibly mediated through the effects of increased mechanical stresses and TGF- β). As expected from previous experiments, the sinusoidal endothelial cells in the normal oxygen environment continue to survive in a differentiated state and express SE-1 only in the lower flow reactors on account of the combined effects of hypoxia as well as the mechanical stimuli from flow rates in the physiological range.

In our experiments the hypoxic environment did not seem to reverse the consequences of high flow on stellate cells. We saw the same pattern of differences between both the flow rates regardless of the oxygen in the environment. This can be explained by the fact that the changes seen with high flow and corresponding increased mechanical stresses in stellate cells (activation and proliferation), which are mediated by TGF- β , would be unaffected by the hypoxic environment since the hypoxia induced VEGF increases would not be expected to counter these effects. On the contrary, according to recent reports hypoxia could potentially further increase TGF- β levels in stellate cells leading to activation (139). The postulated mechanism and interactions by which flow and oxygen affect the survival of non-parenchymal cells in our system has been summarized in Fig 4.5.

Another interesting finding is that while the cells in the normal oxygen environment show measured oxygen uptake rates similar to what has been previously reported in literature (137), the cells in a hypoxic environment display a markedly higher uptake of oxygen when normalized to cell number (Fig 12.B). The explanation for this phenomenon could be due to upregulation of various metabolic and respiratory genes in hepatocytes induced by hypoxia, a finding that has already been reported in literature (140). This would also explain why the calculated difference in oxygen uptake between the low and high flow rates is not to the same extent as the factor of flow rate difference.

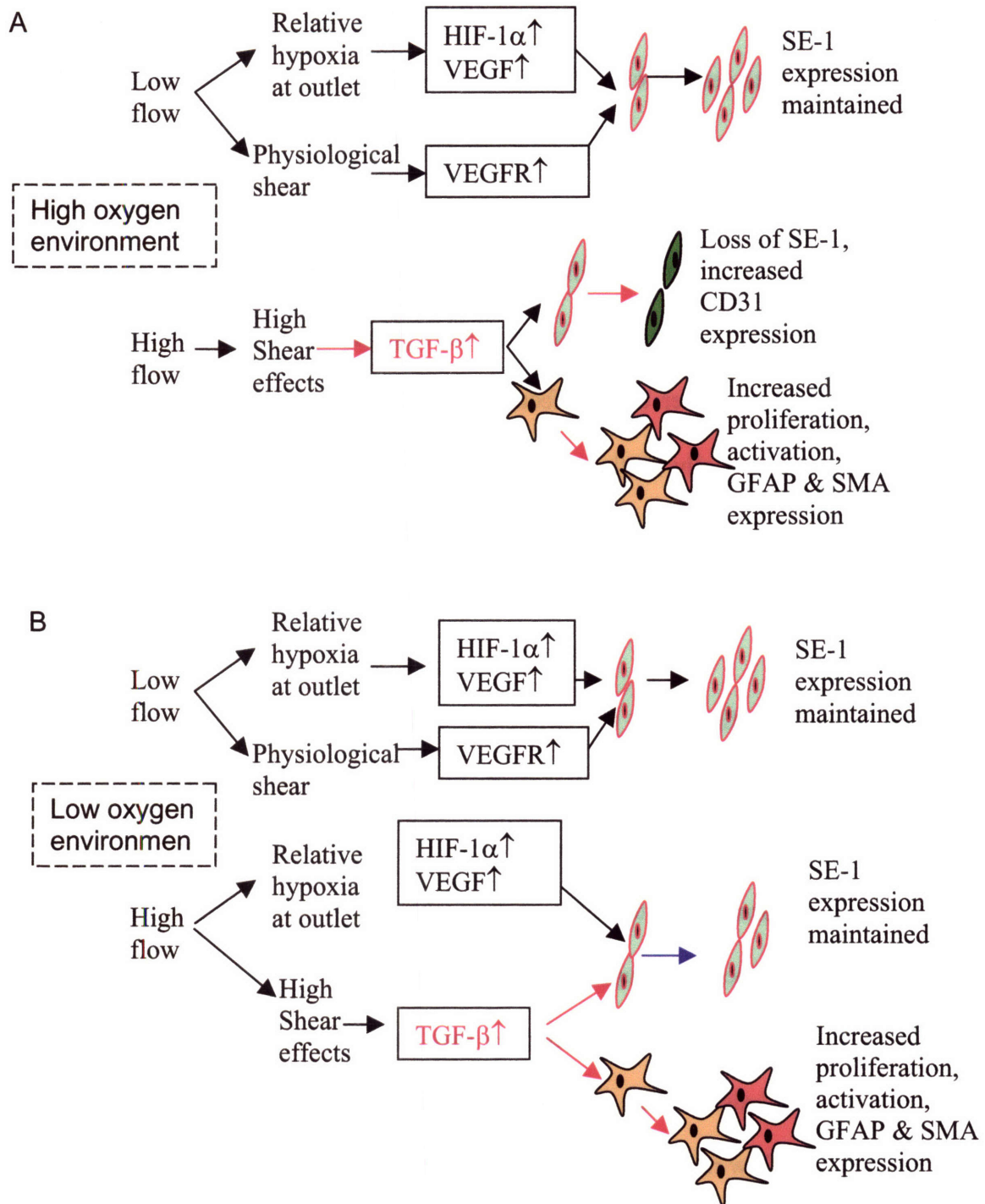


Fig 4.5. Postulated interrelationship of flow and oxygen effects on non-parenchymal survival and phenotype: (A) In a normal oxygen environment, the low flow rate gives rise to positive stimuli for SE-1 survival and phenotype by relative hypoxia as well as physiological shear cues. Higher flow rates are associated with high shear effects, TGF- β upregulation and its effects on SECs (loss of phenotype) and stellate cells (activation and proliferation). (B) However in a hypoxic environment, the relative hypoxia effect is seen at both the flow rates overcoming the effects of TGF- β upregulation on sinusoidal endothelial cells. Stellate cells are unaffected by the oxygen effects and continue to be activated by high flow rates.

Though we have parsed out the effects of flow and oxygen, and suggested that the low flow rate effects are mediated by the hypoxia, it would also be interesting to examine the suggested high flow effects that we postulate are mediated by TGF- β . The following chapter addresses this and looks at the effect of inhibiting this molecule in our system across both the flow rates.

Chapter 5.

Effect Of TGF- β Inhibition On Non-Parenchymal Cell Survival And Phenotype.

5.1.Overall rationale

Our experiments with flow rate and oxygen (described in chapter 4) demonstrated that inhibitory effects of high flow rates on sinusoidal endothelial cells could be overcome by creating a hypoxic environment, possibly due to a compensatory upregulation of other factors. However it was also of interest for us to see if directly inhibiting the cytokine transforming growth factor beta, which we postulated to be responsible for the effects of high flow and shear, could achieve the same effect. After researching literature on different inhibitors, we chose a compound SB- 431542, known for its property to inhibit TGF- β and designed experiments to test its effects in our system.

5.2. System Modifications from earlier experiments

There were a couple of differences in the current set up compared to our earlier experiments. We chose to seed our reactors with freshly isolated cells instead of spheroids in an attempt to overcome the limitations of low endothelial cell incorporation and stellate cell activation that was known to occur prior to introduction of the spheroids into our reactor. Another difference was in the design and overall number of cells seeded into each reactor (Fig 5.1).

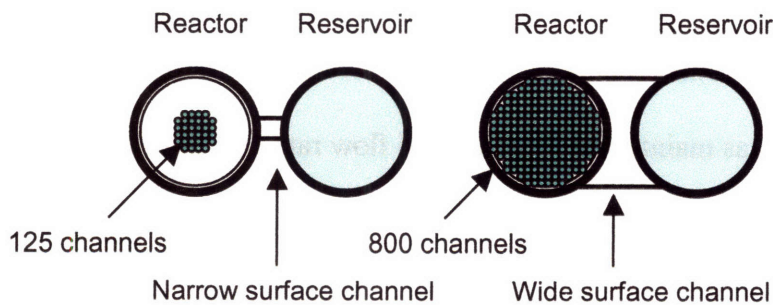


Fig 5.1. Reactor design modifications for larger array scaffolds used in current experiments

The multi-well reactors that we used in our earlier spheroid experiments contained about 125 channels. In the current experiment, the scaffolds had a much higher number of channels per scaffold (about 800). To compensate for the increased requirement of oxygen mass transfer resulting from the larger number of cells seeded into each reactor, the surface channels connecting the reactor well to the reservoir (that allowed re-oxygenation of oxygen during flow) were widened considerably.

5.3. Materials and Methods:

5.3.1. Setting up co-cultures:

Wild type hepatocytes and GFP + endothelial cells were isolated from different animals using the isolation procedures described earlier. Mixed medium containing freshly isolated cells (300,000 hepatocytes and 600,000 endothelial cells) was seeded into the scaffolds of each well of the multi-well reactor to fully pack the channels at the time of seeding. Medium in the reactors was changed every 24 hours and the filter from the reservoir side was replaced after the first day to remove any cells that could have potentially floated over during seeding. For the first 2 days we used mixed medium in our cultures, following which only HGM was used. The flow in the reactors was maintained in the downward direction through the channels for the first 12 hours, following which the direction was reversed. After reversal of flow, one row of wells in the plate (6 reactors) was maintained at an upward flow rate of 1 $\mu\text{l}/\text{channel}/\text{minute}$ while the other was set at 0.2 $\mu\text{l}/\text{channel}/\text{minute}$. For each flow rate, in two wells we added the TGF- β inhibitor SB-431542 into the medium at a concentration of 1 μM . The cultures were maintained for 2 weeks at regular oxygen levels of 20%, 5% CO_2 and 37 $^\circ\text{C}$. During the course of the experiment, the cultures were observed by phase contrast and

fluorescent microscopy. At the end of the 2-week period, scaffolds from 2 wells each from each flow rate, either with or without the added inhibitor were fixed and stained for non-parenchymal cell markers. Oxygen measurements were made from the remaining wells in the system along with estimation of total cell numbers. The experimental layout has been schematically depicted in Fig 5.1 A & B.

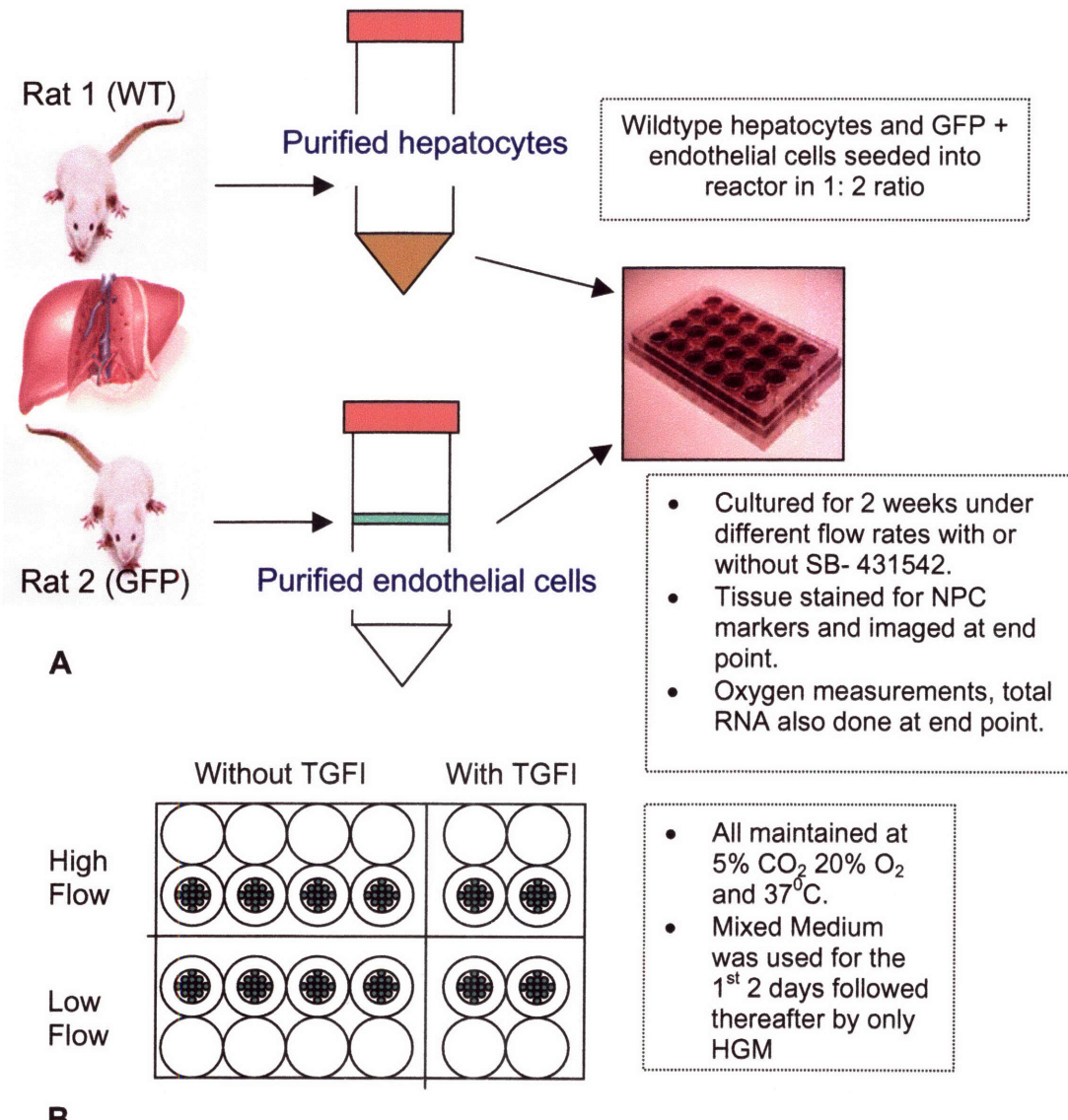


Fig 5.1. Experimental Design to evaluate effect of TGF- β inhibition: (A) Freshly isolated wild type hepatocytes and GFP + endothelial cells were seeded into the scaffolds in the reactor and maintained for 2 weeks. (B) Multiwell layout for evaluating effect of TGF- β inhibition.

5.3.2. Staining for NPC markers and confocal microscopy

Non-parenchymal cells in the tissue at the end of the experimental period were characterized as described previously. Briefly, the scaffolds were fixed in 2% paraformaldehyde for 45 min and cut into multiple segments. These segments were permeabilized with 0.1% Triton-X for 30, mins, washed with PBS and blocked with 5% goat serum for an hour. After overnight incubation with primary antibodies for the various non-parenchymal cell markers, they were washed with 2% BSA in PBS, and incubated with secondary antibody, goat-anti-mouse Cy3, for an hour before washing and placing in chamber slides for confocal microscopy. Spinning disc confocal microscopy was done as described earlier and from z-stacks of images, 3-D composite images were reconstructed. Image acquisition and 3-D reconstruction were performed by using both Metamorph software (Universal Imaging) and Imaris.

5.3.3. Oxygen Measurements And Total Cell Number By RNA Estimation:

Oxygen measurements were made from two of the reactors at each flow rate and oxygen environment as described earlier using the PreSens Oxy-4 system and custom O₂ dipping Probes (v 1.01). Probes were calibrated prior to use with air saturated water and Oakton Zero Oxygen Solution and measurements were made in the reservoir and reactor sides of the system to reflect inlet and outlet concentrations respectively. The sterilized probes were fitted on the lid of the multiwell system, and immersed at a uniform depth in the medium of all the wells being measured. Multiple measurements from each well were recorded using the Oxy 4 software until a steady state measurement was reached. Data was exported into excel format for analysis. Total RNA to estimate the total cell number was isolated from the scaffolds of the wells where oxygen measurements were made, to

normalize the measurements. One mL of Trizol (Invitrogen) was added directly to the removed scaffolds in 6 well plates. RNA isolation was performed using the RNeasy mini kit (Qiagen) according to manufacturer's protocols (for details refer to appendix). The concentration and quality of purified RNA was determined by assessing the ratio of absorbance at 260nm to 280nm.

5.4. Results:

The data presented below is the result of one experiment. Replicate experiments are currently ongoing.

5.4.1. Overall tissue formation:

The cultures were followed microscopically for the course of the experiment (2 weeks), and no differences in pattern were seen between the groups with or without the presence of the TGF- β inhibitor SB-431542. However all the groups showed an overall uneven distribution of tissue in the 800 channel scaffolds as compared to the earlier 125 channel scaffolds we had used previously. Unlike the earlier experiments where almost all the channels were filled with tissue, there were a lot of packed channels in this case interspersed with some empty ones.

5.4.2. Non parenchymal cell staining and oxygen measurements:

Staining of the cultures for the non-parenchymal cell markers showed that addition of SB-431542 reversed the effects of high flow on SECs at a concentration of 1 μ M. As a result, a high amount of SE-1 staining was seen even in the high flow groups. The images from the low flow groups also showed an abundant amount of SE-1 staining, with even the layer of cells that were adhered on the surface of the scaffolds staining for the marker.

Though the high flow rate group without the presence of inhibitor did not stain for SE-1, the overall SE-1 staining pattern in the low flow group without added inhibitor was also lower than that seen at the same flow rate in our earlier experiments.

Addition of SB-431542 at a concentration of 1 μ M seemed to have no effect on the stellate cells in both the flow groups, which demonstrated the same SMA and GFAP staining patterns as noted in the earlier experiments (data not shown).

Measurement of oxygen concentrations from wells demonstrated the same trend in differences as noted earlier between the two flow rates with higher differences seen in the low flow group. However, both the inlet and outlet concentrations at both the flow rates were higher than noted earlier for flow experiments carried out in the previous reactor designs at the similar oxygen levels in the environment. The oxygen uptake rates also followed the same trend as seen earlier, with higher uptake noted in high flow rates.

Low Flow
(0.2 $\mu\text{l}/\text{channel}/\text{min}$)

High Flow
(1 $\mu\text{l}/\text{channel}/\text{min}$)

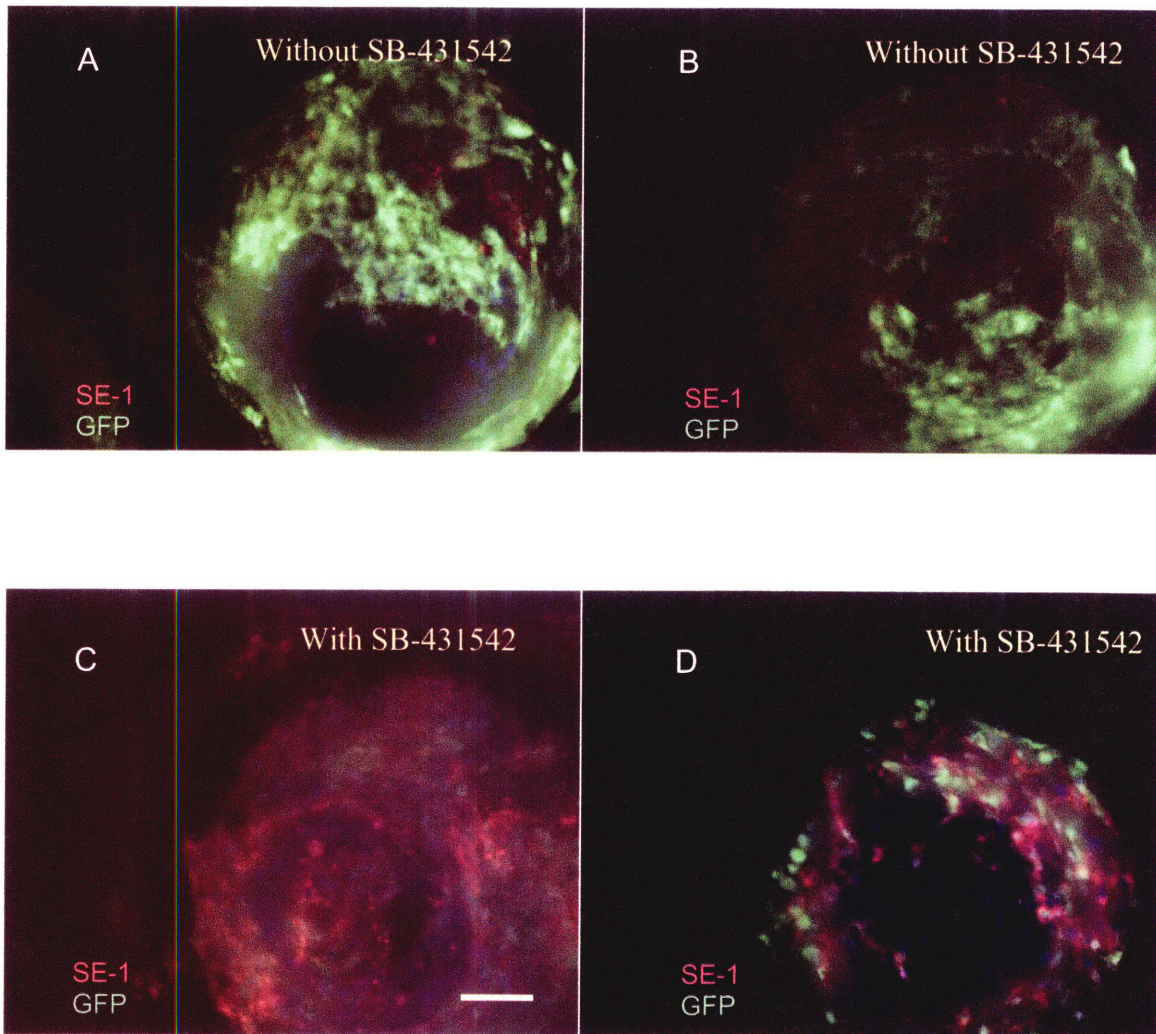


Fig 5.2. Effect of TGF- β inhibition on flow rate effects on sinusoidal endothelial cell survival and phenotype. Confocal images of SE-1 (red) stained co-cultures from single representative channels of reactors either without SB (A & B) or 1 mol SB (C & D) with flow rates of either 0.2 $\mu\text{l}/\text{channel}/\text{min}$ (A & C) or 1 $\mu\text{l}/\text{channel}/\text{min}$ (B & D). Scale bar 50 μm

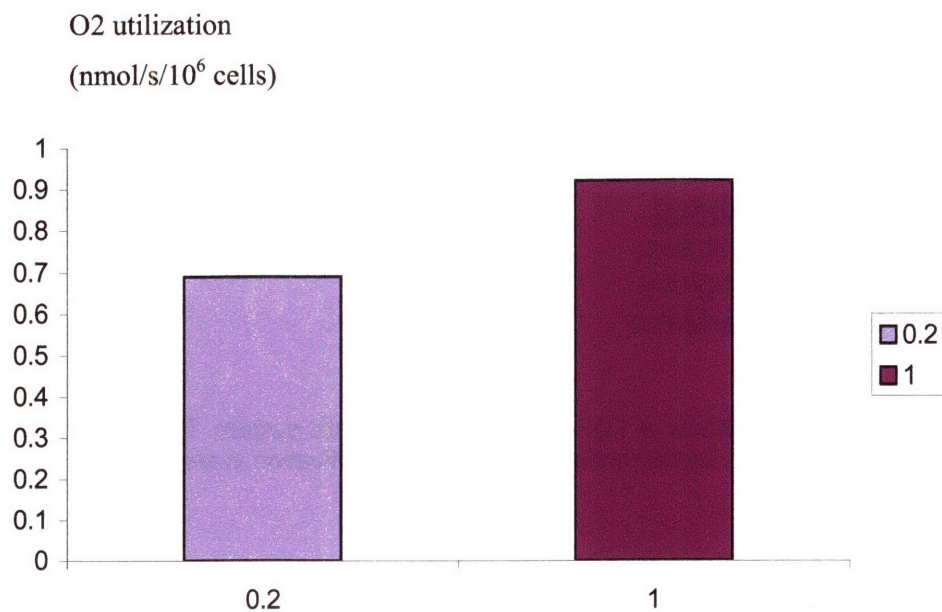
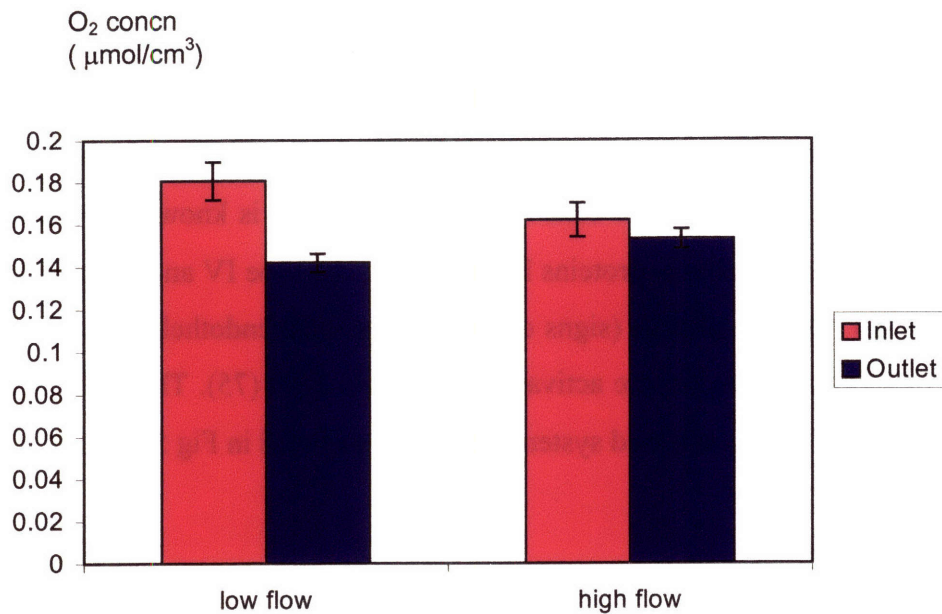


Fig 5.3. Effect of flow rate on oxygen concentrations and uptake in modified reactor system:

(A) Observed concentrations in both reactor and reservoir sides were substantially higher than those seen with the previous design. (B) Calculated oxygen uptake (normalized to recovered cell number estimated by total RNA) followed the earlier observed trend and was higher in the high flow rates.

5.4. Discussion:

After the results from our previous experiments demonstrated that the effects of high flow rates could be overcome in a hypoxic environment, the current set of experiments were aimed at exploring the mechanistic aspect of high flow rates by directly inhibiting the cytokine we suspected to be responsible for its effects. Shear stresses are associated with TGF- β 1 production in endothelial cells (133,141). TGF- β 1 is known to stimulate the synthesis of basement membrane proteins laminin, collagen type IV and entactin (35) in rat liver sinusoidal endothelial cells (signs of loss of sinusoidal endothelial phenotype) and is a major cytokine involved in the activation of stellate cells (75). The sources and effects of TGF- β in an *in vitro* perfused system have been depicted in Fig 5.4.

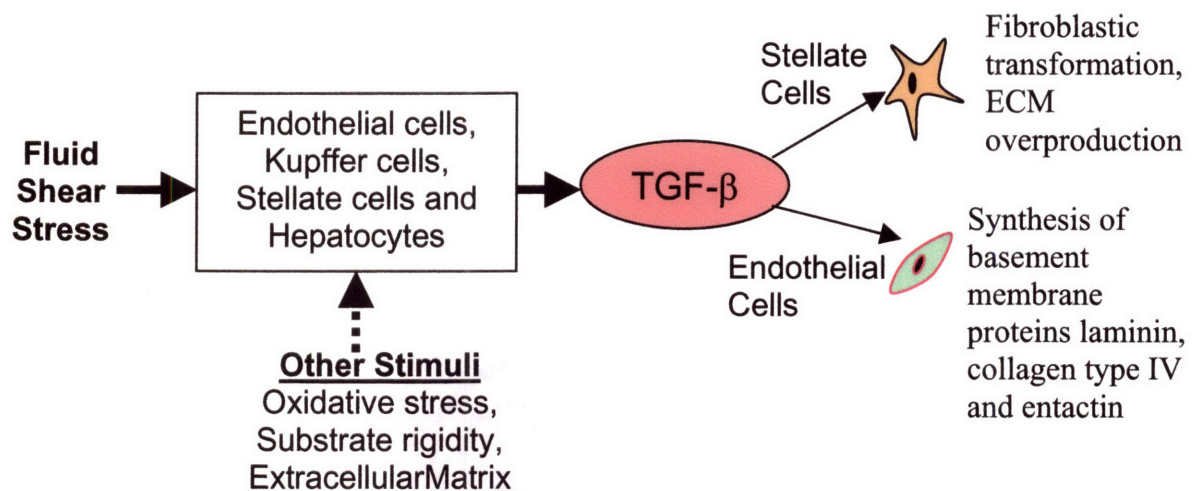


Fig. 5.4. Possible sources and effects of TGF- β in an *in vitro* hepatic system. TGF- β is known to induce effects associated with dedifferentiation in SECs and activation in stellate cells

We chose to explore the mechanistic aspect by examining the role of inhibition of TGF- β on the effects seen with high flow rates. We picked a TGF- β inhibitor, SB-431542, which is known to inhibit the activity of TGF- β 1 activin receptor-like kinases (ALKs), and is selective specifically for ALK-4 (activin type I receptor), ALK-5 (TGF β type I receptor), and ALK-7 (nodal type I receptor) (142). Studies using embryonic stem cell derived endothelial cells (143,144) have shown that it stimulates their proliferation and

differentiation and induces sheet formation at a concentration of 1 μ M. Another study (145) demonstrated its ability to prevent TGF- β induced stimulation of collagen, fibronectin, plasminogen activator inhibitor 1, and connective tissue growth factor gene expression, as well as TGF- β autoinduction, and myofibroblast transdifferentiation in dermal fibroblasts, when used in a concentration of 10 μ M. So far there are no reported studies looking at its effects on adult sinusoidal endothelial cells or hepatic stellate cells.

We carried out flow rate experiments using SB-431542, with an additional modification of seeding using freshly isolated cells instead of spheroids, in an attempt to maximize the SE-1 positive cells and minimize the activated stellate cells we introduce into the system at time zero. Staining results from day 13 demonstrated that SB-431542 reversed the effects of high flow on SECs at a concentration of 1 μ M, with a high amount of SE-1 staining seen in the cultures. This lends support to the postulated TGF- β mediated negative effects of high flow. The SE-1 staining pattern in the low flow group was also increased dramatically as a result of use of SB-431542, possibly due to antagonism of TGF- β produced by non-flow stimuli such as oxidative stress, extracellular matrix, substrate rigidity etc.

The results from our oxygen measurements showed a higher level of saturation of the media compared to the earlier spheroid experiments with similar flow rates. This could possibly be due to two reasons. Our system design modifications that were aimed at ensuring oxygen transfer was enough to sustain the much higher number of cells used were effective in doing so. Secondly the overall packing of channels in a large array scaffold at the seeding density used was not as uniform as that we achieved for the smaller array with spheroids. As a result the interspersed empty channels allow some medium to pass through the scaffold without getting stripped of oxygen providing reservoir and reactor side oxygen values that higher than our earlier experiments at the same flow rates. However the higher oxygen concentrations were beneficial for the purpose of this experiment since we were focusing on reversing the high flow rate effects and any degree of hypoxia could have potentially confounded our results. The postulated mechanism by which SB-431542 acts in our set up have been summarized and represented in Fig 5.5.

At the dosage used (1 μM), SB-431542 showed no demonstrable effect on stellate cell activation by high flow. This could possibly be due to the fact that most published studies using this compound show that a dosage an order of magnitude higher is required to counteract activation due to TGF- β in similar cell types like dermal fibroblasts (145,146). This necessitates future experiments using a higher dosage of SB-431542 to in our system to evaluate its role in preventing stellate activation under high flow rates.

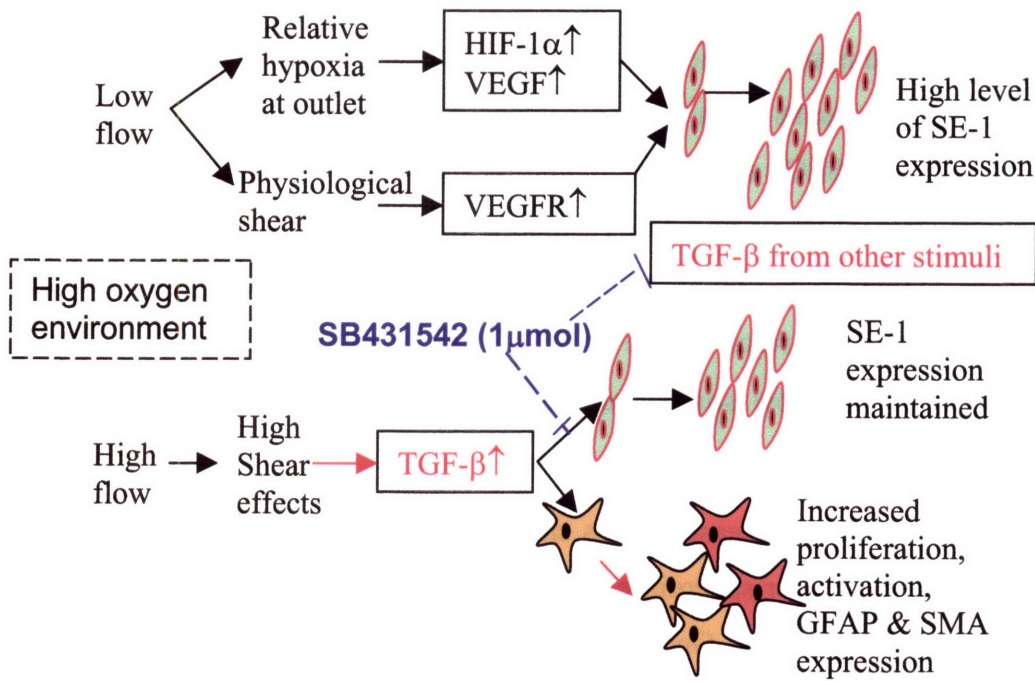


Fig 5.5. Effects of TGF- β inhibition on effects of high flow on non-parenchymal survival and phenotype. SB-431542, a TGF- β 1 inhibitor was found to reverse the effects of high flow on SECs at a concentration of 1 μmol . At the same dosage it showed no demonstrable effect on stellate cell activation by high flow.

The above set of experiments has been completed once and results are awaited from a second set of biological replicates.

Chapter 6:

Summary of Conclusions and Future Directions

6.1. Summary of Conclusions

At the outset, our objective was to design an *in vitro* system that fostered the survival of differentiated sinusoidal endothelial cells by recreating a three dimensional environment recapitulating the necessary stimuli arising out of *in vivo* heterotypic cell-cell contact as well as paracrine interactions. We also wished to provide the necessary stimuli that liver cells experience *in vivo* in the form of shear stresses arising from the flow of blood through the tissue and solute gradients due to circulatory patterns, and evaluate their effect on the survival and phenotype of non-parenchymal cells.

The results of our initial flow experiments with two different flow rates (a lower 0.2 $\mu\text{l}/\text{channel}/\text{min}$ close to physiological values, and a higher 1 $\mu\text{l}/\text{channel}/\text{min}$ representative of pathological conditions such as cirrhosis and portal hypertension) and medium with or without addition of serum and exogenous growth factors showed us that:

- Lower flow rates closer to physiological regimes allow the survival of SE-1 expressing sinusoidal endothelial cells, regardless of the presence of serum and exogenously added growth factors in the medium.
- Higher flow rates, presence of serum and exogenous growth factors in the medium, and scaffold contact were associated with increased proliferation and activation of stellate cells

Though the results showed that microscale flow rates play a significant role in maintaining the balance of non-parenchymal cells, oxygen measurements in the system showed that low flow rates were consistently associated with hypoxic tissue outlet concentrations. This made it important to determine whether the observed effects with

different flow rates were the result of the flow per se or the associated oxygen concentrations and gradients seen across the tissue. In order to decouple these variables we repeated the flow experiments in a normal oxygen environment as before (with 20% O₂) and a relatively hypoxic environment (with 10% O₂). As a result of limited saturation of the medium in the hypoxic environment we were able to achieve lower outlet concentrations even in the high flow rate reactors effectively decoupling the flow and oxygen variables. The experiments from this set of experiments showed us that:

- Retention of SE-1 staining cells was seen even both the flow rates demonstrating that endothelial survival and phenotype at low flow rates was more a function of the hypoxic concentrations, and inducing hypoxic conditions at higher flow rates could even compensate for and overcome any negative effects brought about by direct effects of the flow.
- The relationship of stellate cells with flow rate was unaffected by oxygen concentrations.

While we theorized that hypoxia was helping us overcome negative effects of high flow on sinusoidal endothelial phenotype, we still needed to explore whether the negative effects were mediated by transforming growth factor-beta (TGF- β) that is known to be induced as a result of increased mechanical stress. To achieve this, we added a TGF- β inhibitor SB-431542 in our cultures and repeated the flow rate experiments under normal oxygen concentrations. We found that:

- Inhibiting TGF- β with SB-431542 at a dose of 1 μ M greatly enhanced the presence of SE-1 staining sinusoidal endothelial cells even at high flow rates suggesting that

increased levels of the cytokine may have a role in the loss of phenotype of these cells.

- At the current dosage used (1 μM), SB-431542 had no effect of decreasing the effects seen on stellate cells.

In conclusion we successfully created a three-dimensional flow controlled hepatic culture system that allows balanced survival of hepatocytes and non-parenchymal cells, making it useful as a potential model for studies such as cancer metastasis that require interactions between tumor cells and heterotypic host tissue.

Future Recommendations:

Our studies exploring the effect of flow on the survival and phenotype of SECs used SE-1 (which is used as a staining marker of differentiation for SECs). It would be helpful to confirm the findings of these studies with other phenotypic markers of differentiation such as fenestrations that can be visualized by scanning electron microscopy.

Since our experiments using SB-431542 were aimed at inhibiting the postulated TGF- β effects on SECs at high flow rates, we used a dosage of 1 μM . At this dose, it did not seem to affect stellate cell activation. Published literature using the same compound for decreasing dermal fibroblast activation by TGF- β use a ten fold higher dosage. It might be interesting to plan experiments in our system and evaluate its ability to inhibit stellate cell activation at high flow rates using that dosage, the findings of which could have bearing for its use in cirrhosis.

References

1. Arias IM, Jakoby WB, Popper H, Scachter D, Schafritz DA. Section II.A. Hepatocyte:Metabolism. *The Liver: Biology and Pathobiology, 3rd Ed.* Lippincott Williams & Wilkins, 1997.

Ref Type: Book Chapter

2. Matsumoto T., Kawakami M. The unit-concept of hepatic parenchyma--a re-examination based on angioarchitectural studies. *Acta Pathol.Jpn.*1982; 32 Suppl 2: 285-314.

3. Volwiler W, Willson RA, Larson AM, Ostrow JD. The Liver And Biliary System. *The Gut Course.* University of Washington, Division of Gastroenterology, 2006: 168.

Ref Type: Book Chapter

4. Arias IM, Jakoby WB, Popper H, Scachter D, Schafritz DA. Section IV. The Organ: The Hepatic Microvascular System. *The Liver: Biology and Pathobiology, 3rd Ed.* Lippincott Williams & Wilkins, 1997.

Ref Type: Book Chapter

5. Bloom W., Fawcett D.W. *A Textbook of Histology, 9th Ed.* W. B. Saunders Company, 1968.

Ref Type: Book Chapter

6. Wake K. Structure of the Hepatic Sinusoid. Cells of the hepatic sinusoid. Wisse D.K.E. and Wake, K. 5, 241-246. 2007. Leiden, The Netherlands, Kupffer Cell Foundation. Proceedings of the. International Symposium on Cells of the Hepatic Sinusoid.

7. Arias IM, Jakoby WB, Popper H, Scachter D, Schafritz DA. Section II.C. Sinusoidal Cells. *The Liver: Biology and Pathobiology, 3rd Ed.* Lippincott Williams & Wilkins, 1997.

Ref Type: Book Chapter

8. Braet F., Vanbesien J., De Zanger R., Wisse E. Ageing of the liver sieve and pseudocapillarisation. *Lancet.*2002; 360: 1171-1172.

9. Fehrenbach H., Weiskirchen R., Kasper M., Gressner A. M. Up-regulated expression of the receptor for advanced glycation end products in cultured rat hepatic stellate cells during transdifferentiation to myofibroblasts. *Hepatology.*2001; 34: 943-952.

10. Albanis E., Safadi R., Friedman S. L. Treatment of hepatic fibrosis: almost there. *Curr.Gastroenterol.Rep.*2003; 5: 48-56.

11. Kawada N. Molecular mechanism of stellate cell activation and therapeutic strategy for liver fibrosis. *Comp Hepatol*.2004; 3 Suppl 1: S3.
12. Mabuchi A., Mullaney I., Sheard P., Hessian P., Zimmermann A., Senoo H., Wheatley A. M. Role of Hepatic Stellate Cells in the Early Phase of Liver Regeneration in Rat: Formation of Tight Adhesion to Parenchymal Cells. *Comp Hepatol*.2004; 3 Suppl 1: S29.
13. Malik R., Selden C., Hodgson H. The role of non-parenchymal cells in liver growth. *Semin.Cell Dev.Biol*.2002; 13: 425-431.
14. Bykov I., Ylipaasto P., Eerola L., Lindros K. O. Phagocytosis and LPS-stimulated production of cytokines and prostaglandin E-2 is different in Kupffer cells isolated from the periportal or perivenous liver region. *Scandinavian Journal of Gastroenterology*.2003; 38: 1256-1261.
15. Schuppan D. Structure of the Extracellular-Matrix in Normal and Fibrotic Liver - Collagens and Glycoproteins. *Seminars in Liver Disease*.1990; 10: 1-10.
16. Axel M. G. The cell biology of liver fibrogenesis - an imbalance of proliferation, growth arrest and apoptosis of myofibroblasts. *Cell and Tissue Research*.1998; V292: 447-452.
17. Martinez-Hernandez A., Amenta P. S. The hepatic extracellular matrix. I. Components and distribution in normal liver. *Virchows Arch.A Pathol.Anat.Histopathol*.1993; 423: 1-11.
18. Rojkind M., Giambrone M. A., Biempica L. Collagen types in normal and cirrhotic liver. *Gastroenterology*.1979; 76: 710-719.
19. Griffith L. G., Swartz M. A. Capturing complex 3-D tissue physiology *in vitro*. *Nature Reviews Molecular Cell Biology*.2006; 7: 211-224.
20. Fausto N. Liver regeneration. *Journal of Hepatology*.2000; 32: 19-31.
21. Cressman D. E., Diamond R. H., Taub R. Rapid Activation of the Stat3 Transcription Complex in Liver-Regeneration. *Hepatology*.1995; 21: 1443-1449.
22. Bissell D. M., Wang S. S., Jarnagin W. R., Roll F. J. Cell-Specific Expression of Transforming Growth-Factor-Beta in Rat-Liver - Evidence for Autocrine Regulation of Hepatocyte Proliferation. *Journal of Clinical Investigation*.1995; 96: 447-455.
23. Boulton R., Woodman A., Calnan D., Selden C., Tam F., Hodgson H. Nonparenchymal cells from regenerating rat liver generate interleukin-1 alpha and -1 beta: A mechanism of negative regulation of hepatocyte proliferation. *Hepatology*.1997; 26: 49-58.

24. Schirmacher P., Geerts A., Pietrangelo A., Dienes H. P., Rogler C. E. Hepatocyte Growth-Factor Hepatopoietin-A Is Expressed in Fat-Storing Cells from Rat-Liver But Not Myofibroblast-Like Cells Derived from Fat-Storing Cells. *Hepatology*.1992; 15: 5-11.
25. Morin O., Normand C. Long-Term Maintenance of Hepatocyte Functional-Activity in Coculture - Requirements for Sinusoidal Endothelial-Cells and Dexamethasone. *Journal of Cellular Physiology*.1986; 129: 103-110.
26. Goulet F., Normand C., Morin O. Cellular Interactions Promote Tissue-Specific Function, Biomatrix Deposition and Junctional Communication of Primary Cultured-Hepatocytes. *Hepatology*.1988; 8: 1010-1018.
27. Nahmias Y., Schwartz R. E., Hu W. S., Verfaillie C. M., Odde D. J. Endothelium-mediated hepatocyte recruitment in the establishment of liver-like tissue *in vitro*. *Tissue Engineering*.2006; 12: 1627-1638.
28. Krause P., Markus P. M., Schwartz P., Unthan-Fechner K., Pestel S., Fandrey J., Probst I. Hepatocyte-supported serum-free culture of rat liver sinusoidal endothelial cells. *Journal of Hepatology*.2000; 32: 718-726.
29. Edwards S., Lalor P. F., Nash G. B., Rainger G. E., Adams D. H. Lymphocyte traffic through sinusoidal endothelial cells is regulated by hepatocytes. *Hepatology*.2005; 41: 451-459.
30. Mochida S., Ishikawa K., Toshima K., Inao M., Ikeda H., Matsui A., Shibuya M., Fujiwara K. The mechanisms of hepatic sinusoidal endothelial cell regeneration: A possible communication system associated with vascular endothelial growth factor in liver cells. *Journal of Gastroenterology and Hepatology*.1998; 13: S1-S5.
31. Sato T., El Assal O. N., Ono T., Yamanoi A., Dhar D. K., Nagasue N. Sinusoidal endothelial cell proliferation and expression of angiopoietin/Tie family in regenerating rat liver. *Journal of Hepatology*.2001; 34: 690-698.
32. Shimizu H., Miyazaki M., Wakabayashi Y., Mitsunashi N., Kato A., Ito H., Nakagawa K., Yoshidome H., Kataoka M., Nakajima N. Vascular endothelial growth factor secreted by replicating hepatocytes induces sinusoidal endothelial cell proliferation during regeneration after partial hepatectomy in rats. *Journal of Hepatology*.2001; 34: 683-689.
33. Modis L., Martinez-Hernandez A. Hepatocytes modulate the hepatic microvascular phenotype. *Lab Invest*.1991; 65: 661-670.
34. Deleve L. D., Wang X. D., Hu L. P., McCuskey M. K., McCuskey R. S. Rat liver sinusoidal endothelial cell phenotype is maintained by paracrine and autocrine regulation. *American Journal of Physiology-Gastrointestinal and Liver Physiology*.2004; 287: G757-G763.

35. Neubauer K., Kruger M., Quondamatteo F., Knittel T., Saile B., Ramadori G. Transforming growth factor-beta 1 stimulates the synthesis of basement membrane proteins laminin, collagen type IV and entactin in rat liver sinusoidal endothelial cells. *Journal of Hepatology*.1999; 31: 692-702.
36. Pinzani M., Gesualdo L., Sabbah G. M., Abboud H. E. Effects of Platelet-Derived Growth-Factor and Other Polypeptide Mitogens on Dna-Synthesis and Growth of Cultured Rat-Liver Fat-Storing Cells. *Journal of Clinical Investigation*.1989; 84: 1786-1793.
37. Paralkar V. M., Vukicevic S., Reddi A. H. Transforming Growth-Factor-Beta Type-1 Binds to Collagen-Iv of Basement-Membrane Matrix - Implications for Development. *Developmental Biology*.1991; 143: 303-308.
38. Swartz M. A. Signaling in morphogenesis: transport cues in morphogenesis. *Current Opinion in Biotechnology*.2003; 14: 547-550.
39. Pinkse G. G. M., Voorhoeve M. P., Noteborn M., Terpstra O. T., Bruijn J. A., de Heer E. Hepatocyte survival depends on beta 1-integrin-mediated attachment of hepatocytes to hepatic extracellular matrix. *Liver International*.2004; 24: 218-226.
40. Pinkse G. G. M., Jiawan-Lalai R., Bruijn J. A., de Heer E. RGD peptides confer survival to hepatocytes via the beta 1-integrin-ILK-pAkt pathway. *Journal of Hepatology*.2005; 42: 87-93.
41. Nagaoka M., Ise H., Akaike T. Immobilized E-cadherin model can enhance cell attachment and differentiation of primary hepatocytes but not proliferation. *Biotechnology Letters*.2002; 24: 1857-1862.
42. Lampugnani M. G., Dejana E. Interendothelial junctions: structure, signalling and functional roles. *Curr.Opin.Cell Biol*.1997; 9: 674-682.
43. Ruoslahti E. RGD and other recognition sequences for integrins. *Annu.Rev Cell Dev.Biol*.1996; 12: 697-715.
44. Couvelard A., Scoazec J. Y., Feldmann G. Expression of Cell-Cell and Cell-Matrix Adhesion Proteins by Sinusoidal Endothelial-Cells in the Normal and Cirrhotic Human Liver. *American Journal of Pathology*.1993; 143: 738-752.
45. Mcguire R. F., Bissell D. M., Boyles J., Roll F. J. Role of Extracellular-Matrix in Regulating Fenestrations of Sinusoidal Endothelial-Cells Isolated from Normal Rat-Liver. *Hepatology*.1992; 15: 989-997.
46. Iwamoto H., Sakai H., Nawata H. Inhibition of integrin signaling with Arg-Gly-Asp motifs in rat hepatic stellate cells. *Journal of Hepatology*.1998; 29: 752-759.
47. Gressner A. M. Cytokines and Cellular Crosstalk Involved in the Activation of Fat-Storing Cells. *Journal of Hepatology*.1995; 22: 28-36.

48. Jarnagin W. R., Rockey D. C., Koteliansky V. E., Wang S. S., Bissell D. M. Expression of variant fibronectins in wound healing: cellular source and biological activity of the EIIIA segment in rat hepatic fibrogenesis. *The Journal of Cell Biology*.1994; 127: 2037-2048.
49. Awata R., Sawai H., Imai K., Terada K., Senoo H., Sugiyama T. Morphological comparison and functional reconstitution of rat hepatic parenchymal cells on various matrices. *Journal of Gastroenterology and Hepatology*.1998; 13: S55-S61.
50. Korff T., Augustin H. G. Integration of endothelial cells in multicellular spheroids prevents apoptosis and induces differentiation. *Journal of Cell Biology*.1998; 143: 1341-1352.
51. Buhler R., Lindros K. O., Nordling A., Johansson I., Ingelmannsundberg M. Zonation of Cytochrome-P450 Isozyme Expression and Induction in Rat-Liver. *European Journal of Biochemistry*.1992; 204: 407-412.
52. Anundi I., Lahteenmaki T., Rundgren M., Moldeus P., Lindros K. O. Zonation of Acetaminophen Metabolism and Cytochrome-P450 2E1-Mediated Toxicity Studied in Isolated Periportal and Perivenous Hepatocytes. *Biochemical Pharmacology*.1993; 45: 1251-1259.
53. Jungermann K., Katz N. Functional Hepatocellular Heterogeneity. *Hepatology*.1982; 2: 385-395.
54. Wisse E., Dezanger R. B., Jacobs R., McCuskey R. S. Scanning Electron-Microscope Observations on the Structure of Portal Veins, Sinusoids and Central Veins in Rat-Liver. *Scanning Electron Microscopy*.1983; 1441-1452.
55. Wake K., Sato T. Intralobular Heterogeneity of Perisinusoidal Stellate Cells in Porcine Liver. *Cell and Tissue Research*.1993; 273: 227-237.
56. Shigeki A., Masayuki I. Physiological role of sinusoidal endothelial cells and Kupffer cells and their implication in the pathogenesis of liver injury. *Journal of Hepato-Biliary-Pancreatic Surgery*.2000; V7: 40-48.
57. Braet F., Shleper M., Paizi M., Brodsky S., Kopeiko N., Resnick N., Spira G. Liver sinusoidal endothelial cell modulation upon resection and shear stress *in vitro*. *Comp Hepatol*.2004; 3: 7.
58. Sakata R., Ueno T., Nakamura T., Ueno H., Sata M. Mechanical stretch induces TGF-beta synthesis in hepatic stellate cells. *European Journal of Clinical Investigation*.2004; 34: 129-136.
59. Smedsrod B., Johansson S., Pertoft H. Studies *In vivo* and *In vitro* on the Uptake and Degradation of Soluble Collagen Alpha-1(I) Chains in Rat-Liver Endothelial and Kupffer Cells. *Biochemical Journal*.1985; 228: 415-424.

60. Maher J. J., Mcguire R. F. Extracellular-Matrix Gene-Expression Increases Preferentially in Rat Lipocytes and Sinusoidal Endothelial-Cells During Hepatic-Fibrosis *In vivo*. *Journal of Clinical Investigation*.1990; 86: 1641-1648.
 61. DeZanger R, Braet F, Augustin HG, Wisse E. Prolongation of hepatic endothelial cell cultures by phorbol myristate acetate. In: Wisse E, Kohn EC, Barakat AI, eds. *Cells of the Hepatic Sinusoid 6*. Leiden: Kupffer Cell Foundation, 2007: 97-101.
- Ref Type: Book Chapter
62. Deleve L. D., Wang X. D., McCuskey M. K., McCuskey R. S. Rat liver endothelial cells isolated by anti-CD31 immunomagnetic separation lack fenestrae and sieve plates. *American Journal of Physiology-Gastrointestinal and Liver Physiology*.2006; 291: G1187-G1189.
 63. Ohmura T., Enomoto K., Satoh H., Sawada N., Mori M. Establishment of a novel monoclonal antibody, SE-1, which specifically reacts with rat hepatic sinusoidal endothelial cells. *J Histochem.Cytochem*.1993; 41: 1253-1257.
 64. Zhang Y. J., Ikejima K., Honda H., Kitamura T., Takei Y., Sato N. Glycine prevents apoptosis of rat sinusoidal endothelial cells caused by deprivation of vascular endothelial growth factor. *Hepatology*.2000; 32: 542-546.
 65. Samarasinghe D. A. Culture of sinusoidal endothelial cells from rat liver. *Journal of Gastroenterology and Hepatology*.1998; 13: 851-854.
 66. Enomoto K., Nishikawa Y., Omori Y., Tokairin T., Yoshida M., Ohi N., Nishimura T., Yamamoto Y., Li Q. Cell biology and pathology of liver sinusoidal endothelial cells. *Med.Electron Microsc*.2004; 37: 208-215.
 67. Irving M. G., Roll F. J., Huang S., Bissell D. M. Characterization and Culture of Sinusoidal Endothelium from Normal Rat-Liver - Lipoprotein Uptake and Collagen Phenotype. *Gastroenterology*.1984; 87: 1233-1247.
 68. Yamane A., Seetharam L., Yamaguchi S., Gotoh N., Takahashi T., Neufeld G., Shibuya M. A New Communication-System Between Hepatocytes and Sinusoidal Endothelial-Cells in Liver Through Vascular Endothelial Growth-Factor and Flt Tyrosine Kinase Receptor Family (Flt-1 and Kdr/Flk-1). *Oncogene*.1994; 9: 2683-2690.
 69. Ross M. A., Sander C. M., Kleeb T. B., Watkins S. C., Stolz D. B. Spatiotemporal expression of angiogenesis growth factor receptors during the revascularization of regenerating rat liver. *Hepatology*.2001; 34: 1135-1148.
 70. Elvevold K., Nedredal G. I., Revhaug A., Bertheussen K., Smedsrod B. Long-term preservation of high endocytic activity in primary cultures of pig liver sinusoidal endothelial cells. *European Journal of Cell Biology*.2005; 84: 749-764.

71. Friedman S. L., Roll F. J., Boyles J., Arenson D. M., Bissell D. M. Maintenance of Differentiated Phenotype of Cultured Rat Hepatic Lipocytes by Basement-Membrane Matrix. *Journal of Biological Chemistry*.1989; 264: 10756-10762.
 72. Geerts A., Vrijssen R., Rauterberg J., Burt A., Schellinck P., Wisse E. *In vitro* Differentiation of Fat-Storing Cells Parallels Marked Increase of Collagen-Synthesis and Secretion. *Journal of Hepatology*.1989; 9: 59-68.
 73. Senoo H., Hata R. Extracellular-Matrix Regulates and L-Ascorbic-Acid 2-Phosphate Further Modulates Morphology, Proliferation, and Collagen-Synthesis of Perisinusoidal Stellate Cells. *Biochemical and Biophysical Research Communications*.1994; 200: 999-1006.
 74. Senoo H., Imai K., Sato M., Kojima N., Miura M., Hata R. I. Three-dimensional structure of extracellular matrix reversibly regulates morphology, proliferation and collagen metabolism of perisinusoidal stellate cells (vitamin A-storing cells). *Cell Biology International*.1996; 20: 501-512.
 75. Friedman S. L. Molecular regulation of hepatic fibrosis, an integrated cellular response to tissue injury. *Journal of Biological Chemistry*.2000; 275: 2247-2250.
 76. LeCluyse E. L. Human hepatocyte culture systems for the *in vitro* evaluation of cytochrome P450 expression and regulation. *Eur.J Pharm.Sci*.2001; 13: 343-368.
 77. Sivaraman A., Leach J. K., Townsend S., Iida T., Hogan B. J., Stolz D. B., Fry R., Samson L. D., Tannenbaum S. R., Griffith L. G. A microscale *in vitro* physiological model of the liver: predictive screens for drug metabolism and enzyme induction. *Curr.Drug Metab*.2005; 6: 569-591.
 78. Powers M. J., Domansky K., Kaazempur-Mofrad M. R., Kalezi A., Capitano A., Upadhyaya A., Kurzawski P., Wack K. E., Stolz D. B., Kamm R., Griffith L. G. A microfabricated array bioreactor for perfused 3-D liver culture. *Biotechnol.Bioeng*.2002; 78: 257-269.
 79. Powers M. J., Janigian D. M., Wack K. E., Baker C. S., Beer S. D., Griffith L. G. Functional behavior of primary rat liver cells in a three-dimensional perfused microarray bioreactor. *Tissue Eng*.2002; 8: 499-513.
 80. Domansky K, Sivaraman A, Griffith L.G.. Micromachined Bioreactor for in Vitro Cell Self-Assembly and 3-D Tissue Formation. In: Andersson H and van den Berg A, eds. *Lab-on-Chips for Cellomics. Micro and Nanotechnologies for Life Science*. 13. Netherlands: Kluwer Academic Publishers, 2006: 319-346.
- Ref Type: Book, Chapter
81. Liotta L. A., Kohn E. C. The microenvironment of the tumor-host interface. *Nature*.2001; 411: 375-379.

82. Fuchs E., Raghavan S. Getting under the skin of epidermal morphogenesis. *Nature Reviews Genetics*.2002; 3: 199-209.
83. Loreal O., Levavasseur F., Fromaget C., Gros D., Guillouzo A., Clement B. Cooperation of Ito Cells and Hepatocytes in the Deposition of An Extracellular-Matrix *In vitro*. *American Journal of Pathology*.1993; 143: 538-544.
84. Rojkind M., Novikoff P. M., Greenwel P., Rubin J., Rojasvalencia L., Decarvalho A. C., Stockert R., Spray D., Hertzberg E. L., Wolkoff A. W. Characterization and Functional-Studies on Rat-Liver Fat-Storing Cell-Line and Freshly Isolated Hepatocyte Coculture System. *American Journal of Pathology*.1995; 146: 1508-1520.
85. Billiar T., Curran R., Hoffman R., Bentz B., Simmons R. Ng-Monomethyl-L-Arginine (Nmma) Blocks Kupffer Cell Suppression of Hepatocyte Protein-Synthesis But Not Tnf Or Il-1 Release in Response to Lps. *Journal of Leukocyte Biology*.1988; 44: 292.
86. Matsuo R., Ukida M., Nishikawa Y., Omori N., Tsuji T. The Role of Kupffer Cells in Complement Activation in D-Galactosamine Lipopolysaccharide-Induced Hepatic-Injury of Rats. *Acta Medica Okayama*.1992; 46: 345-354.
87. Fraslin J. M., Kneip B., Vaulont S., Glaise D., Munnich A., Guguenguillouzo C. Dependence of Hepatocyte-Specific Gene-Expression on Cell-Cell Interactions in Primary Culture. *Embo Journal*.1985; 4: 2487-2491.
88. Schrode W., Mecke D., Gebhardt R. Induction of glutamine synthetase in periportal hepatocytes by cocultivation with a liver epithelial cell line. *Eur.J Cell Biol*.1990; 53: 35-41.
89. Fry J. R., Bridges J. W. A novel mixed hepatocyte-fibroblast culture system and its use as a test for metabolism-mediated cytotoxicity. *Biochem Pharmacol*.1977; 26: 969-973.
90. Shimaoka S., Nakamura T., Ichihara A. Stimulation of Growth of Primary Cultured Adult-Rat Hepatocytes Without Growth-Factors by Coculture with Nonparenchymal Liver-Cells. *Experimental Cell Research*.1987; 172: 228-242.
91. Elsdale T., Bard J. Collagen substrata for studies on cell behavior. *J Cell Biol*.1972; 54: 626-637.
92. Hay E. D., Dodson J. W. Secretion of collagen by corneal epithelium. I. Morphology of the collagenous products produced by isolated epithelia grown on frozen-killed lens. *J Cell Biol*.1973; 57: 190-213.
93. Emerman J. T., Pitelka D. R. Maintenance and induction of morphological differentiation in dissociated mammary epithelium on floating collagen membranes. *In vitro*.1977; 13: 316-328.

94. Bissell M. J. The differentiated state of normal and malignant cells or how to define a "normal" cell in culture. *Int.Rev.Cytol.*1981; 70: 27-100.
95. Ingber D. E., Folkman J. How does extracellular matrix control capillary morphogenesis? *Cell.*1989; 58: 803-805.
96. Bissell M. J., Radisky D. C., Rizki A., Weaver V. M., Petersen O. W. The organizing principle: microenvironmental influences in the normal and malignant breast. *Differentiation.*2002; 70: 537-546.
97. Ingber D. E. Cancer as a disease of epithelial-mesenchymal interactions and extracellular matrix regulation. *Differentiation.*2002; 70: 547-560.
98. Roskelley C. D., Srebrow A., Bissell M. J. A hierarchy of ECM-mediated signalling regulates tissue-specific gene expression. *Curr.Opin.Cell Biol.*1995; 7: 736-747.
99. Radisky D., Muschler J., Bissell M. J. Order and disorder: the role of extracellular matrix in epithelial cancer. *Cancer Invest.*2002; 20: 139-153.
100. Cunha G. R., Hayward S. W., Wang Y. Z. Role of stroma in carcinogenesis of the prostate. *Differentiation.*2002; 70: 473-485.
101. Knight B., Laukaitis C., Akhtar N., Hotchin N. A., Edlund M., Horwitz A. R. Visualizing muscle cell migration in situ. *Curr.Biol.*2000; 10: 576-585.
102. Roskelley C. D., Desprez P. Y., Bissell M. J. Extracellular matrix-dependent tissue-specific gene expression in mammary epithelial cells requires both physical and biochemical signal transduction. *Proc Natl Acad Sci U S A.*1994; 91: 12378-12382.
103. Li A. P., Colburn S. M., Beck D. J. A simplified method for the culturing of primary adult rat and human hepatocytes as multicellular spheroids. *In vitro Cell Dev.Biol.*1992; 28A: 673-677.
104. Yuasa C., Tomita Y., Shono M., Ishimura K., Ichihara A. Importance of cell aggregation for expression of liver functions and regeneration demonstrated with primary cultured hepatocytes. *J Cell Physiol.*1993; 156: 522-530.
105. Takezawa T., Yamazaki M., Mori Y., Yonaha T., Yoshizato K. Morphological and immuno-cytochemical characterization of a hetero-spheroid composed of fibroblasts and hepatocytes. *J Cell Sci.*1992; 101 (Pt 3): 495-501.
106. Tong J. Z., De Lagausie P., Furlan V., Cresteil T., Bernard O., Alvarez F. Long-term culture of adult rat hepatocyte spheroids. *Exp.Cell Res.*1992; 200: 326-332.

107. Lin K. H., Maeda S., Saito T. Long-term maintenance of liver-specific functions in three-dimensional culture of adult rat hepatocytes with a porous gelatin sponge support. *Biotechnol.Appl.Biochem.*1995; 21 (Pt 1): 19-27.
108. Gerlach J. C. Use of hepatocyte cultures for liver support bioreactors. *Adv.Exp.Med.Biol.*1994; 368: 165-171.
109. Martin Y., Vermette P. Bioreactors for tissue mass culture: design, characterization, and recent advances. *Biomaterials.*2005; 26: 7481-7503.
110. Morin J. P., Preterre D., Keravec V., Thuillez C. Rotating wall vessel as a new *in vitro* shear stress generation system: application to rat coronary endothelial cell cultures. *Cell Biol.Toxicol.*2003; 19: 227-242.
111. MacDonald J. M., Wolfe S. P., Roy-Chowdhury I., Kubota H., Reid L. M. Effect of flow configuration and membrane characteristics on membrane fouling in a novel multicoaxial hollow-fiber bioartificial liver. *Ann.N.Y.Acad Sci.*2001; 944: 334-343.
112. Zeilinger K., Holland G., Sauer I. M., Efimova E., Kardassis D., Obermayer N., Liu M., Neuhaus P., Gerlach J. C. Time course of primary liver cell reorganization in three-dimensional high-density bioreactors for extracorporeal liver support: an immunohistochemical and ultrastructural study. *Tissue Eng.*2004; 10: 1113-1124.
113. Song J. W., Gu W., Futai N., Warner K. A., Nor J. E., Takayama S. Computer-controlled microcirculatory support system for endothelial cell culture and shearing. *Anal.Chem.*2005; 77: 3993-3999.
114. Kellner K., Liebsch G., Klimant I., Wolfbeis O. S., Blunk T., Schulz M. B., Gopferich A. Determination of oxygen gradients in engineered tissue using a fluorescent sensor. *Biotechnol.Bioeng.*2002; 80: 73-83.
115. Glicklis R., Merchuk J. C., Cohen S. Modeling mass transfer in hepatocyte spheroids via cell viability, spheroid size, and hepatocellular functions. *Biotechnol.Bioeng.*2004; 86: 672-680.
116. Matsumura T., Thurman R. G. Measuring rates of O₂ uptake in periportal and pericentral regions of liver lobule: stop-flow experiments with perfused liver. *Am.J Physiol.*1983; 244: G656-G659.
117. Matsumura T., Yoshihara H., Jeffs R., Takei Y., Nukina S., Hijioka T., Evans R. K., Kauffman F. C., Thurman R. G. Hormones increase oxygen uptake in periportal and pericentral regions of the liver lobule. *Am.J Physiol.*1992; 262: G645-G650.

118. Guppy M., Leedman P., Zu X., Russell V. Contribution by different fuels and metabolic pathways to the total ATP turnover of proliferating MCF-7 breast cancer cells. *Biochem J.*2002; 364: 309-315.
119. Andersson H., van den B. A. Microfabrication and microfluidics for tissue engineering: state of the art and future opportunities. *Lab Chip.*2004; 4: 98-103.
120. Rigby P. J., Goldie R. G. Confocal microscopy in biomedical research. *Croat.Med.J.*1999; 40: 346-352.
121. Ishiguro S., Arai S., Monden K., Adachi Y., Funaki N., Higashitsuji H., Fujita S., Furutani M., Mise M., Kitao T., . Identification of the thromboxane A2 receptor in hepatic sinusoidal endothelial cells and its role in endotoxin-induced liver injury in rats. *Hepatology.*1994; 20: 1281-1286.
122. Naito M., Hasegawa G., Ebe Y., Yamamoto T. Differentiation and function of Kupffer cells. *Med.Electron Microsc.*2004; 37: 16-28.
123. Griffith L. G., Naughton G. Tissue engineering--current challenges and expanding opportunities. *Science.*2002; 295: 1009-1014.
124. Domansky K, Inman W, Serdy J, Griffith LG. Multiwell Cell Culture Plate Format with Integrated Microfluidic Perfusion System. 6112, 61120F-1-61120F-7. 2006. San Jose. Proceedings of SPIE, Microfluidics, BioMEMS, and Medical Microsystems IV. 1-23-2006.
125. Domansky K, Inman W, Serdy J, Griffith LG. Perfused Microreactors for Liver Tissue Engineering. 2005. Shanghai. Proceedings of the 27th International Conference of the IEEE-EMBS. 9-1-2005.
126. Smedsrod B., Pertoft H., Eggertsen G., Sundstrom C. Functional and Morphological Characterization of Cultures of Kupffer Cells and Liver Endothelial-Cells Prepared by Means of Density Separation in Percoll, and Selective Substrate Adherence. *Cell and Tissue Research.*1985; 241: 639-649.
127. Ito S., Nakanishi H., Ikehara Y., Kato T., Kasai Y., Ito K., Akiyama S., Nakao A., Tatematsu M. Real-time observation of micrometastasis formation in the living mouse liver using a green fluorescent protein gene-tagged rat tongue carcinoma cell line. *International Journal of Cancer.*2001; 93: 212-217.
128. Block G. D., Locker J., Bowen W. C., Petersen B. E., Katyal S., Strom S. C., Riley T., Howard T. A., Michalopoulos G. K. Population expansion, clonal growth, and specific differentiation patterns in primary cultures of hepatocytes induced by HGF/SF, EGF and TGF alpha in a chemically defined (HGM) medium. *J Cell Biol.*1996; 132: 1133-1149.
129. Braet F., Dezanger R., Sasaoki T., Baekeland M., Janssens P., Smedsrod B., Wisse E. Methods in Laboratory Investigation - Assessment of A Method of

Isolation, Purification, and Cultivation of Rat-Liver Sinusoidal Endothelial-Cells. Laboratory Investigation.1994; 70: 944-952.

130. Knook D. L., Sleyster E. C. Separation of Kupffer and Endothelial Cells of Rat-Liver by Centrifugal Elutriation. Experimental Cell Research.1976; 99: 444-449.
131. Tokairin T, Nishikawa Y, Doi YK, Watanabe H, Yoshioka T, Su M, Omori Y, Enomoto K. A highly specific isolation of rat sinusoidal endothelial cells by the immunomagnetic bead method using SE-1 monoclonal antibody. Journal of Hepatology 36[6], 725-733. 2002.
132. Pinzani M. Hepatic Stellate (Ito) Cells - Expanding Roles for A Liver-Specific Pericyte. Journal of Hepatology.1995; 22: 700-706.
133. Ohno M., Cooke J. P., Dzau V. J., Gibbons G. H. Fluid Shear-Stress Induces Endothelial Transforming Growth-Factor-Beta-1 Transcription and Production - Modulation by Potassium Channel Blockade. Journal of Clinical Investigation.1995; 95: 1363-1369.
134. Xu B., Broome U., Uzunel M., Nava S., Ge X. P., Kumagai-Braesch M., Hultenby K., Christensson B., Ericzon B. G., Holgersson J., Sumitran-Holgersson S. Capillarization of hepatic sinusoid by liver endothelial cell-reactive autoantibodies in patients with cirrhosis and chronic hepatitis. American Journal of Pathology.2003; 163: 1275-1289.
135. Braet F., Muller M., Vekemans K., Wisse E., Le Couteur D. G. Antimycin A-induced defenestration in rat hepatic sinusoidal endothelial cells. Hepatology.2003; 38: 394-402.
136. Hellerbrand C., Stefanovic B., Giordano F., Burchardt E. R., Brenner D. A. The role of TGF beta 1 in initiating hepatic stellate cell activation *in vivo*. Journal of Hepatology.1999; 30: 77-87.
137. Rotem A., Toner M., Tompkins R. G., Yarmush M. L. Oxygen-Uptake Rates in Cultured Rat Hepatocytes. Biotechnology and Bioengineering.1992; 40: 1286-1291.
138. Semenza G. L. Signal transduction to hypoxia-inducible factor 1. Biochemical Pharmacology.2002; 64: 993-998.
139. Shi Y. F., Fong C. C., Zhang Q., Cheung P. Y., Tzang C. H., Wu R. S., Yang M. Hypoxia induces the activation of human hepatic stellate cells LX-2 through TGF-beta signaling pathway. FEBS Lett.2007; 581: 203-210.
140. Sonna L. A., Cullivan M. L., Sheldon H. K., Pratt R. E., Lilly C. M. Effect of hypoxia on gene expression by human hepatocytes (HepG2). Physiological Genomics.2003; 12: 195-207.

141. Lum R. M., Wiley L. M., Barakat A. I. Influence of different forms of fluid shear stress on vascular endothelial TGF-beta 1 mRNA expression. *International Journal of Molecular Medicine*.2000; 5: 635-641.
142. Inman G. J., Nicolas F. J., Callahan J. F., Harling J. D., Gaster L. M., Reith A. D., Laping N. J., Hill C. S. SB-431542 is a potent and specific inhibitor of transforming growth factor-beta superfamily type I activin receptor-like kinase (ALK) receptors ALK4, ALK5, and ALK7. *Molecular Pharmacology*.2002; 62: 65-74.
143. Watabe T., Nishihara A., Mishima K., Yamashita J., Shimizu K., Miyazawa K., Nishikawa S., Miyazono K. TGF-beta receptor kinase inhibitor enhances growth and integrity of embryonic stem cell-derived endothelial cells. *Journal of Cell Biology*.2003; 163: 1303-1311.
144. Watabe T., Yamashita J. K., Mishima K., Miyazono K. TGF-beta signaling in embryonic stem cell-derived endothelial cells. *Methods Mol.Biol*.2006; 330: 341-351.
145. Mori Y., Ishida W., Bhattacharyya S., Li Y., Platanius L. C., Varga J. Selective inhibition of activin receptor-like kinase 5 signaling blocks profibrotic transforming growth factor beta responses in skin fibroblasts. *Arthritis Rheum*.2004; 50: 4008-4021.
146. Hasegawa T., Nakao A., Sumiyoshi K., Tsuchihashi H., Ogawa H. SB-431542 inhibits TGF-beta-induced contraction of collagen gels by normal and keloid fibroblasts. *Journal of Dermatological Science*.2005; 39: 33-38.

Appendices

Appendix 1 - HGM formulation

HGM is made with the base medium DMEM (Gibco 11054-020) with the additives listed below. For every 500mL bottle of DMEM add the following:

Chemical name	Amount to add	Final concentration	Stock concentration	Order information
L-proline	0.015g	0.03g/L	N/A	Sigma P-4655
L-ornithine	0.05g	0.1g/L	N/A	Sigma O-6503
Niacinamide	0.153g	0.305g/L	N/A	Sigma N-0636
D-(+)-glucose	0.5g	2g/L	N/A	Sigma G-7021
D-(+)-galactose	1g	2g/L	N/A	Sigma G-5388
Bovine serum albumin	1g	2g/L	N/A	Sigma A-9647
Trace metal:				
ZnCl ₂	5µl of stock	0.0544 mg/L		5.44 mg/mL
ZnSO ₄ ·7H ₂ O	5µl of stock	0.075 mg/L		7.5 mg/mL
CuSO ₄ ·5H ₂ O	5µl of stock	0.02 mg/L		2 mg/mL
MnSO ₄	5µl of stock	0.025 mg/L		2.5mg/mL
Sterile filter the solution and add the following				
Penicillin- Streptomycin ¹	0.5 mL	10 unit/mL 10 µg/mL	10,000 unit/mL 10 mg/mL	Sigma P-0781
L-glutamine ²	2.5 mL	1 mM	200 mM	Gibco 25030-081
Insulin-Transferrin- Sodium Selenite ³	500 µl	5 mg/L 5 mg/L 5 µg/L	5 g/L 5 g/L 5 mg/L	Roche 1074547
Dexamethasone ⁴	400 µl	0.1 µM	0.05 mg/mL	Sigma D-8893
EGF ⁵	200 µl	20 ng/mL	0.050 mg/mL	Collaborative 40001

Appendix 2 - Protocol For Isolation and Viability Test of Hepatocytes

Materials:

Ice Bucket, Pre-Autoclaved Funnel with 300 μ m mesh, Trypan Blue, Hemostat and tissue forceps, DAG [500 ml DMEM (Gibco 11054-020) with 1 gm of added bovine serum albumin (Sigma A-9647) and gentamycin]

Procedure:

1. Prepare an ice bucket with 4- 50mL centrifuge tubes filled with 40ml DAG.
2. Obtain the liver from the perfusionist. Also take with you a flat ice pack, an autoclaved funnel with 100- μ m mesh, and a hemostat and tissue forceps with tips wrapped in sterile gauze.
3. In the hood, gently pour the liver with 30ml DAPS into a 100mm petri dish. Use the hemostat and forceps to peel back the capsule on each lobe.
4. Use the hemostat to clamp down on the connective tissue of the liver, and gently agitate the liver by knocking the hinge part of the hemostat on the sidewall of the petri dish. Your other hand should hold the petri dish to prevent it from sliding off the ice pack which may become slippery due to condensation. Try to keep most of the liver submerged under liquid and pay attention not to squeeze the liver between the bottom of the dish and the tip of the hemostat. The tip of the hemostat should not touch the bottom of the dish.
5. Break more areas of the capsules if the liver is not breaking up well. Otherwise, when the solution looks like the color of caramel, the shaking should be enough.
6. Prepare a clean 50ml tube and place the funnel into it. Place the remains of the liver on the mesh with the hemostat. Use a pipette to transfer all liquid into the tube through the mesh.

7. Replace the liver in the Petri dish and wash again with 40mL DAPS to isolate all the cells you can. Filter this as before into another 50mL tube.
8. Dispose of the mesh and the liver remains. Equilibrate the two tubes by pouring the liquid back and forth between the two tubes. Pour down the walls of the tube to minimize stress to cells.
9. Spin the two cone tubes of cell solution at 50g for 3 minutes at 4°C.
10. Remove supernatant (save it if NPC's are needed). Re-suspend the cell pellets with fresh DAPS, 40mL per tube. Carefully pour each tube of DAPS into the tubes with the cell pellet. Be careful not to let liquid directly land on top of the pellets. Tilt both tubes so that the liquid is flowing slowly on the tube wall. After both 40ml tubes of DAPS are transferred, cap the tube with cells and start re-suspending cells by rocking both tubes gently. Do this until the pellet is completely in suspension.
11. Spin again at 50g for 3 minutes at 4°C.
12. During this spin, prepare the Trypan blue: 700uL DAPS, 200ul Trypan blue.
13. Remove supernatant (save it if NPC's are needed). Re-suspend each cell pellet with 20mL of fresh DAPS. Make sure that when pipetting in the liquid, the liquid flows slowly on the wall instead of hitting the pellets directly. Pour one tube of solution into the other to consolidate down to one tube (about 45mL total).
14. Take 100µm from the tube and place it into the Trypan blue tube. Use the hemacytometer to count the cell viability and cell concentration as the first final count. Count all 8 squares.
15. Record on the Hepatocyte count document and save under the date.

Appendix 3 – Protocol For Isolation and Viability Test of Primary Liver Endothelial Cells

Materials:

PBS (Gibco 10010-031); Percoll (Sigma-Aldrich P-4937); EGM-2 (Cambrex CC-3162); Hoechst (Molecular Probes H-3570); Sytox Orange (Molecular Probes S11368)

Procedure:

1. Perform perfusion as described in appendix 2 but with the flow rate at 15mL/min.
2. After the perfusion, reserve supernatants from the first two 50g spins. Save the hepatocyte pellets if desired.
3. During the spins in step 2, layer the Percoll. Prepare 30 mL of 50% Percoll by mixing 15mL Percoll and 15mL PBS in a 50 ml conical tube. Prepare 30 mL of 25% Percoll by mixing 22.5mL PBS and 7.5mL Percoll divide equally into two conical tubes. Using a 10 ml pipette, draw up about 14.5mL of the 50% Percoll and place the pipette tip at the bottom of the 25% Percoll. Very gradually load the 50% Percoll underneath the 25% Percoll in order to get two distinct layers.
4. Spin the supernatants from step 2 at 100g for 5min at 24⁰C. Reserve the supernatant and discard the pellets.
5. Spin the supernatants from step 4 at 350g for 7 min. Discard the supernatant. Break up the pellets before re-suspending them in a total of 20mL of PBS.
6. Very gently load 10mL of cell suspension on top of 25% Percoll in the bilayer.
7. Transfer the two tubes to the centrifuge without disturbing them. Set brake setting to 0 and acceleration to 1. (Centrifuge 5804R) Spin at 900g for 20min.
8. You can now see two rings of cells separated out. Carefully suction liquid until the total level reaches 20mL removing the first ring. Collect 10 ml including the cell layer

forming the second ring (at about 15mL mark) until about 10mL is left in the tube. You should now have 20mL of cell suspension in PBS/Percoll collected from 2 tubes.

9. Add to this tube equal volume of PBS. Spin at 900g for 10min. Suction off the supernatant, break up the pellet, and re-suspend the pellet in EGM-2.

10. Combine 900 μ l of EGM-2, 2 μ l of Hoechst, 2 μ l of Sytox Orange, and 100 μ l of cell suspension. Count in a Hemocytometer using the DAPI filter. Sytox orange (dead nuclei) show up as bright green, and Hoechst (all live nuclei) show up as blue.

11. The cells are ready to be used.

Appendix 4 - Protocol for Immuno-Fluorescent Staining of Isolated Non-parenchymal Cells

Materials:

PBS (Gibco 10010-031), 2% paraformaldehyde (EMS) primary antibodies [SE-1 (IBL America), CD31 (Chemicon), ED2 (Serotec), GFAP (Serotec), or SMA (Sigma)], secondary antibody goat-anti-mouse Cy3 (Jackson ImmunoResearch), Hoechst nuclei stain (Molecular Probes)

Procedure

1. Place sterilized glass coverslips in the wells of a 24-well plate and coat them with type 1 rat tail collagen (30 μg / mL) for 2 hours before aspirating off the excess solution.
2. Plate freshly isolated endothelial cell fractions on the collagen-coated glass slips at 300,000 cells per well.
3. Allow cells to attach to the coverslips for 4 hours and wash cells quickly with 1x PBS.
4. Fix cells in 2% paraformaldehyde in PBS for 20 minutes to 1 hour at room temperature. If staining cannot be done right away, store cells in PBS at 4°C until ready to stain.
5. Rinse cells in PBS.
6. Permeabilize cells in 0.1% Triton-X in PBS for 30 minutes at room temperature.
7. Wash well with PBS.
8. Wash cells with PBG (0.5% BSA and 0.15% glycine in 1x PBS).
9. Block with 5% Goat serum for 30 minutes at room temperature.
10. Wash well with PBG.
11. Add the appropriate primary antibody (SE-1, CD31, ED2, GFAP, or SMA) diluted in PBG and incubate for 2 hours at room temperature.

12. Wash well with PBG at room temperature.
13. Dilute secondary antibody (goat-anti-mouse Cy3) in PBG (1:100 dilution) and incubate for 1 hour at room temperature. Cover with foil to avoid light exposure.
14. Wash with PBG.
15. Wash with PBS.
16. Incubate with nuclear stain (Hoechst dye) for about a minute and immediately wash with PBS.
17. Mount cover slip with mounting medium and allow it to set.
18. Slides can be stored at 4°C until ready to image.

Appendix 5 – Assembly And Priming Of Multiwell Reactors

Materials:

1 Lid (A 96 Well Plate Lid works fine), 1 Polyurethane Membrane, 1 Fluidic Plate, 1 Pneumatic Plate, 14 Hex Screws, 1 Hexdriver, 1 Reactor Controller, 50 mL warm mixed medium (37°C).

Procedure (Done entirely inside a sterile hood under sterile conditions)

Reactor Assembly:

1. Sterilize base of pneumatic plate by spraying ethanol being careful not to get it in the fluidic channels.
2. Dry pneumatic plate and place polyurethane membrane on top of the pneumatic plate aligning the holes in the membrane around the screw holes. Make sure to eliminate folds and when handling the membrane, try to only touch the corners and keep the membrane as sterile as possible.
4. Place fluidic plate over the pneumatic plate and membrane.
5. Flip the assembly over and make sure that the membrane covers all the fluidic channels.
6. Tighten screws starting from the middle and working outward. Do not tighten all the way first. Screw in all screws, and then go back and tighten until the membrane becomes clear between the fluidic and pneumatic plates. This is a sign that you have a good seal.
7. Once you have a good seal, cover the fluidic plate with the lid; you are ready to prime the reactor.

Priming the Reactor:

1. Fill each reservoir well with roughly 1.5 mL of mixed medium.

2. Connect the pump controller to the vacuum and pressure sources. Both gauges should read 30 ± 5 kPa when flowing.
3. Connect the tubing from the controller to the reactor assembly.
4. Turn on the controller to UPWARD setting.
5. Begin flowing in the UPWARD setting.
6. Look to see if fluid is pumping into the reactor well.
7. Once you have verified that your system is functioning, fill reactor wells and make sure fluid connects across the surface channel.
8. You should set up your reactor the day before and allow running overnight in incubator and refreshing media before seeding cells.

Appendix 6 – Protocol For Co-culture Spheroid Formation

Materials:

1 500 mL spinner flasks (Bellco Glass Vineland, NJ), Sigmacote (Sigma), Plastic funnel, Glass beaker, 50 μ m- and 300 μ m-pore size filters (SEFAR America)

Procedure

1. Prepare the spinner flasks a day before the perfusion by coating its inner walls and paddle attachments with Sigmacote. Let it air dry and rinse with milli-Q water. Autoclave the flask with 100mL of milli-Q water for 45min of sterilization under the wet cycle.
2. Immediately after cell isolation, seed 40×10^6 endothelial cells and 20×10^6 hepatocytes into the spinner flask with 100mL of mixed medium (containing 50 ml each of HGM and EGM-2). Let it spin at 85rpm in the incubator set at 37°C and 8.5% CO₂ for 48 hours.
3. Cut a 10cm x 10cm square of 50 μ m filter and use a rubber band to secure it onto a 100mL glass beaker. Cut a 10cm x 10cm square of 300 μ m filter and secure onto a plastic funnel with autoclave tape. Wrap both in separate autoclave blue papers and autoclave for at least 45min of sterilization under the dry cycle.
4. On the day of seeding, assemble and prime reactors as described in appendix 4.
5. In the sterile hood, fill a 100mm Petri dish with 30mL of mixed medium and set it on an ice pack. On the side, prepare another 30mL of mixed medium in a 50mL tube and set it on ice.
6. Using a 50 ml pipette, sieve the spheroids from the flask through the 300 μ m-filter funnel into two 50mL tubes.
7. Pipette the contents from the 50mL tubes through the 50 μ m-filter beaker to select out all spheroids between 50 μ m and 300 μ m in diameter.
8. Carefully remove the rubber band and invert and submerge the filter in the Petri dish. Shake it in solution to release all the spheroids. Collect the solution into a 50mL tube.

9. Spin at 40g for 2 minutes at 4°C.

10. Remove supernatant and resuspend cells with the mixed medium set aside earlier.

Store it on ice.

Appendix 7 – Setup and Seeding the Multiwell Reactors

Materials:

1 Assembled Reactor, Prior autoclaved components: Packed Filters (24), Gaskets (12), Filter Supports (12), Glass Dish (1), Sterile Tweezers (1) and Tamping Tool (1), Prior ethanol sterilized polycarbonate scaffolds that are soaked in Type 1 rat tail collagen (30 µg / mL) for 2 hours and dried for an hour (12), P1000 Pipette, Wide Orifice Tips, Reactor Controller, Spheroids OR cell isolates, Mixed medium, Sterile PBS,

Procedure (Done entirely inside a sterile hood under sterile conditions)

Setting Up Reactor Wells:

1. Place all filter supports in 50 mL Falcon Tube.
2. Fill Falcon Tube with PBS and tap the bottom of the tube to remove trapped bubbles from filter supports.
3. Place all gaskets in dish of PBS.
4. Place gaskets in all of the reactor wells. Push down with tamping tool.
5. Pour filter supports into glass dish or 90 mm petri dish.
6. Place filter support in all reactor wells with concentric rings facing up.
7. Push down with tamping tool.
8. Rinse filter gently in PBS and then place one filter in all wells.
9. Rinse scaffolds gently in PBS, and gently place one in each reactor well.
10. Put one retaining ring in each well. Push them down firmly enough to ensure that the ring is tight and the path of the fluid is through the filter and scaffold and not around it.

Seeding Spheroids/Cells

1. Aspirate as much media as possible from both the reactor and reservoir leaving a thin layer of media above the scaffold in the reactor well and the filter in the reservoir well as to not introduce air bubbles beneath the filter.
2. Add back cold, fresh medium to the reactor well only. Do not create a fluidic connection between the reactor well and reservoir well.
3. Make sure that the reactor is set for downward flow through the scaffold.
4. Pause flow
5. Using a P1000 pipette, hold pipette straight up and slowly pipette the desired amount of the spheroids/ cell suspension in a pattern over the scaffold.
6. Check seeding under microscope. If poorly distributed, using the wide orifice tips aspirate from periphery in a circular motion and pipette over channels again
7. Resume downward flow and fill reservoir to fill line with media (approximately 2.5 mL - 2.7 mL). Make sure that you have no dry spots across the fluidic channel.
8. Set the controller for reverse flow and select a flowrate. Set a reversal time of 8 hours.

Appendix 8 – Maintaining And Disassembling The Multiwell Reactors

Materials:

1 Assembled Reactor, Prior autoclaved components: Packed Filters (12), 10 ml pipette, Aspirator, Sterile Tweezers (1) and Tamping Tool (1), Petri Dish (2), 1% BSA Solution Reactor Controller, 50 ml medium warmed to 37⁰C (HGM or mixed depending on experiment design), Sterile PBS, Hexdriver, Bleach solution, 1-3% 7X Solution

Procedure (Done entirely inside a sterile hood under sterile conditions)

Changing Reservoir Side Filters (only 24 hours post seeding) and Medium (Every Day):

1. Soak 12 new filters in petri dish filled with 1% BSA Solution.
2. Remove the reactor from the incubator and transfer it carefully to the hood without spilling media from the channels.
3. Under the hood, remove the lid from the reactor and aspirate off any media from the lid and on the surface of the reactor plate. Aspirate media from the reservoirs by taking your aspirator tip and bringing it to the top of the retaining ring and aspirating off the media. Be careful to not aspirate off media to the point of creating air bubbles under the filter as this interrupts the flow through the reactor.
4. Aspirate media from reactor wells by taking your aspirator tip near the wall of the reactor well. Be sure not to aspirate media directly from above the cells. Be sure to leave approximately 1 - 2 mm of media above the cells as to not disrupt them significantly.
5. (Done only 24 hours post seeding) Remove retaining ring from reservoir side, and place aside in petri dish filled with PBS. Remove filters from reservoir and discard. Gently place new BSA-soaked filters in reservoir. Tamp in place. Put one retaining ring in each well, and push down firmly with tamping tool to ensure tight fluidic seal.

6. Put 2.5 ml of new warm media in each reservoir well being careful to keep your pipette clear of bubbles. Make sure that you have no dry spots across the fluidic channel as this will disrupt oxygen transport.
7. Cover your reactor and return your reactor to the incubator.
8. Make sure the pressure and vacuum gauges are set between 30 ± 5 .

Harvesting Samples from the Reactor

1. Stop the controller. Remove the retaining ring from above the scaffold.
2. Gently grab both sides of the scaffold with a tweezers and remove scaffold for the analyses your experiment requires.
3. Remove remaining reactor components and place in bleach solution.
4. Perform a mechanical diagnostic to verify that flow rates in all wells were functional and accurate. Aspirate media from reactor well and the bridge between the reactor and reservoir wells and then from reservoir wells making sure to not introduce air bubbles in pumping system. Add 500 μL to reservoir well. Select and test the flowrate by beginning UPWARD flow and recording the time taken to empty the reservoir wells.

Disassembling The Reactor.

1. To disassemble and clean your reactor, unscrew assembly screws and clean screws, if needed.
2. Separate fluidic and pneumatic plate.
3. Discard polyurethane membrane. Soak fluidic and pneumatic plates in bleach solution for an hour. Rinse with deionized water and soak in 7X Solution for 2 hours.
5. Rinse with milliQ water and dry. Clear debris in channels using compressed air.

Appendix 9 - Protocol For Immuno-Fluorescent Staining Of Co-Culture Spheroids Or Tissue From Reactor Scaffolds

Materials:

PBS (Gibco 10010-031), 2% paraformaldehyde (EMS) primary antibodies [SE-1 (IBL America), CD31 (Chemicon), ED2 (Serotec), GFAP (Serotec), or SMA (Sigma)], secondary antibody goat-anti-mouse Cy3 (Jackson ImmunoResearch), Hoechst nuclei stain (Molecular Probes)

Procedure

1. If staining spheroids, obtain them as described in Appendix –6 and resuspend them in 10 ml of PBS. Dispense about 500 μ l of the spheroid suspension into separate 2 ml centrifuge tubes for each of the primary antibodies and a negative control and spin them down.

OR

In case of the reactor polycarbonate scaffolds, remove them as described in Appendix 8 and place them in the wells of 12 well plates. Wash once with PBS.

2. Aspirate out the PBS gently from the samples.

3. Fix spheroids/reactor tissue by adding 1000 μ l of 2% paraformaldehyde in PBS for 1 hour at room temperature. Make sure that the spheroids are resuspended in the centrifuge tubes. Use a nutator to constantly mix the tubes/12 well plates. If staining cannot be done right away, store samples in PBS at 4°C until ready to stain.

5. Spin down the spheroids. Wash spheroids/reactor scaffolds with PBS.

6. Permeablize spheroids in tubes/ reactor samples in plates by adding 500 μ l of 0.1% Triton-X in PBS. Continue rotating the tubes/12 well plates on a nutator for 45 minutes at room temperature.

7. Spin down the spheroids. Wash spheroids/reactor scaffolds with PBS.

8. Spin down the spheroids. Wash spheroids/reactor scaffolds with 2% BSA in 1x PBS.
9. Spin down the spheroids. Block spheroids/reactor scaffolds with 500 μ l of 5% Goat serum. Continue rotating the tubes/12 well plates on a nutator for 60 minutes at room temperature.
10. Spin down the spheroids. Wash spheroids/reactor scaffolds with 2% BSA in 1x PBS.
11. Cut the scaffold into multiple pieces with each piece containing numerous channels filled with tissue. Transfer these pieces into separate wells of a 24 well plate labeled for the respective primary antibody being stained.
12. Add the appropriate primary antibody (SE-1, CD31, ED2, GFAP, or SMA) diluted in 2% BSA in 1x PBS and incubate overnight at 4⁰C. The dilutions are as per manufacturers instructions or adjusted for the specific instance. Continue rotating the tubes/24 well plates on a nutator overnight at 4⁰C while they are incubating with the antibody.
13. Spin down the spheroids. Wash spheroids/reactor scaffolds three times with 2% BSA in 1x PBS.
14. Dilute secondary antibody (goat-anti-mouse Cy3) in 2% BSA in 1x PBS. (1:100 dilution) and incubate for 1 hour at room temperature. Incubate simultaneously with nuclear stain (1:5000 dilution) Draq 5 (Alexis). Cover with foil to avoid light exposure.
15. Spin down the spheroids. Wash spheroids/reactor scaffolds three times with 1x PBS.
16. Resuspend spheroids in 200 μ l of PBS. Add spheroids using a wide orifice pipette tip into the channels of a Labtek chamber slide. In the case of reactor scaffolds, place them in similar chamber slides and submerge in PBS.
17. Samples are now ready for confocal microscopy. After microscopy, the chamber slides can be sealed with parafilm and stored at 4⁰C.

Appendix 10 – Protocol For Oxygen Measurement In Reactor System

Materials:

Oxy 4 meter, custom O₂ dipping Probes (v 1.01), reactor assembly with seeded tissue, Oakton Zero Oxygen Solution (Sodium Sulfide) MilliQ Water, magnetic stirrer bar, thermometer.

Procedure:

Calibration

1. Air saturated water value (100%): Fill a wide beaker filled with MilliQ Water stirred constantly with a magnetic stirrer bar and record the temperature. First use the Fibox 3 single dipping probe to make O₂ measurement at 5-min intervals till the reading stabilizes reflecting air saturated water value (100%). Now immerse the custom probes for the Oxy 4 into the water. Start the Oxy 4 software. Make measurements by setting all intervals to 1 min and the temperature set to the thermometer reading. Calibrate probes by clicking on the Calibration tab and entering the pressure and temperature of the 100% standard followed by choosing the “Calibrate all” option.
2. Zero O₂ solution (0 %) O₂: Fill a 500 ml bottle with the zero O₂ solution with a stirrer bar in the bottom. Follow the rest of the calibration steps as described above.

Wash all the probes with MilliQ water to get rid of any remaining zero O₂ solution.

Measurement in Reactors

1. Mount the probes on the lid and make sure the heights of all the probes are adjusted to the same desired depth by placing a reference sheet of uniform thickness across the lid.
2. Spray the lid and probes down thoroughly with ethanol and leave under the hood sitting on its side allowing it to dry for 30 minutes under cover of an aluminium foil.

3. Replace the lid with the mounted probes onto the reactor under sterile conditions and replace the reactor with the lid and probes into the incubator. Attach the probes to the connectors of the optic fibre cables (preferably coming in from the back of the incubator to minimize bending of the cables).
4. Ensure all the connectors are properly attached to the probes before running the Oxy 4 software. On the logging tab select all channels specifying where you want the file it creates to be saved. On the measurement tab check the box marked “locked” under the sampling rate and channel temperature to have similar settings for all probes.
5. Set O₂ sampling measurements at 5-15 mins for a steady state measurement. Click the “All Channels” button and after 2 readings are made, monitor the data by clicking on the “All Channels” tab to display all the readings concurrently.
6. To stop logging click on the “All channels” button under the measurement tab before you start disconnecting the probes.
7. Data can be exported and read in Excel using the import feature. The data set is semicolon delimited and each channel is stored as a separate text file.

Cleaning up and Storage

1. Wash the probes with MilliQ water and spray down with Ethanol and blow dry very gently with air. At all times be very careful with the tips of the probes.
2. Replace inside box and cover with Aluminium foil to prevent the sensors from photo damage.

Appendix 11 - Protocol for RNA isolation from samples in Trizol

(Adapted from the Trizol and RNeasy Kit user manuals)

Materials:

Trizol (Invitrogen), chloroform (Sigma-Aldrich), ethanol, RNeasy Kit (Qiagen), RNase-free water.

Procedure:

1. For reactor samples, drop each scaffold into a well of a 6 well plate with 1000 μ L trizol. Freeze the samples immediately in the -80°C freezer.
2. Thaw samples on ice. Homogenize the tissue with a 3mL syringe connected with 20-gauge needle for at least 5-10 cycles of pumping in and out. Repeat this step with a 25-gauge needle.
3. Transfer trizol solution to a centrifuge tube. Each tube should contain 1mL or less of Trizol solution. For every mL of Trizol, add 250 μ l of chloroform. Vortex on the highest setting and let settle for 2 minutes at room temperature.
4. Spin at 12,000 rpm for 15 minutes in the cold room.
5. Fill a centrifuge tube with RNase-free water and warm it to 55°C .
6. Remove the aqueous phase on top and place into a new centrifuge tube. Add equal volume of ice-cold 70% ethanol. Pipette up and down to mix. If the total volume at this point is more than 650 μ L, repeat step 6-7 until all solution has been passed through the column. Return the rest of the Trizol sample to -80°C freezer for further DNA or protein isolation.
7. Load the mixture onto an RNeasy column with maximum volume of 650 μ l. Spin for 15 sec. at 10,000 rpm at room temperature.
8. Collect the flow-through and run it through the column again using step 6. Discard the flow-through.

9. Add 700µl RW1 to the column. Spin for 15 sec. at 10,000 rpm. Discard the flow through and replace the collection tube with a new one.
10. Add 500µl RPE buffer (make sure ethanol has been added) and spin for 15 sec. at 10,000 rpm. Discard the flow-through.
11. Repeat the last step.
12. Spin the column again to collect any excess liquid. Discard the collection tube and the flow-through. Place the column into a 1.5mL collection tube with a closeable top.
13. Load 30-50µl of 55°C RNase-free water into the column. Spin for 1 min at 10,000 rpm to elute the RNA.
14. If more than 30µg of RNA is expected, repeat the last step with the same tube.
15. Store in the -80°C freezer.